Studies on Catalysis by Nano Titania Modified with Metals and Nonmetals

Thesis submitted to

Cochin University of Science and Technology

in partial fulfillment of the requirements for

the award of the degree of

Doctor of Philosophy

in

Chemistry

Under the Faculty of Science

by

DHANYA T. P.

Department of Applied Chemistry

Cochin University of Science and Technology

Kochi - 682 022

November 2012

Studies on Catalysis by Nano Titania Modified with Metals and Nonmetals

Ph. D. Thesis under the Faculty of Science

Author:

Dhanya T. P.
Research Fellow, Department of Applied Chemistry
Cochin University of Science and Technology
Kochi, India 682 022
E mail: dhanyatp_2006@yahoo.co.in

Guide:

Dr. S. Sugunan
Professor (Emeritus)
Department of Applied Chemistry
Cochin University of Science and Technology
Kochi, India 682 022
Email: ssg@cusat.ac.in

Department of Applied Chemistry
Cochin University of Science and Technology
Kochi, India 682 022

November 2012

DEPARTMENT OF APPLIED CHEMISTRY
COCHIN UNIVERSITY OF SCIENCE AND TECHNOLOGY
KOCHI - 682 022, INDIA

Dr. S. Sugunan
Professor (Emeritus)

Mob: 9447609478
ssg@cusat.ac.in

Certificate

This is to certify that the research work presented in the thesis entitled **"Studies on Catalysis by Nano Titania Modified with Metals and Nonmetals"** is an authentic record of research work carried out by Smt. Dhanya T. P. under my supervision at the Department of Applied Chemistry, Cochin University of Science and Technology, in partial fulfillment of the requirements for the degree of Doctor of Philosophy in Chemistry and that no part thereof has been included for the award of any other degree.

Kochi-22
07/11/12

Dr. S. Sugunan
(Supervising Guide)

Declaration

I hereby declare that the thesis entitled **"Studies on Catalysis by Nano Titania Modified with Metals and Nonmetals"** is the bonafide report of the original work carried out by me under the supervision of Dr. S. Sugunan at the Department of Applied Chemistry, Cochin University of Science and Technology and no part thereof has been included in any other thesis submitted previously for the award of any degree.

Kochi-22
07/11/12

Dhanya T. P.

To my parents and husband…

Acknowledgement

First and foremost, praises and thanks to God, Almighty, for His showers of blessings throughout my research work to complete the research successfully.

I have indeed immense pleasure to express my deepest sense of gratitude and obligation to my guide Prof. Dr. S. Sugunan, Department of Applied Chemistry for constant encouragement, invaluable advice, and excellent guidance given to me. I shall ever remain grateful to him.

I would like to express my heartfelt thanks to Dr. K. Sreekumar, Head, Department of Applied chemistry for providing me the necessary facilities for carrying out my research. I sincerely thank Dr. K. Girish Kumar, former Head, Applied Chemistry Department for the timely help and support during the period of this work. I also express my heartfelt thanks to Dr.S.Prathapan, my doctoral committee member for the support and suggestions. I express my thanks to all teaching and nonteaching staffs of Applied Chemistry Department for their help and warm wishes.

I greatfully acknowledge Dr. Suguna Yasodharan and Dr. V. Sivanandan Achari, School of Environmental Studies, CUSAT for their timely help in doing TOC analysis. I would also like to acknowledge Bindya, Raji, Anju, Deepa, Asha and Chitra for their help and assistance. I acknowledge with thanks Dr. Jagannath, BARC for XPS study, STIC-CUSAT and SAIF- IIT Chennai for providing me the necessary instrumental analysis data.

I sincerely thank my teachers of Department of Chemistry, Calicut University from the depth of my heart.

Iwould also like to thank my seniors Dr. Sanjay, Dr. Suja, Dr. Radhika and my labmates Rose miss, Reshmi, Cimi, Joyes miss, Bolie, Nisam, Soumini, Ambili, Rajesh,

Mothi, Reni and Sandhya for their loving support. I thank all my friends of other labs of Applied Chemistry department. My special thanks to my hostel mates Shimi, Sisy, Remya, Priya, Haseena, Uma, Sujisha for their constant support and sisterly affection. I find myself lucky to have friends like them in my life. I express my warm thanks to my colleagues of chemistry department, NSS College Ottapalam.

My deepest gratitude goes to my parents for their unflagging love and support throughout my life. I would like to express my deep love for my mother whose selfless sacrificial life, great efforts with pain and unceasing prayers enabled me to reach the present position in life. I have no suitable word that can fully describe her everlasting love to me.

I wish to express my dearest thanks to my husband, who has given me all his loving care and support. He is my best friend and a role model for me .As for my husband, I find it difficult to express my appreciation because it is so boundless. Without his encouragement and understanding it would have been impossible for me to finish this work. I dedicate this thesis to him with all my love.

My special thanks to my brother-in-law, sister and my sweet kannan for their support.

I am forever grateful to my grandparents. The relationships and bonds that I have with my grandparents hold an enormous amount of meaning to me. For as long as I can remember, and in all aspects of my life, both of them have been my biggest sources for inspiration. I would not be where I am today without them.

Dhanya. T. P.

Preface

Semiconductor photocatalysis has received much attention during last three decades as a promising solution for both energy generation and environmental problems. Heterogeneous photocatalytic oxidation allows the degradation of organic compounds into carbon dioxide and water in the presence of a semiconductor catalyst and UV light source. The •OH radicals formed during the photocatalytic processes are powerful oxidizing agents and can mineralise a number of organic contaminants. Titanium dioxide (TiO_2), due to its chemical stability, non-toxicity and low cost represents one of the most efficient photocatalyst. However, only the ultraviolet fraction of the solar radiation is active in the photoexcitation processes using pure TiO_2 and although, TiO_2 can treat a wide range of organic pollutants the effectiveness of the process for pollution abatement is still low.

A more effective and efficient catalyst therefore must be formulated. Doping of TiO_2 was considered with the aim of improving photocatalytic properties.

In this study TiO_2 catalyst was prepared using the sol-gel method. Metal and nonmetal doped TiO_2 catalysts were prepared. The photoactivity of the catalyst was evaluated by the photodegradation of different dyes and pesticides in aqueous solution.

High photocatalytic degradation of all the pollutants was observed with doped TiO_2. Structural and optical properties of the catalysts were characterized using XRD, BET surface area, UV-Vis. DRS, CHNS analysis, SEM, EDX, TEM, XPS, FTIR and TG. All the catalysts showed the anatase phase. The presence of dopants shifts the absorption of TiO_2 into the visible region indicating the possibility of using visible light for photocatalytic processes.

Contents

.....ꕥ.....

Chapter

1

Introduction

Contents

Heterogeneous photocatalysis is an emerging technique valuable for water and air purification. This method has gained significant impetus over the years as it offers the advantage of destroying a wide range of water and air pollutants. Conventional techniques such as activated carbon are becoming unacceptable because they do not destroy the pollutants but only transfer the contaminants from one phase to another. The absolute toxicity of the pollutants, however, is not diminished. The new oxidation technology known as Advanced Oxidation Processes (AOPs) appears as an emerging technology for the complete mineralization of the organic and inorganic pollutants. Among AOPs, heterogeneous photocatalysis using semiconductor nanomaterials for the waste water purification appears to be the most promising technology, because the photoactivated semiconductors can completely decompose (mineralize) various kinds of pollutants that are refractory, toxic, and non-biodegradable, to CO_2, water and mineral acids under mild conditions. This chapter describes the basics and the application of heterogeneous photocatalysis.

1.1 Photocatalysis

The prefix photo, defined as "light". Catalysis is the process where a substance participates in modifying the rate of a chemical transformation of the reactants without being altered in the end. This substance which increases the rate of a reaction by reducing the activation energy is known as the catalyst. Hence, photocatalysis is a reaction which uses light to activate a substance which modifies the rate of a chemical reaction without being involved itself and the photocatalyst is the substance which can modify the rate of chemical reaction using light irradiation. Chlorophyll of plants is a typical natural photocatalyst. The difference between chlorophyll photocatalyst to man-made nano photocatalyst is, usually chlorophyll captures sunlight to turn water and carbon dioxide into oxygen and glucose, but on the contrary photocatalyst creates strong oxidation agent and electronic holes to breakdown the organic matter to carbon dioxide and water in the presence of photocatalyst and light (fig.1.1).

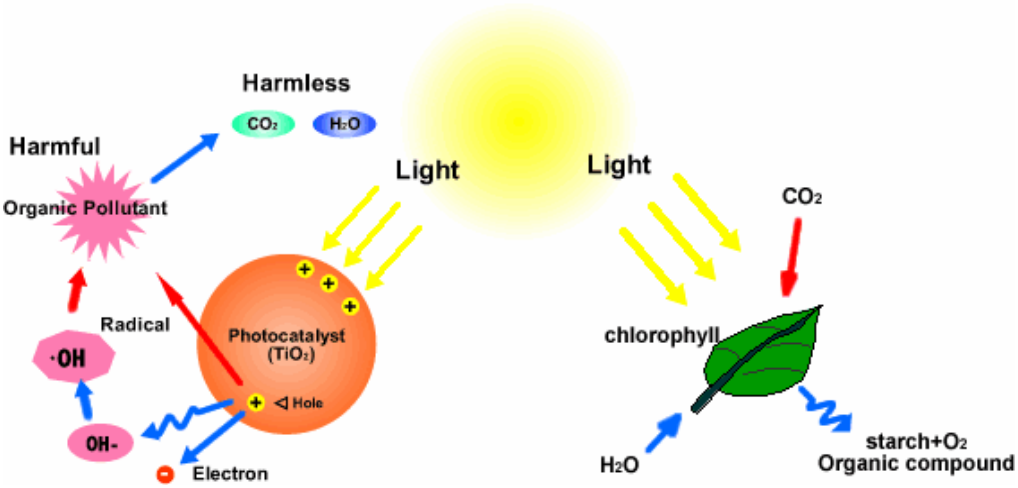

Fig. 1.1 Photocatalysis and photosynthesis

A semiconductor immersed into a solvent (in most cases water) and illuminated with photons exceeding its band gap energy will be called a photocatalyst provided that at its surface it is able to catalyze reactions with $\Delta G < 0$ [1].For thermodynamically unfavourable reactions ($\Delta G > 0$), the energy of UV irradiation is converted into chemical energy and the term ‘‘photosynthesis’’ applies.

Photocatalytic reactions have been extensively studied. Photocatalytic reactions are classified into two categories: ‘‘down-hill’’ and ‘‘up-hill’’ reactions. Degradation such as photo-oxidation of organic compounds using oxygen molecules is generally a down-hill reaction. The reaction proceeds irreversibly. In this reaction, a photocatalyst work as a trigger to produce $O_2^{\cdot -}$, $OH^{\cdot}$ as active species for oxidation at the initial stage. This type of reaction is regarded as a photo induced reaction and has been extensively studied using titanium dioxide photocatalyst. On the other hand, water splitting into H_2 and O_2 is accompanied by a largely positive change in the Gibbs free energy ΔG^O = 237 kJ/mol and is an up-hill reaction. In this reaction, photon energy is converted into chemical energy as seen in photosynthesis by green plants. Therefore, this type of reaction is called artificial photosynthesis [2,3].

Semiconductor photocatalysis has received much attention during last three decades as a promising solution for both energy generation and environmental problems. Since the discovery of Fujishima and Honda [4] that water can be decomposed into hydrogen and oxygen using a semiconductor (TiO_2) electrode under UV irradiation, extensive works have been carried out to produce hydrogen from water splitting using a variety of semiconductor photocatalysts. In recent years, scientific and engineering interest in

heterogeneous photocatalysis has also been focused on environmental applications such as water treatment and air purification.

1.2 History of Photocatalysis

In the mid 1920s, the semiconductor ZnO began attracting attention for use as a sensitizer for the decomposition of both organic and inorganic photoreactions, and TiO_2 was soon after investigated for its photodegradation characteristics [5]. Most of the primitive work in semiconductor photochemistry took place in the 1960s. In the 1970's solar energy was being studied due to a need for more available renewable resources and environmental concerns; photochemistry was looked upon for the storage and usage of solar energy. In 1972, Fujishima and Honda discovered the photocatalytic splitting of water on TiO_2 electrodes [4]. This event marked the beginning of a new era in heterogeneous photocatalysis. In the early 1980s, TiO_2 was used for the first time to sensitize reactions in the photo mineralization of selected organics. In the 1980's and 1990's there came an increasing concern for environmental preservation and clean up. As a result some environmental scientists have looked at photochemistry for air, water, and soil clean up. TiO_2 catalyzed photochemistry can accomplish the mineralisation, which is the degradation of organic compounds to H_2O and CO_2 and its inorganic substituants. Over the years, many semiconductors with photocatalytic properties have been either thoroughly or partially investigated including TiO_2 (3.2 eV), $SrTiO_3$ (3.4 eV), Fe_2O_3 (2.2 eV), CdS (2.5 eV), WO_3 (2.8 eV), ZnS (3.6 eV), $FeTiO_3$ (2.8 eV), ZrO_2 (5 eV), V_2O_5 (2.8 eV), Nb_2O_5 (3.4 eV), SnO_2 (3.5 eV), as well as many others [6]. Of the semiconductors tested, their uses and applications vary depending on the individual properties of the photocatalyst. During the last few years, semiconductor mediated photo catalysis has been reported as a promising route to destroy toxic and hazardous

organic substances in industrial wastewater and drinking water. In most cases, a complete oxidative destruction of pollutants has been observed and the end products include CO_2, H_2O and inorganic ions. The harvest of sunlight for photocatalysis has been a tremendous boon to the process, on account of the economic feasibility, ease of large scale operation and process efficiency.

1.3 Mechanism of Photocatalysis

In the absence of a catalytically active substance, the oxidation of the most hydrocarbons proceeds rather slowly, which can be explained by kinetic arguments. A photocatalyst decreases the activation energy of a given reaction. In the result of photoinduced processes often particles with strong oxidation and reduction ability occur.

A heterogeneous photocatalytic system consists of semiconductor particles (photocatalyst) which are in close contact with a liquid or gaseous reaction medium. Exposing the catalyst to light, excited states are generated which are able to initiate subsequent processes like redox reactions and molecular transformations.

In fig.1.2 a simplified reaction scheme of photocatalysis is shown. Due to their electronic structure, which is characterized by a filled valence band (VB) and an empty conduction band (CB), semiconductors (metal oxides or sulphides such as ZnO, CdS, TiO_2, Fe_2O_3, and ZnS) can act as sensitizers for light-induced redox processes. The energy difference between the lowest energy level of the CB and the highest energy level of the VB is the so-called band gap energy (E_{bg}). It corresponds to the minimum energy of light required to make the material electrically conductive.

When a photon with an energy of hν exceeds the energy of the band gap, an electron(e^-) is promoted from the valence band to the conduction band leaving a hole(h^+) behind. In electrically conducting materials, i.e. metals, the produced charge carriers are immediately recombined. In semiconductors a portion of this photoexcited electron-hole pairs diffuse to the surface of the catalytic particle and take part in the chemical reaction with the adsorbed donor (D) or acceptor (A) molecules. The holes can oxidize donor molecules (1) whereas the conduction band electrons can reduce appropriate electron acceptor molecules (2).

$$D + h^+ \rightarrow D^{\cdot +} \text{ ---------- (1)}$$

$$A + e^- \rightarrow A^{\cdot -} \text{ ---------- (2)}$$

A characteristic feature of semiconducting metal oxides is the strong oxidation power of their holes h^+. They can react with water (3) to produce the highly reactive hydroxyl radical (•OH). Both the holes and the hydroxyl radicals are very powerful oxidants, which can be used to oxidize most organic contaminants

$$H_2O + h^+ \rightarrow OH^{\cdot} + H^+ \text{ ---------- (3)}$$

In general, air oxygen acts as electron acceptor (4) by forming the super-oxide ion $O2^{\cdot -}$

$$O_2 + e^- \rightarrow O_2^{\cdot -} \text{ ---------- (4)}$$

Super-oxide ions are also highly reactive particles, which are able to oxidize organic materials [7,8].

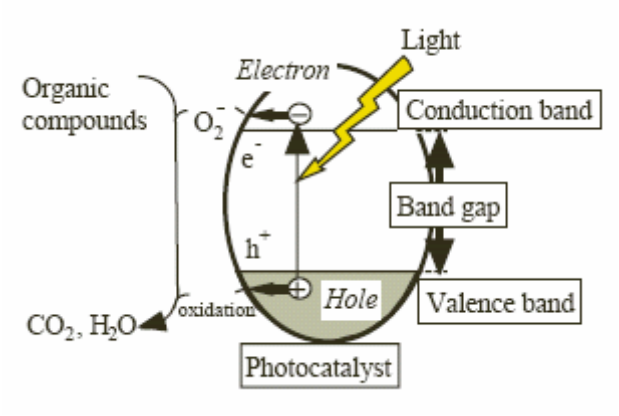

Fig. 1.2 Mechanism of photocatalysis

The overall process is the semiconductor mediated photocatalysed oxidative mineralisation of the organic pollutant and can be represented by the following equation:

$$\text{Pollutant} + O_2 \xrightarrow[h\nu \geq E_{bg}]{\text{Semiconductor}} CO_2 + \text{Water}$$

1.4 Basic Functions of Photocatalyst

1.4.1 Sterilizing Effect

Photocatalyst does not only kill bacteria cells, but also decompose the cell itself. The titanium dioxide photocatalyst has been found to be more effective than any other antibacterial agent, because the photocatalytic reaction works even when there are cells covering the surface and while the bacteria are actively propagating. The end toxin produced at the death of cell is also expected to be decomposed by photocatalytic action. Titanium dioxide does not deteriorate and it shows a long-term anti-bacterial effect. Generally speaking, disinfection by titanium oxide is three times stronger than chlorine, and 1.5 times stronger than ozone.

1.4.2 Deodorizing Effect

On the deodorizing application, the hydroxyl radicals accelerate the breakdown of any Volatile Organic Compounds or VOCs by destroying the molecular bonds. This will help to combine the organic gases to form a single molecule that is not harmful to humans and thus enhance the air cleaning efficiency. Some of the examples of odor molecules are: Tobacco odor, formaldehyde, nitrogen dioxide, gasoline, and many other hydrocarbon molecules in the atmosphere. Air purifier with TiO_2 can prevent smoke and soil, pollen, bacteria, virus and harmful gas as well as seize the free bacteria in the air with the help of the highly oxidizing effect of photocatalyst.

1.4.3 Air Purifying Effect

The photocatalytic reactivity of titanium oxides can be applied for the reduction or elimination of polluted compounds in air such as NO_x, cigarette smoke, as well as volatile compounds arising from various construction materials. Also, high photocatalytic reactivity can be applied to protect lamp-houses and walls in tunneling, as well as to prevent white tents from becoming sooty and dark. Atmospheric constituents such as chlorofluorocarbons (CFCs) and CFC substitutes, greenhouse gases, and nitrogenous and sulfurous compounds undergo photochemical reactions either directly or indirectly in the presence of sunlight. In a polluted area, these pollutants can eventually be removed.

1.4.4 Antifogging

Generally when moist air comes in contact with glass, small droplets of water are formed, and the glass becomes fogged. On titanium dioxide coated glass, the water forms a continuous flat sheet, so that there is no fogging.

Fogging of the surface of mirrors and glass occurs when humid air condenses, with the formation of many small water droplets, which scatter light. On a super hydrophilic surface, no water droplets are formed. Instead, a uniform film of water can form on the surface, and this film does not scatter light.

1.4.5 Self-Cleaning

Most of the exterior walls of buildings become soiled from automotive exhaust fumes, which contain oily components. When the original building materials are coated with a photocatalyst, a protective film of titania provides the self-cleaning building by becoming antistatic, super oxidative, and hydrophilic. The hydrocarbon from automotive exhaust is oxidized and the dirt on the walls washes away with rainfall, keeping the building exterior clean at all times [9].

1.4.6 Water Purification

Photocatalyst coupled with UV lights can oxidize organic pollutants into nontoxic materials, such as CO_2 and water and can disinfect certain bacteria. This technology is very effective at removing further hazardous organic compounds and at killing a variety of bacteria and some viruses in the secondary wastewater treatment.

1.4.7 Photocatalytic Water Splitting

Photocatalytic water splitting is the term for the production of hydrogen (H_2) and oxygen (O_2) from water by directly utilizing the energy from light. Hydrogen fuel production has gained increasing attention as oil and other nonrenewable fuels become increasingly depleted and expensive. Water splitting holds particular interest since it utilizes the inexpensive natural

resource water. Photocatalytic water splitting has the advantage of the simplicity of using a powder in solution and sunlight to produce H_2 and O_2 from water [10].

1.5 Advantages of Photocatalysis

- Complete mineralisation of pollutants
- Use of near UV or solar light
- No addition of other chemicals
- Operation at room temperature

1.6 Semiconductors as Photocatalysts

For conventional redox reactions, one is interested in either reduction or oxidation of a substrate. However, in the case of water splitting one has to carry out both the redox reactions simultaneously namely, the reduction of hydrogen ions ($2H^+ + 2e- \rightarrow H_2$) as well as oxygen evolution from the hydroxyl ions ($2OH^- + 2H+ \rightarrow H_2O + 1/2O_2$). The system that can promote both these reactions simultaneously is essential. Since in the case of metals the top of the valence band (measure of the oxidizing power) and bottom of the conduction band (measure of the reducing power) are almost identical they cannot be expected to promote a pair of redox reactions separated by a potential of nearly 1.23 V.

Therefore one has to resort to systems where the top of the valence band and bottom of the conduction band are separated at least by 1.23V. This situation is obtainable with semiconductors as well as with insulators. If the valence band is completely filled with electrons and the bandgap lies between 0 and 5 eV, it will be called a semiconductor. A material with a bandgap higher than 5 eV is called an insulator (fig.1.3). However insulators are not

appropriate due to the high value of the band gap which demands high energy photons to create the appropriate excitons for promoting both the reactions Therefore, it is clear that semiconductors are suitable materials for the promotion of water splitting reaction [11-13].

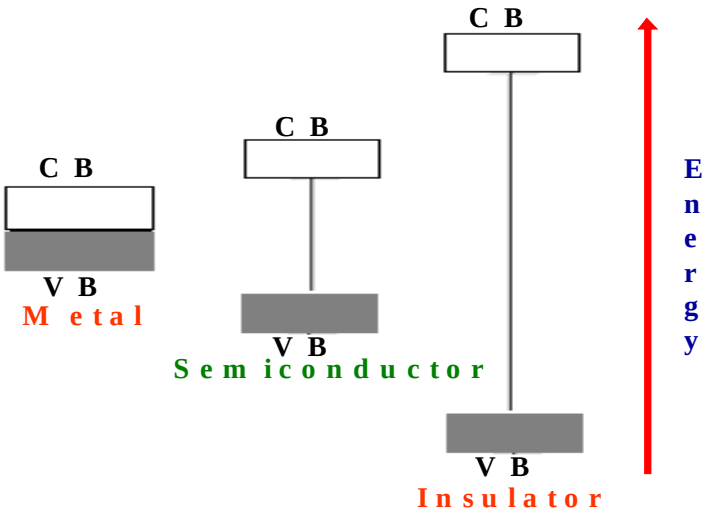

Fig. 1.3 Band gap of available materials

The ability of a semiconductor to undergo photoinduced electron transfer to adsorbed particles is governed by the band energy positions of the semiconductor and the redox potentials of the adsorbates. The relevant potential level of the acceptor species is thermodynamically required to be below the conduction band of the semiconductor. The potential level of the donor is required to be above the valence band position of the semiconductor in order to donate an electron to the empty hole [7,14].

The band-edge positions of some semiconductors are presented in fig.1.4 [14].

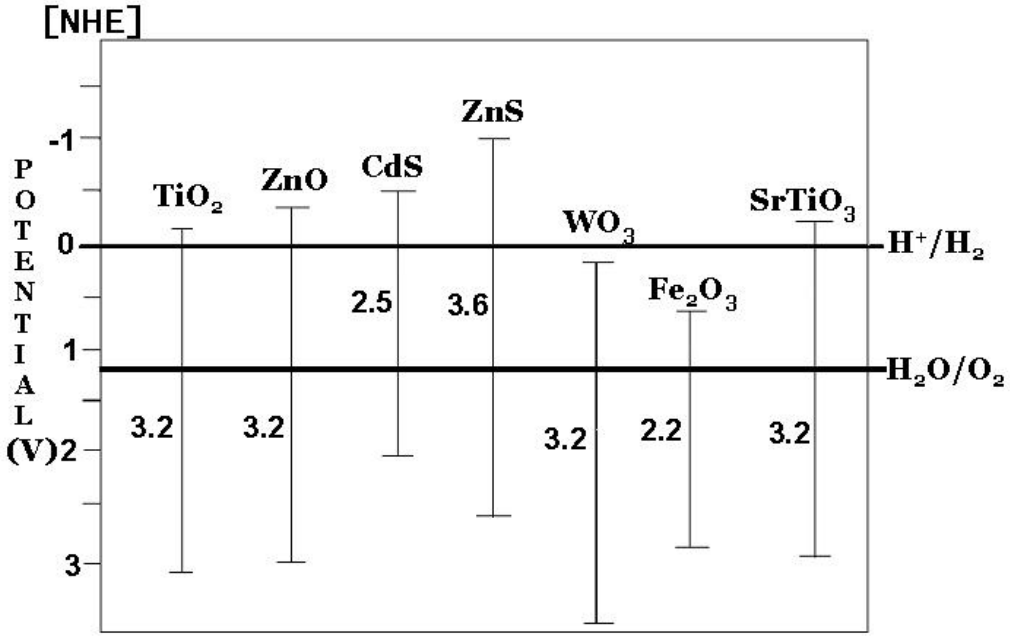

Fig.1.4 Band energy position of semiconductors

1.7 TiO_2 as Photocatalyst

Titanium dioxide is one of the basic materials in everyday life. It has been widely used as white pigment in paints, cosmetics and foodstuffs. Titanium is the ninth most abundant element and constitutes about 0.63% in weight of the earth's crust. Minerals rutile and ilmenite, $FeTiO_3$, are the main ores of this element [7,15,16].

Titanium dioxide occurs in three crystalline forms rutile, anatase and brookite, and additionally as two high pressure forms, a monoclinic baddeleyite-like form and an orthorhombic α-PbO_2-like form. The most common form is rutile which is also the most stable form. Anatase and brookite both convert to rutile upon heating [17]. Rutile, anatase and brookite all contain six coordinated titanium.

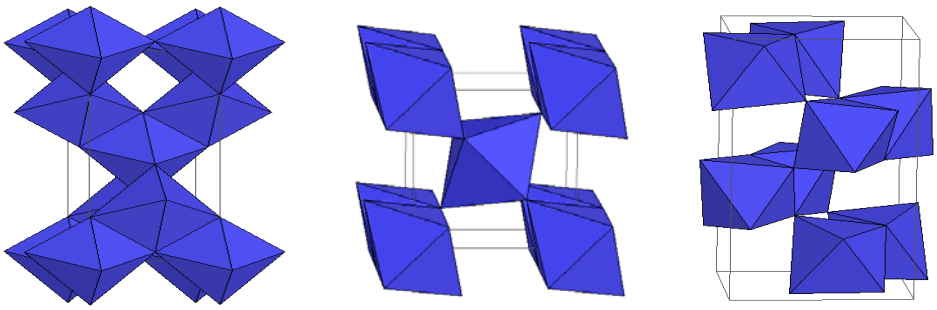

(a) **(b)** **(c)**

Fig. 1.5 Bulk structures of (a) anatase, (b) rutile and (c) brookite

Two different crystal structures of TiO_2, rutile and anatase, are commonly used in photocatalysis, with anatase showing a higher photocatalytic activity [14,15,18]. The structure of rutile and anatase can be described in terms of chains of TiO_6 octahedra. The two crystal structures differ by the distortion of each octahedron and by the assembly pattern of the octahedra chains [19-22]. Although rutile is generally considered the most stable polymorph, differences in the Gibbs free energy of formation between rutile and anatase are small [22,23]. Anatase can be easily obtained by synthesis at low temperature treatments (below 400^{o}C), but rutile frequently starts to appear at moderate temperatures (400–600^{o}C) and it becomes the predominant phase after annealing at higher temperatures [19,22]. The band gaps are 3.2 and 3.0 eV for anatase and rutile, respectively [19,22-27]. Each Ti^{4+} ion is surrounded by an octahedron of six O^{2-} ions. The octahedron in rutile is not regular, showing a slight orthorhombic distortion. The octahedron in anatase is significantly distorted so that its symmetry is lower than that of orthorhombic. The Ti-Ti distances in anatase are greater (3.79 and 3.04 A^{o} vs 3.57 and 2.96 A^{o} in rutile) whereas the Ti-O distances are shorter than in rutile (1.934 and 1.980 A^{o} in anatase vs 1.949 and 1.980 A^{o} in rutile) [28]. In the rutile structure each octahedron

is in contact with 10 neighbor octahedrons (two sharing edge oxygen pairs and eight sharing corner oxygen atoms) while in the anatase structure each octahedron is in contact with eight neighbors (four sharing an edge and four sharing a corner). These differences in lattice structures cause different mass densities and electronic band structures between the two forms of TiO_2. The difference in their photocatalytic activity arises from their different lattice structures and electronic band structures [29,30]. Although rutile has a wide variety of applications primarily in the pigment industry, anatase phase with a band gap of 3.2eV has proven to be most active crystal structure of TiO_2, largely because of its favorable energy band positions and high surface area.

Due to the presence of a small amount of oxygen vacancies, which are compensated by the presence of Ti^{3+} centres, TiO_2 is an n-type semiconductor. The valence band of this material is mainly formed by the overlapping of the oxygen 2p orbitals, whereas the lower part of the conduction band is mainly constituted by the 3d orbitals, with t_{2g} symmetry, of Ti^{4+} cations. The titanium has no electrons in its valence shell when it is in the oxidation state of +4, resulting in an empty t_{2g}-band. The bandgap is the gap between the filled p-band (valence band) and the empty t_{2g}-band (conduction band) [12].

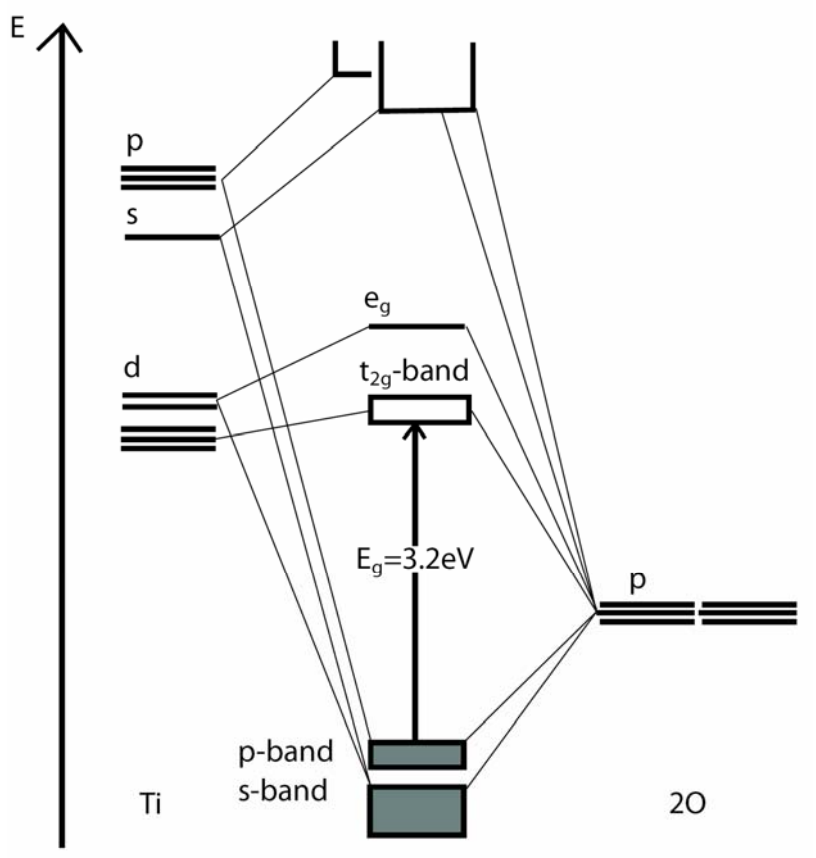

Fig. 1.6 The bonding situation in titanium dioxide (TiO_2)

The empty $t_{2g}$and completely filled p-band of TiO_2 makes it a semi-conductor with a bandgap of 3.2 eV. This is in the ultraviolet region

E = hν, E: energy h: Plank's constant ν: frequency

$\nu = c / \lambda$ c: light speed λ : wavelength

Therefore, $E = hc / \lambda$

1.8 Advantages of TiO_2 as Photocatalyst

TiO_2 has dominated the field of photocatalysis in terms of research, characterization, and applications. The reason for TiO_2's widespread use comes from its moderate band gap, nontoxicity, high surface area, low cost,

recyclability, high photoactivity, wide range of processing procedures, and its excellent chemical and photochemical stability. It should also be noted that TiO_2 is ranked as one of the top 50 most available chemicals.

With a band gap of 3.2eV, a photon would need a wavelength equal to or shorter than 385nm to electronically excite this semiconductor, meaning that it needs UV energy. TiO_2's band gap, although favorable for UV photocatalysis, subjects TiO_2 to low efficiency yields in solar applications (its largest potential market) since less than 5% of the sun's energy is emitted at wavelengths below 385nm. Therefore, whereas the anatase form of TiO_2 is considered an ideal photocatalyst for UV applications, in its unmodified form it is rendered highly inefficient for visible light applications.

Stability is a critical factor in photocatalytic reactions. Metal sulphide semiconductors, for instance, although having a desirably small band gap, are susceptible to photoanodic corrosion due to the energetically unfavorable position of their valance band edge. The photocatalytic lifetime of these semiconductors is therefore extremely short, where the exact time depends on the reaction environment. The ideal photocatalyst should be photochemically stable and therefore insusceptible to any type of corrosion in all reaction environments. ZnO has a similar bandgap to that of TiO_2 as shown in fig. 1.4 and is expected to exhibit similar photocatalytic capacity to that of TiO_2, provided that this property is largely dependent on the energy level of CB and VB. Therefore, it has been comparatively studied with TiO_2 in terms of its photocatalytic performance. The main drawback of ZnO in an aqueous environment is, however, its chemical instability:[31-39]

$$ZnO + 2H_{aq}^{+} \rightleftharpoons Zn_{aq}^{2+} + H_2O$$

$$ZnO + H_2O \rightleftharpoons Zn(OH)_2$$

Hence, the pH range in which ZnO is found to be stable is very limited [40]. The implementation of ZnO photocatalytic systems has not flourished like TiO_2 systems have, mainly because of their unsatisfactory photostability. Under prolonged optical irradiation, ZnO suffers from photodecomposition, which is mainly attributed to the oxidation of ZnO from the solid phase into the aqueous phase by holes [41].

Photocatalytic reactions are usually involved with some form of environmental purification (water, air, etc.), it is considered counterproductive to use toxins such as carcinogens as a means for purification. The largest impact of the problem of toxicity in the field of visible light activated photocatalysis is related to the semiconductor CdS, which is a known carcinogen, mutagen, and irritant. CdS, although unfavourable because of its quick electron-hole pair recombination times, is considered ideal as far as energy band edge positions are concerned. Its band gap (2.5eV) is small enough to absorb green light. TiO_2, on the other hand, has been considered environmentally friendly, adding to its appeal as a photocatalyst. TiO_2 has been used in applications involving both direct and indirect contact with humans with negligible associated health risks.

Ideally, a semiconductor photocatalyst for the purification of water should be chemically and biologically inert, photocatalytically active, easy to produce and use and activated by sunlight. Not surprisingly, no semiconductor perfectly fits this demanding list of requirements, although the semiconductor titanium dioxide, comes close, falling down on its inability to absorb visible light. TiO_2 is having following unique properties:-

- Strong oxidising power
- Non toxicity
- Long term photo stability

- Cost effectiveness
- Biologically and chemically inert

In fact titanium dioxide has a bandgap energy, $E_{bg} \cong 3.2 - 3.0$ eV, and so is only able to absorb UV light (typically < 380 nm) which represents a small fraction, ca. 6%, of the solar spectrum. However, the other very positive features of titanium dioxide as a semiconductor photocatalyst, such as high photoactivity, chemical and photochemical robustness and inexpense, far outweigh its deficient spectral profile overlap with the solar spectrum. As a result, titanium dioxide has become the semiconducting material for research and for use in commercial photocatalytic reactors in the field of semiconductor photocatalysis.

1.9 Visible Light Photocatalyst

The main drawback of TiO_2 photocatalyst is actually the wide bandgap, as it only allows very limited utilization of solar energy. More recently, significant efforts have also been made to develop new or modified semiconductor photocatalysts that are capable of using visible-light (λ = 400–700 nm). These includes metal ion doping [42-45], non-metallic element doping C [46-48], S [49,50], N [51-56] and sensitization with organic dyes or small band-gap semiconductors such as CdS.

Metal ion doping has been primarily studied to enhance the photocatalytic activity under UV irradiation. In recent years, however, extensive research work have been focused on visible-light induced photocatalysis by metal ion-doped semiconductor, since some of these have shown the extended absorption spectra into visible-light region. This property has been explained by the excitation of electrons of dopant ion to the conduction band of semiconductor (i.e., a metal to conduction band charge-transfer). Numerous metal ions, including transition

metal ions (e.g., vanadium, chromium, iron, nickel, cobalt, ruthenium and platinum) and rare earth metal ions (e.g., lanthanum, cerium and ytterbium) have been investigated as potential dopants for visible-light induced photocatalysis. However, metal ion dopant can also serve as a recombination center, resulting in decreased photocatalytic activities.

The studies of visible-light active semiconductors doped with nonmetallic elements such as nitrogen (N), sulphur (S) and carbon (C) have been intensively carried out since the study of N doped TiO_2 by Asahi and coworkers in 2001[51]. It was originally proposed that N doping of TiO_2 can shift its photo-response into the visible region by mixing of p states of nitrogen with 2p states of lattice oxygen and increase photocatalytic activity by narrowing the TiO_2 band-gap. However, more recent studies have shown both theoretically and experimentally that the nitrogen species result in localized N 2p states above the valence band and the electronic transitions from localized N 2p state to the conduction band are made in TiO_2 under visible-light irradiation [57-59]. Unlike metal ion doping, non-metallic dopants replace lattice oxygen and are less likely to form recombination centres.

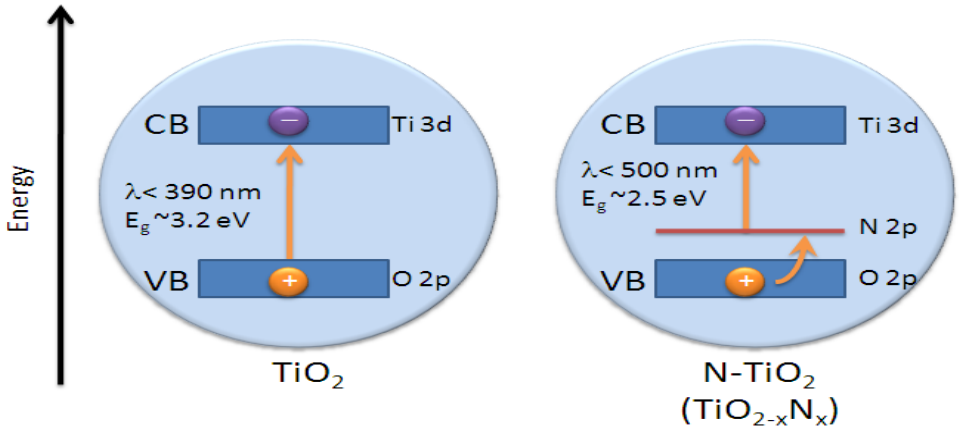

Fig. 1.7 Bandgap of pure and N doped titania

Sensitization methods are widely used to utilize visible-light for energy conversion. In case of sensitization with organic dyes, dye molecule electrons excited by visible light can be injected to the conduction band of semiconductor to initiate the catalytic reactions. Similarly, sensitization is made by coupling a large bandbap semiconductor with a small band-gap semiconductor with a more negative conduction level (i.e., hybrid or composite photocatalyst).

1.10 Synthesis Method for Nanosized Titanium Dioxide

1.10.1 Sol-Gel Method

In a sol-gel process, a colloidal suspension or a sol is typically formed from the hydrolysis and polymerization reactions of the precursors, which are usually inorganic metals salts or metal organic compounds such as metal alkoxides. Complete polymerization and loss of solvent leads to the transition from the liquid sol into solid gel phase. Sol gel method is usually used to synthesise nanosized TiO_2 thin film or powder. This method is generally desirable in synthesis of nanosized TiO_2 due to its better control in particle size, homogeneity in particle distribution and has good adhesion properties. Nanosized TiO_2 have been synthesized with the sol-gel method from acid or base catalyzed hydrolysis of a metal alkoxides [60,61]. This method involves the formation of TiO_2 sol or gel by hydrolysis and followed by condensation of titanium alkoxides. The high hydrolysis rate of titanium alkoxides may cause uncontrolled local precipitation, resulting in decreased photocatalytic activity [62]. Since the study of Larbot *et al*., [63] has shown an excellent control of the hydrolysis rate of titanium alkoxide through esterification reaction. Acetic acid was added to control the hydrolysis, stabilize the sol and preventing the precipitation of TiO_2.

1.10.2 Hydrothermal Method

Hydrothermal method is normally conducted in a steel pressure vessel called autoclaves with or without Teflon (poly-tetrafluoroethylene) liners under controlled temperature and pressures in the presence of aqueous solution. This method offers a lot of advantages to yield high purity nanosized TiO_2 at relatively faster rates under elevated water vapour pressure and temperature with minimum contamination. The moderate temperatures that used in this method of preparation can reduce the energy cost and enhance the reactivity of the nanosized TiO_2.

1.10.3 Solvothermal Method

The solvothermal method is almost identical to the hydrothermal method except the solvent that used in this method is organic media such as methanol, 1,4-butanol or toluene under pressure at low temperature. However, the temperature can be elevated much higher than in the hydrothermal method, since the organic solvents with high boiling point can be chosen. The solvothermal method normally has a better control than hydrothermal method of the size, shape distributions and the crystallinity of nanosized TiO_2. Nanosized TiO_2 can be synthesized through solvothermal method with or without the assistant of surfactants [64].

1.10.4 Chemical Vapour Deposition

Chemical vapour deposition is mainly industrial chemical processes, which is based upon the reaction of vaporizable metal alkoxides with oxygen or steam in the gas phase. These processes are normally used to form coatings to alter the mechanical, electrical, optical, thermal, wear resistance and corrosion resistance properties of various substrates. It usually occurs within a vacuum chamber and thermal energy will heat the gases in the coating

chamber to drive the deposition reaction. As a result, a desired thin film will be deposited on the material [65].

1.11 Factors Affecting Photoactivity

The photocatalytic activity of TiO_2 towards a specific reaction depends on both its physicochemical properties and external conditions. The influential physicochemical properties include the morphology, primary particle size, degree of aggregation, surface area, and crystalline structures, while the external conditions involve the irradiation intensity, the pH of the aqueous system, the presence/absence of electron/hole scavengers, and the bias potential if applied to TiO_2 film photoelectrodes. These factors often interactively affect the overall photocatalytic activity [66].

Particle size, degree of aggregation and surface area determine the adsorption ability of TiO_2 photocatalysts for substrate molecules, which has proved to be a prerequisite for many photocatalytic reactions to proceed efficiently. Most currently used and commercially available photocatalyst powders, consist of nanocrystalline primary particles that are aggregated to form secondary structures with dimensions in the micrometer range. Aggregation of particles would inevitably reduce their total surface area exposed to the outer environment.

The pH of the aqueous environment of the TiO_2 particles appears to be one of the most influential external conditions determining their photocatalytic activity. Apparently, the surface adsorption behavior towards ionic species can be directly modified by changing the pH of the solution: at lower pH, the TiO_2 surface is protonated to be positively charged which favors the adsorption of anionic species from the solution; at higher pH, the surface is negatively charged thus repelling anionic species from approaching the surface [29].

1.12 Advanced Oxidation Processes (AOPs)

Advance oxidation processes (AOPs) are examples of environmental friendly approaches for treating the effluent containing the toxic chemicals, refractory and biodegradable compounds. Typically AOPs are ambient temperature and pressure process that involve in situ generation of highly reactive species such as hydroxyl radical (•OH). The •OH radicals are powerful oxidizing reagents with an oxidation potential of 2.80 V and exhibits faster rates of oxidation reactions as compared to that using conventional oxidants like hydrogen peroxide or $KMnO_4$ [4]. Among AOPs, photocatalytic oxidation (PCO) has proved to be of real interest as efficient tool for degrading aquatic organic contaminants. PCO involves the acceleration of photoreaction in presence of semiconductor photocatalyst. One of the major applications of PCO is heterogeneous photocatalysis to effect total mineralization of liquid phase organic contaminants. The term "photocatalytic degradation" usually refers to complete photocatalytic oxidation or photomineralization, essentially to CO_2, H_2O, NO_3^-, PO_4^{3-} and halides ions [65].

1.13 Objectives of the Present Work

The aim of this research is to develop a photocatalyst with high photoactivity, which is stable and capable of degrading and mineralizing a wide class of organic compounds using visible light. The specific objectives of this research are:

- Preparation of titania by sol–gel route.
- Modification by doping with metals and non metals to provide efficient catalyst systems for the photo degradation of a variety of harmful chemicals including dyes and pesticides.

- Characterisation using a variety of standard techniques including XRD, BET surface area, CHN, SEM, EDX, TEM, FTIR, UV-Vis. DRS, TG and XPS.
- Study of activity of these catalysts towards photocatalysis for the degradation of some dyes like Acid Orange7, Acid Red1, Methylene Blue, Crystal Violet and Acid Blue 25.
- Study of the photocatalytic mineralisation of some pesticides like 2,4-D, Dazomet, Monolinuron, Phosphamidon and 2,4,5-T.
- Evaluation of the degradation of 4-Nitrophenol and Acetophenone in visible light in the presence of the photocatalysts.

References

[1] Huanjun Zhang, Guohua Chen, Detlef W. Bahnemann, J. Mater. Chem., 19 (2009) 5089.

[2] Akihiko Kudo, Catalysis Surveys from Asia, 7 (2003) 31.

[3] Fujishima, T.N. Rao, D.A. Tryk, J. Photochem. Photobiol. C,1 (2000) 1.

[4] Fujishima, K.Honda, Nature, 238 (1972) 37.

[5] A. Mills, S. Le Hunte, J. Photochem. Photobiol. A, 108 (1997)1.

[6] Y. Xu, M. Schoonen, American Mineralogist, 85 (2000) 543.

[7] Roland Benedix, Frank Dehn, Jana Quaas, Marko Orgass, Lacer No.5 (2000)157.

[8] Y .Goswami, Advances in Solar Energy, 10 (1995) 165.

[9] A. Fujishima, T.N Rao, D.A. Tryk, J. Photochem. Photobiol. C. Photochemistry Reviews, 1 (2000) 1.

[10] Akihiko Kudo, Pure Appl. Chem., 79(2007)1917.

[11] B.Viswanathan, Bull. Catal. Soc. India, 2 (2003) 71.

[12] J. F. M. Oudenhoven, F. J. E. Scheijen, M. Wolffs, Chemistry of Catalytic System 2: Photocatalysis, (2004) 1

[13] L. Linsebigler, Guangquan Lu, John T. Yates, Chem. Rev.,95 (1995) 735

[14] G. Magesh, B. Viswanathan, R. P. Viswanath, T. K. Varadarajan. Photo/ Electrochemistry & Photobiology in the Environment. Energy and Fuel, (2007).

[15] D. Marıa, Hernandez-Alonso, Fernando Fresno, Silvia Suareza, Juan M. Coronado, Energy Environ. Sci., 2 (2009) 1231.

[16] O. Carp, C. L. Huisman, A. Reller, Prog. Solid State Chem., 3 (2004) 33.

[17] Greenwood, N. Norman, A. Earnshaw, Chemistry of the Elements, Oxford: Pergamon., (1984) 1117.

[18] Augustynski, J. Electrochem. Acta., 38(1993)43.

[19] J. Maira, K. L.Yeung, C. Y. Lee, P. L. Yue , C. K. Chan, J. Catal., 192 (2000) 185.

[20] L. Linsebigler, G. Lu, J. T. Yates, Chem. Rev., 95 (1995)735.

[21] T. L. Thompson, J. T. Yates, Chem. Rev., 106 (2006) 4428.

[22] X. Chen, S. S. Mao, Chem. Rev., 107 (2007) 2891.

[23] H. Z. Zhang, J. F. Banfield, J. Phys. Chem. B, 104 (2000) 3481.

[24] J. M. Herrmann, Catal. Today, 53 (1999) 115.

[25] M. R. Hoffmann, S. T. Martin, W. Choi, D. W. Bahnemann, Chem. Rev., 95(1995) 69.

[26] A. Mills, S. Le Hunte, J. Photochem. Photobiol. A, 108 (1997)1.

[27] A. Fujishima, T. N. Rao, D. A. Tryk, J. Photochem. Photobiol. C, 1 (2000) 1.

[28] J. K. Burdett, T. Hughbands, J. M. Gordon, J. W. Richardson, J. V. Smith, J. Am. Chem. Soc., 109(1987)3639.

[29] Huanjun Zhang, Guohua Chen, Detlef W. Bahnemann, J. Mater. Chem., 19 (2009) 5089.

[30] L. Linsebigler, G. Q. Lu, J. T. Yates, Chem. Rev., 95 (1995)735.

[31] M. Gratzel, Nature, 414(2001) 338.

[32] C.Richard, New J. Chem., 18(1994) 443.

[33] A. Khodja, T. Sehili, J. F. Pilichowski, P. Boule, J. Photochem. Photobiol. A-Chem., 141(2001) 231.

[34] L. Q. Jing, B. F. Xin, F. L. Yuan, B. Q. Wang, K. Y. Shi, W. M. Cai, H. G. Fu, Appl. Catal. A-Gen., 275(2004) 49.

[35] O. Seven, B. Dindar, S. Aydemir, D. Metin, M. A. Ozinel, S. Icli, J. Photochem. Photobiol. A-Chem., 165 (2004) 103.

[36] N. Daneshvar, D. Salari, A. R. Khataee, J. Photochem.Photobiol. A-Chem., 162 (2004) 317.

[37] S. Sakthivel, B. Neppolian, M. V. Shankar, B. Arabindoo, M. Palanichamy, V. Murugesan, Sol. Energy Mater. Sol. Cells, 77 (2003) 65.

[38] M. C. Yeber, J. Rodriguez, J. Freer, N. Duran, H. D. Mansilla, Chemosphere, 41 (2000) 1193.

[39] L. Amalric, C. Guillard, P. Pichat, Res. Chem. Intermed., 20 (1994) 579.

[40] W. Bahnemann, C. Kormann , M. R. Hoffmann, J. Phys. Chem., 91 (1987) 3789.

[41] A. Fujishima, T. Kato, E. Maekawa, K. Honda, Bulletin of The Chemical Society of Japan, 54 (1981) 1671.

[42] M. Anpo, I. Y. Chihashi, M. Takeuchi, H. Yamashita, Res. Chem. Intermed., 24 (1998) 143.

[43] W. Y .Choi, A. Termin, M. R. Hoffmann, Angew. Chem. Int. Ed., 33 (1994) 1091.

[44] W. Y .Choi, A.Termin, M. R. Hoffmann, J. Phys. Chem., 98 (1994) 13669.

[45] X. Z. Li, F. B. Li, Environ. Sci. Technol., 35 (2001) 2381.

[46] S. Sakthivel, H. Kisch, Angew. Chem. Int. Ed., 42 (2003) 4908.

[47] S. U. M .Khan, M.A l. Shahry, W. B. Ingler, Science, 297(2002) 2243.

[48] Y. Nakano, T. Morikawa, T. Ohwaki, Y. Taga, Appl. Phys. Lett., 87 (2005) 52111.

[49] T. Umebayashi, T. Yamaki, H. Itoh, K. Asai, Appl. Phys. Lett., 81 (2002) 454.

[50] T. Umebayashi, T. Yamaki, S .Tanaka, K. Asai, Chem. Lett., 32 (2003) 330.

[51] R. Asahi, T. Morikawa, T. Ohwaki, K. Y .Aoki, Taga, Science, 293 (2001) 269.

[52] X. B. Chen, C.Burda, J. Phys. Chem. B, 108(2004) 15446.

[53] Di Valentin, C. Pacchioni, G. A. Selloni, Phys. Rev. B, 70(2004).

[54] J.Y. Lee, J. Park, J. H. Cho, Appl. Phys. Lett., 87(2005) 56.

[55] S. Sato, R. Nakamura, S. Abe, Appl. Catal. A, 284(2005) 131.

[56] M. Mrowetz, W. Balcerski, A. J. Colussi, M. R. Hoffman, J. Phys. Chem. B, 108(2004) 17269

[57] M.Batzill, E. H.Morales, U.Diebold, Phys. Rev. Lett., 96(2006).

[58] S. Livraghi, M. C. Paganini, E. Giamello, A. Selloni, C. Di Valentin, G. Pacchioni, J. Am. Chem. Soc.,128(2006) 15666.

[59] C. Di Valentin, G. Pacchioni, A. Selloni, S. Livraghi, E. Giamello, J. Phys. Chem. B, 109 (2005) 11414.

[60] Y. Bessekhouad, D .Robert, J. V. Weber, J Photochem Photobiol A Chem., 157 (2003) 47.

[61] A .Chemseddine, T. Moritz, Eur J. Inorg. Chem., 2 (1999) 235.

[62] J.F. Zhu, J.L. Zhang, F. Chen, M.Anpo, Mater Lett., 59 (2005) 3378.

[63] A. Larbot, I. Laaziz, J. Marignan, J.F. Quinson. J Non-Cryst Solids, 147-148 (1992) 157.

[64] S.W. Yang, L.Gao, Mater Chem Phys., 99 (2006) 437.

[65] Sze M. Lam, Jin C. Sin, Abdul R. Mohamed, Recent Patents on Chemical Engineering, 1 (2008) 209.

[66] M. R. Hoffmann, S. T. Martin, W. Y. Choi , D. W. Bahnemann, Chem. Rev., 95 (1995) 69.

.....ꕥ.....

Chapter

2

Materials and Experimental Methods

Contents

Catalyst characterization is the most important part of a catalytic research. Since heterogeneous catalytic reactions begin with the adsorption of reactant on the surface of the catalyst, the study of the catalyst surface is important. The information obtained from the characterization process can help in understanding the relationship between the catalytic behaviour and the composition and structure of the catalyst. However, although many characterization techniques can provide valuable results on the catalyst properties, the most useful and meaningful information always comes from a combination of several characterization techniques.

2.1 Introduction

The experimental work in this study can be divided into three (3) major stages.

i) Catalysts preparation

ii) Catalysts characterization

iii) Photocatalytic activity measurements

In this chapter, the experimental procedure and the different characterisation techniques used are presented.

2.2 Catalyst Preparation

TiO_2 doped with metals and non metals are prepared through sol-gel technique. Pure titania was also prepared in order compare with the doped catalysts.

2.3 Materials Used

Materials	Company
Titanium tetra isopropoxide	Sigma Aldrich
Urea	Merck
Thiourea	Merck
Ethanol	Merck
Nitric acid	Merck
Silver nitrate	Merck
Ammoniumhepta molybdate tetrahydrate	Merck
Methylene Blue	Sigma Aldrich
Acid Orange 7	Sigma Aldrich
Acid Red1	Sigma Aldrich
Acid Blue 25	Sigma Aldrich
Crystal Violet	Sigma Aldrich
2,4 –Dichloro phenoxy acetic acid	Sigma Aldrich
2,4 ,5–Trichloro phenoxy acetic acid	Sigma Aldrich
Monolinuron	Sigma Aldrich
Phosphamidon	Sigma Aldrich
Dazomet	Sigma Aldrich
Acetophenone	Merck
4-Nitrophenol	Merck

2.4 Method of Preparation

2.4.1 Preparation of nitrogen doped titania.

Nitrogen doped TiO_2 catalyst was prepared through sol gel method using Titanium isopropoxide(TTIP) and urea [1]. In this method titanium isopropoxide and urea was taken in the mole ratio 1:5. The urea solution was added drop wise to a mixture of titanium isopropoxide and ethanol. After stirring for 24 hours at room temperature it was dried at 60^oC and then calcined at 400^oC for 4 hours. The same procedure was adopted to synthesise N doped catalysts with TTIP : urea in the mole ratio 1:2 and 1:10.

2.4.2 Preparation of nitrogen and sulphur codoped titania.

Sol gel method was used to prepare N-S codoped TiO_2. Instead of urea, thiourea was used to prepare N-S codoped titania [2].Three different catalysts with TTIP : thiourea in the mole ratio 1:2, 1:5 and 1:10 were prepared. Pure titania catalyst was also prepared to compare the results with the doped one.

2.4.3 Preparation of metal doped titania

The metal doped photocatalysts with different metal concentrations (metal load- 0.5, 1.0, and 3.0 wt%) were prepared by the sol–gel method as follows. Titanium isopropoxide, ammonium heptamolybdate tetrahydrate and silver nitrate were used as precursors. 12.5 ml of TTIP was dissolved in 25 ml of absolute alcohol with stirring for 10 minutes; then 0.25 ml of HNO_3 was added dropwise to the above solution under stirring for 30 minutes. Another solution containing metal salt in the required stoichiometry was slowly added into the above solution, stirred for two hours and the transparent sol was obtained. The gel was prepared by aging the sol for 24 hours at room temperature. The gel was dried at 60^oC. The dried solids were ground in an agate mortar until fine and homogeneous powder was obtained. Before

characterization, all the samples were calcined in air at 400^{o}C for 4 hours. Thus Mo and Ag, doped titania catalysts were prepared [3].

2.5 Catalyst Notations

Silver doped TiO_2(0.5wt%Ag)	AgT1
Silver doped TiO_2(1wt%Ag)	AgT2
Silver doped TiO_2 (3wt%Ag)	AgT3
Molybdenum doped TiO_2(0.5wt%Mo)	MoT1
Molybdenum doped TiO_2(1wt%Mo)	MoT2
Molybdenum doped TiO_2(3wt%Mo)	MoT3
N dopedTiO_2(TTIP:Urea 1:2mole ratio)	U1
N dopedTiO_2(TTIP:Urea 1:5mole ratio)	U2
N dopedTiO_2 (TTIP:Urea 1:10mole ratio)	U3
N-S codoped TiO_2(TTIP:thiourea 1:2mole ratio)	TU1
N-S codoped TiO_2(TTIP:thiourea 1:5mole ratio)	TU2
N-S codoped TiO_2(TTIP:thiourea 1:10mole ratio)	TU3
Undoped titania	T

2.6 Characterization Tools

Catalyst characterization is the most important part of a catalytic research. The information obtained from the characterization process can help in understanding the relationship between the catalytic behaviour and the composition and structure of the catalyst. However, although many characterization techniques can provide valuable results on the catalyst properties, the most useful and meaningful information almost always comes from a combination of several characterization techniques [4].

In this research, the structural, chemical and optical properties of the catalysts were investigated. Characterization techniques such as X-ray Diffraction Analysis(XRD), BET surface Area, UV-Vis Diffuse Reflectance Spectroscopy(UV-Vis.DRS), CHNS Elemental analysis, Scanning Electron Microscopy(SEM), Energy Dispersive X-ray Analysis(EDX), Transmission Electron Microscopy(TEM), Fourier Transform Infrared Spectroscopy(FTIR), X-ray Photoelectron Spectroscopy(XPS) and Thermogravimetric Analysis (TG) were employed. The extent of phoyocatalytic degradation was tested using UV–Visible spectrophotometer and mineralization was examined by measuring the Total Organic Carbon (TOC) in the solution.

2.6.1 X-ray Diffraction Analysis (XRD)

X-ray diffraction is a versatile, non-destructive technique, used for identifying the crystallographic phases present in solid materials and powders and for analyzing structural properties. The main applications of XRD analysis include characterization of crystalline materials, determination of unit cell dimensions and measurement of sample purity. It is one of the oldest and most frequently applied techniques in catalyst characterization.

X-ray diffractometer is not limited to just measuring crystalline materials. It can also be used to investigate amorphous materials despite the fact that these do not give sharply defined peaks. X-ray diffraction works on the principle that X-rays form predictable diffraction patterns when interacting with a crystalline matrix of atoms. The diffraction patterns can easily be converted into information about the location of atoms within the matrix and from those positions, the exact crystalline structure can be determined.

The Powder Xray Diffractometer utilises an X ray source that is aimed at the sample, a detector that is also pointing at the sample, and these

components move so that a wide range of diffraction angles (2θ) is scanned. During a typical experiment the sample position is fixed while the source and detector scan a specified range of angles typically 5 to 70 degrees (2θ) for analysis. The scan rate is chosen to provide the desired quality of results; slower scans provide high quality results than faster.

X Rays of the incident beams are in phase when they reach the sample. Some rays reflect off the first plane, others of the second and other parallel planes and these will reemerge from the sample if they are in phase. This will only happen when the incident angle and interplanar spacing are such that the path difference travelled by each ray is equal to the integral values of wavelength. When X ray beam hits the sample and diffracted, we can measure the distance between the planes of the atoms that constitute the sample by applying Bragg's law $n\lambda=2d\sin\theta$, where n is the order of diffraction λ is the wavelength of incident X ray beam d is the distance between adjacent planes of atoms and θ is the angle of incidence. This law relates the wavelength of electromagnetic radiation to the diffraction angle and the lattice spacing in a crystalline sample. These diffracted X-rays are then detected, processed and counted. By scanning the sample through a range of angles, all possible diffraction directions of the lattice should be attained due to the random orientation of the powdered material.

The crystal phases of the catalysts were determined by X-ray diffraction (XRD) analysis. XRD patterns of the samples were obtained using Bruker AXS D8 advance X ray diffractometer using CuKα radiation. Data were collected over the angle of 2θ between 10° to 70° [5]. Crystallite size was determined by using Scherrer's equation [6-10]

$$D=0.9\lambda/\beta(\Pi/180)\cos\theta.$$

where D is the crystallite size λ is the wavelength of X ray radiation, β is the full width of half maximum and θ is the diffraction angle.

2.6.2 Surface Area Measurements

The surface area is an important property of a material in catalysis applications. The ability to measure surface area is hence extremely important in comparing and evaluating materials for these applications as it can influence their effectiveness and reactivity. The BET method is the most common one for measuring surface area of materials and involved in measuring how much gas is adsorbed onto the surface of the material in question; normally nitrogen gas is used for this purpose [10-12].

BET theory aims to explain the physical adsorption of gas molecules on a solid surface and serves as the basis for an important analysis technique for the measurement of the specific surface area of a material. In 1938, Stephen Brunauer, Paul Hugh Emmett, and Edward Teller published an article about the BET theory in a journal for the first time; "BET" consists of the first initials of their family names.

The concept of the theory is an extension of the Langmuir theory, which is a theory for monolayer molecular adsorption, to multilayer adsorption with the following hypotheses: (a) gas molecules physically adsorb on a solid in layers infinitely; (b) there is no interaction between each adsorption layer; and (c) the Langmuir theory can be applied to each layer. The resulting BET equation is expressed by (1):

$$P / [V(P_0-P)] = 1/V_mC + [(C-1)/V_mC][P/P_0] \quad \text{---------- (1)}$$

P and P_0 are the equilibrium and the saturation pressure of adsorbates at the temperature of adsorption, V is the adsorbed gas quantity (in volume units), and V_m is the monolayer adsorbed gas quantity. C is the BET constant.

Equation (1) is an adsorption isotherm and can be plotted as a straight line with P/[V(P_0-P)] on the y-axis and P/P_0 on the x-axis according to experimental results. This plot is called a BET plot. The linear relationship of this equation is maintained only in the range of $0.05 < P / P_0 < 0.35$. The value of the slope and the y-intercept of the line are used to calculate the monolayer adsorbed gas quantity V_m and the BET constant C. The specific surface area is given by the equation

$$SA\ (BET) = V_m A_m N_0 / W \times 22414$$

Where N_0 is the Avogadro number A_m is the molecular cross sectional area of the adsorbate (0.162nm^2 for nitrogen) and W is the weight of the sample [13].

BET Surface area was measured using Micrometritics Tristar 3000 surface area analyzer. The samples were activated at 90^{o}C for 30 minutes and degassed at 350^{o}C for 4 hours.

2.6.3 UV-Visible Diffuse Reflectance Spectroscopy (UV-Vis. DRS)

Diffuse reflectance is an excellent sampling tool for powdered or crystalline materials. This technique is useful in determining the absorption edge of the catalyst. It gives information regarding electronic transition between orbitals or bands in the case of atoms, ions or molecules. Electronic transitions may be classified as metal centered transitions [d-d or (n-1)d-ns] and charge transfer transitions.

TiO_2 is a semiconductor with a large band gap, therefore the optical band gap E_{bg} can be determined. The reflectance (R) data were obtained from the optical spectra. Here the influence of doping on the electronic spectrum was studied by diffuse reflectance spectroscopy [10,14].

The UV- DRS were obtained in the range 300-800nm on Labomed UV VIS DOUBLE BEAM UVD 500 Spectrophotometer equipped with an integrating sphere assembly using $BaSO_4$ as reflectance standard. The wavelength at the onset of reflection was taken and band gap was calculated using the equation $E_{bg}=1240/\lambda$. where λ is the wavelength in nanometer [15-17].

2.6.4 CHNS Analysis

This technique determines the presence of the elements like carbon, hydrogen, nitrogen and sulphur in a given substance and gives the result as percentage amount of these atoms against the total weight. Since this technique specifically determines these four elements this instrument is called as "CHN/S Analyzer"

In this technique the substance under study is combusted under oxygen stream in a furnace at high temperatures. The end products of the combustion would be mostly the oxides of the concerned elements in the form of gases. These are then separated and carried to the detector using inert gases like helium or argon. It is one of the few analytical techniques that give a clear quantitative measurement of the carbon, hydrogen, nitrogen and sulphur[18].

The CHNS elemental analysis is mainly applicable for organic compounds and inorganic complexes. In the present work the percentage of nitrogen and sulphur in the prepared catalysts was determined by CHNS analysis. The elemental analysis was performed on Elementer Vario EL III CHN analyzer.

2.6.5 Scanning Electron Microscopy (SEM)

Electron microscopes are instruments that use a beam of highly energetic electrons to examine objects on a very fine scale. This examination can yield information on the topography of samples (surface feature) and morphology the sample (shape and size).

The Scanning Electron Microscope (SEM) produces images by scanning the surface of a specimen with a beam probe of electrons, which is synchronized in a rastering pattern with the electron beam of a cathode ray tube (CRT or television picture tube). Low energy secondary electrons produce a signal that is strongly influenced by topography. When this signal is displayed on the CRT, the resulting image can be interpreted as a three dimensional representation of the specimen surface. It should be noted that the SEM image shows mainly outer surface detail and texture but not the interior detail. The instrument comprises of a heated filament as source of electron beam, condenser lenses, aperture, evacuated chamber for placing the sample, electron detector, amplifier, CRT with image forming electronics, etc. Scanning electron microscopy has been applied to the surface studies of metals, ceramics, polymers, composites and biological materials for both topography as well as compositional analysis [13].

In this study the surface morphology of the catalysts are characterized using SEM. The SEM micrographs of the samples were taken using JOEL Model JSM -6390LV scanning electron microscope with a resolution of 1.38eV

2.6.6 Energy Dispersive X-ray Analysis (EDX)

EDX is used to confirm the existence of dopants in the thin films. By elemental analysis data conducted using EDX can be used to detect the existence of dopants in the catalyst. All dopants, which were not detectable in

the XRD analysis, were observed by EDX. This is because the percentage amount of elements given in the EDX data represent the total amount of that individual element in the sample. No information on the type of species that a particular element formed can be extracted from the data. EDX spectra of the samples were recorded in a JOEL Model JED-2300 instrument

2.6.7 Transmission Electron Microscopy (TEM)

Transmission electron microscopy has been used extensively for measuring the size of small metal particles. The electron microscope uses an electron beam; the electron gun consists of a tungsten anode and beam aperture control. An electron lens system can focus the electron beam with very narrow cross section at the point where it strikes the specimen. The transmitted electrons pass through another set of electron optics to finally fall on a fluorescent screen where the image is produced and can be recorded on a photographic film [13].

TEM pictures give the particle size and their distribution. The image is projected on a screen and the particles in different size range are counted .The size distribution in the measured range can be plotted as a histogram. The high resolution TEM images provide the actual morphology with accurate particle size and phase purity.

The TEM analysis was carried out in an ultra high resolution analytical electron microscope JOEL3010

2.6.8 Fourier Transform Infrared Spectroscopy (FTIR)

The vibrational energy levels of a molecule can be studied by infrared spectroscopic method. In FTIR Spectroscopy sample is exposed to all frequencies at the same time, the source used is not monochromatic and all the

wave numbers are simultaneously used, it is much faster and the time domain spectrum is converted to a frequency domain spectrum by Fourier transform.

In FTIR, the un-dispersed light beam is passed through the sample and the absorbance at all wavelengths is received at the detector simultaneously. A computerized mathematical manipulation (known as "Fourier Transform") is performed on this data, to obtain absorption data for each and every wavelength. To perform this type of calculations interference of light pattern is required for which the FT-IR instrumentation contains two mirrors, one fixed and one moveable with a beam splitter in between them. Before scanning the sample a reference or a blank scanning is required.

Since most FTIR spectra of the adsorbed molecules are recorded in the transmission mode, sample preparation needs some care .The finely powdered sample is prepared in the form of a thin self-supporting wafer. It should be thin to transmit enough radiation and at the same time should contain enough catalysts to hold a sufficient number of adsorbed molecules. Infrared spectroscopy has variety of applications in catalysis. Determination of bulk structure of the catalysts, information of some of the peculiarities of the surface such as the presence of surface hydroxyl groups can be obtained .The study of Bronsted and Lewis acidity of solids is also another application of IR spectroscopy. The FTIR Spectra of samples were recorded through Thermo Nicolet AVATAR 370 DTGS model FTIR with KBr pellets in the range 400-4000cm^{-1} [12, 13].

2.6.9 X-Ray Photoelectron Spectroscopy (XPS)

X-ray photoelectron spectroscopy (XPS) has long been recognized as a primary tool for the detection of chemical species at the surface of solids. This technique allows direct characterization of the catalyst surface. It gives

information on the elemental composition and oxidation states of the elements on the solid surface before and after reaction test.

XPS is based on the photoelectric effect. Kinectic energy E_K of an electron emitted from an atom present in a gaseous molecule is given as

$$E_K = h\nu - E_B.$$

where $h\nu$ is the photon energy and E_B is the binding energy of electron. When atom in a molecule or solid absorbs photon, ionization and the emission of a core (inner shell) electron with a specific binding energy occurs. The kinetic energy distribution of the emitted photoelectrons can be measured using any appropriate electron energy analyzer and a photoelectron spectrum can thus be recorded. The XPS obtained is a plot of peak intensities versus binding energy, E_B. For each and every element, there will be a characteristic binding energy associated with each core atomic level [13].

The presence of peaks at particular energies indicates the presence of a specific element in the sample under study. The intensity of the peaks is also related to the concentration of the element within the sample. As the electron binding energies are dependent on the chemical environment of the atom, XPS can provide chemical bonding information as well [19].

XPS data were recorded in an indigenously developed electron spectrometer equipped with Thermo VG Clamp-2 Analyser and a Mg Kα X-ray source (1253.6 eV, 30mA × 8 kV). A thin sample wafer of 12 mm in diameter was used in these studies. As an internal reference for the absolute binding energy of C 1s peak at 284.6 eV was used.

2.6.10 Thermogravimetric Analysis (TG)

Thermogravimetric Analysis finds its application in finding the purity, integrity, crystallinity and thermal stability of the chemical substances under study. Sometimes it is used in the determination of the composition of complex mixtures. In this technique the change in sample weight is measured while the sample is heated at a constant rate (or at constant temperature), under air (oxidative) or nitrogen (inert) atmosphere. It is commonly used to determine the absorbed moisture content, calcination temperature and stability limit of the catalyst.

In TG analysis the sample is placed in a sample pan which is attached to a sensitive microbalance assembly and is subsequently placed into high temperature furnace. The balance measure the initial sample weight at room temperature and then continuously monitors changes in sample weight as heat is applied to samples. From the thermogram, information about dehydration, decomposition of various forms of products at various temperatures can be obtained.

The TG analysis were done on a Perkin Elmer Pyris Diamond thermogravimetric/differential thermal analyser by heating the samples at a rate of 10^{o}C /min from room temperature to 800^{o}C in nitrogen atmosphere with samples mounted on a platinum sample holder [12].

2.7 Photocatalytic Activity Studies

Photocatalytic activity of the prepared samples was measured by studying the degradation of different dyes and pesticides in aqueous solution. The major advantage of these systems is that they are able to achieve the degradation of organic pollutants by using visible light under ambient conditions [20]. The experiment was carried out using an Oriel Uniform

Illuminator 150 W Xe ozone free lamp with filters. 280-420nm dichoric mirror for UV light, and 420-630nm dichoric mirror (cold mirror) for visible irradiation were used.

Dyes (Methylene Blue, Acid Orange 7, Acid Blue 25, Crystal Violet and Acid Red1) pesticides (2,4–Dichlorophenoxyacetic acid, 2,4,5–Trichlorophenoxy acetic acid, Monolinuron, Phosphamidon and Dazomet) Acetophenone, 4-Nitrophenol were selected as pollutants for the photocatalytic degradation.

The studies were carried out by taking 10 ml of 10^{-4} M solution of dyes and 1g/L of catalyst. The solution was stirred for 30 minutes before irradiation to attain the adsorption desorption equilibrium. After irradiation the solution was centrifuged and percentage degradation was studied by measuring the absorbance using a SPECTRASCAN UV 2600 DOUBLEBEAM UV VIS spectrophotometer [21,22].

The effect of time, catalyst concentration, dopants on the percentage degradation was studied. In the case of pesticides, acetophenone and 4-nitrophenol the percentage mineralisation was studied using TOC analysis [23-25].

2.8 TOC Analysis

The element carbon is the most common form that can be found everywhere. Its measurement at trace levels is very important, especially, in the fields of environmental pollution. Among these, monitoring the organic compounds in the environment is important, since inorganic carbon constitutes to only a lesser extent having its presence with carbonates, bicarbonates and dissolved carbon dioxide. Hence, it is customary to find out the presence of

carbon as Total Organic Carbon, which represents the quantity of carbon present in water as organic matter, either dissolved or suspended [26].

TOC is a measure of the amount of carbon in a sample originating from organic matter only. The test is run by burning the sample and measuring the CO_2 produced. The principle of the TOC involves complete oxidation of carbonaceous materials to carbon dioxide and water by catalytic combustion or by chemical oxidation. The released carbon dioxide is measured using an IR detector since this molecule strongly absorbs in the IR region. In cases, wherein the measurement of inorganic carbon is necessitated then it is done within the same instrument by purging air through the sample placed in acid solution. This will create the formation of carbon dioxide and water from the inorganic carbonates and bicarbonates. A typical analysis for TOC measures both the total carbon present as well as the so called "inorganic carbon" (IC), the latter representing the content of dissolved carbon dioxide and carbonic acid salts. Subtracting the inorganic carbon from the total carbon yields TOC.

References

[1] D. Klauson, E. Portjanskaja, S. Preis, Environ. Chem .Lett ., 6 (2008) 35.

[2] Xiang Li, Rongchun Xiong, Gang Wei, Catal Lett., 125 (2008) 104.

[3] Jinkai Zhou, Yuxin Zhang, X.S. Zhao, Ajay K. Ray, Ind. Eng. Chem. Res., 45 (2006) 3503.

[4] H. Kominami, Y. Ishi, M. Kohno, S. Konishi, Y. Kera, B .Ohtani, Catal. Lett., 91(2003)41.

[5] D. dela Cruz Romero, G. Torres Torres, J. C. Arevalo , R. Gomez, A. Aguilar Elguezabal, J. Sol-Gel Sci Technol., 56 (2010)219.

[6] Veda Ramaswamy, Preeti Awati, A.V. Ramaswamy, Topics in Catalysis, 38 (2006) 251.

[7] T. Lopez, J. A. Moreno, R. Gomez, X. Bokhimi, J. A. Wang, H. Yee-Madeira,G. Pecchic, P. Reyesc, J. Mater. Chem., 12 (2002) 714.

[8] Horst Kisch, Shanmugasundaram Sakthivel, Marcin Janczarek, Dariusz Mitoraj, J. Phys. Chem. C, 111 (2007) 11445.

[9] Neelam Jagtap, Mahesh Bhagwat, Preeti Awati, Veda Ramaswamy, Thermochimica Acta., 427 (2005) 37.

[10] Freddy E. Oropeza, J. Harmer, R. G. Egdell, Robert G. Palgrave, Phys. Chem. Chem. Phys., 12(2010) 960.

[11] R. Sasikalaa, V. Sudarsana, C. Sudakarb, R. Naikb, L. Panickerc, S.R. Bharadwaja, International Journal of hydrogen energy, 34 (2009) 610 5.

[12] Xiaoqing Qiu, Liping Li, Jing Zheng, Junjie Liu, Xuefei Sun, Guangshe Li, J. Phys. Chem. C, 112(2008) 12242.

[13] D.K.Chakrabarthy, B.Viswanathan, Heterogeneous catalysis New age international (2007).

[14] Huaming Yang, Xiangchao Zhang, J. Mater. Chem., 19(2009) 6907.

[15] Horst Kisch, Shanmugasundaram Sakthivel, Marcin Janczarek, Dariusz Mitoraj J. Phys. Chem. C, 111 (2007) 11445.

[16] Aditi, Fernandes, Bulletin of the Catalysis Society of India, 4 (2005) 131.

[17] A.R. Gandhe, J.B. Fernandes, Journal of Solid State Chemistry, 178 (2005) 2953.

[18] Studies on photocatalysis by titania doped with non-metals, PhD thesis K.M Rajesh.

[19] Jun Zhang, Chunxu Pan, Pengfei Fang, Jianhong Wei, Rui Xiong, Applied Materials & interfaces,2(2010) 1173 .

[20] Chuncheng Chen, Wanhong Ma, Jincai Zhao, Chem. Soc. Rev., 39 (2010) 4206.

[21] S.F. Villanueva, S. S. Martınez, Solar Energy Materials & Solar Cells, 91 (2007) 1492.

[22] Mohamed Mokhtar Mohameda, Mater M. Al-Esaimi, Journal of Molecular Catalysis A: Chemical, 255 (2006) 53.

[23] Kan Wang, Jianying Zhang, Liping Lou, Shiying Yang, Yingxu Chen, Journal of Photochemistry and Photobiology A: Chemistry, 165 (2004) 201.

[24] Ioannis K. Konstantinou, Triantafyllos A. Albanis, Applied Catalysis B: Environmental, 49 (2004) 1.

[25] M. Qamar, M. Muneer, D. Bahnemann, Journal of Environmental Management, 80 (2006) 99.

[26] www.wikipedia .org

.....ഌ൹.....

Chapter

3

Results and Discussions

Contents

Characterization of the catalysts was conducted using XRD, BET surface area CHNS, XPS, SEM, EDX, TEM, FTIR and UV-Vis.DRS. Each individual technique gives information on different properties of the catalyst such as crystallinity of the catalyst, the elemental composition, oxidation states, absorption properties and the band gap values. However, the integration of all the data obtained could give overall information on the properties of a good catalyst.

3.1 Introduction

This chapter focuses on the catalyst characterization elaborating on the identification of the phase structure, surface area, elemental analysis, surface morphology, absorption properties (UV-Vis) and band gap of the prepared catalysts. Characterization was conducted on all catalyst samples. All the characterizations were carried out on the catalyst samples before photoreaction.

Metal-doping of TiO_2 has been extensively explored as a way to improve photoactivity under visible light [1-5]. Some metal elements such as Mo and Ag have been employed to tune the electronic structure and enhance the photocatalytic activity of TiO_2. However in some cases metal doping can result in thermal instability and increasing career trapping which may decrease the photocatalytic efficiency [6-8].

On the other hand, doping of TiO_2 with nonmetals is another widely used approach to increase the photocatalytic activity. Recently many efforts have been made to modify TiO_2 with non-metals such as B, C,N,S and F to efficiently extend the photo response from UV to visible light region [9-11].In this work an attempt have been made to modify TiO_2 with non metals such as N and S.

Doping with suitable transition metal ions allows extending the light absorption of large band gap semiconductors to the visible region. A comparison of the results reported in the literature for doped samples is not easy because the experimental conditions under which the runs are carried out and the preparation methods of the samples are usually different. Moreover, it is well known that bare anatase and rutile TiO_2 samples also show very different photoactivities, depending on their electronic and surface physicochemical properties. Nevertheless, it is worth pointing out that the

photoactivity cannot be straight forwardly related to only few properties because it depends on all of them [12].

TiO_2 powders doped with some metals (molybdenum, silver) and non metals(nitrogen, nitrogen-sulphur) have been prepared by solgel method. The samples have been characterized by X-ray Diffraction Analysis (XRD), BET surface Area, UV-Vis Diffuse Reflectance Spectroscopy (UV Vis.DRS), CHNS Elemental analysis, Scanning Electron Microscopy (SEM), Energy Dispersive X-ray Analysis (EDX), Transmission Electron Microscopy (TEM), X-ray Photoelectron Spectroscopy(XPS), Fourier Transform Infrared Spectroscopy (FTIR), and Thermogravimetric Analysis(TG) .

3.2 Optimization of Catalysts

In this work Mo and Ag doped catalysts with different metal concentrations (0.5, 1,3wt %) were prepared. Nonmetal doped catalysts were also prepared using sol gel method. Urea, ammonium chloride, liquid ammonia, nitric acid, ammonium carbonate and triethylamine, thiourea and ammonium fluoride were used as sources of dopant. They are characterised by different techniques such as CHNS, UVDRS, and XRD. From these we selected the N and N-S codoped catalysts prepared using urea and thiourea. Three different N doped catalysts with TTIP and urea in 1:2, 1:5, and 1:10 mole ratios were prepared. The same method was adopted for the preparation of N-S codoped catalysts.In case of metal doped catalysts maximum degradation was observed with 1wt% metal doped catalysts (AgT2andMoT2) and in the case of N and N-S codoped catalysts maximum degradation was observed for catalysts prepared in 1:5 mole ratio of TTIP andurea/thiourea (U2and TU2).TU2 showed better activity for photocatalytic degradation of different organic pollutants and so it was used for study of effect of operational parameters.

3.3 X-ray Diffraction Analysis (XRD)

The crystalline structure of the photocatalysts was investigated by using XRD technique. Data were collected over the angle of 2θ between 10 ° up to 70°

The XRD patterns of the synthesised N doped and N-S codoped TiO_2 are shown in fig. 3.1 and 3.2.

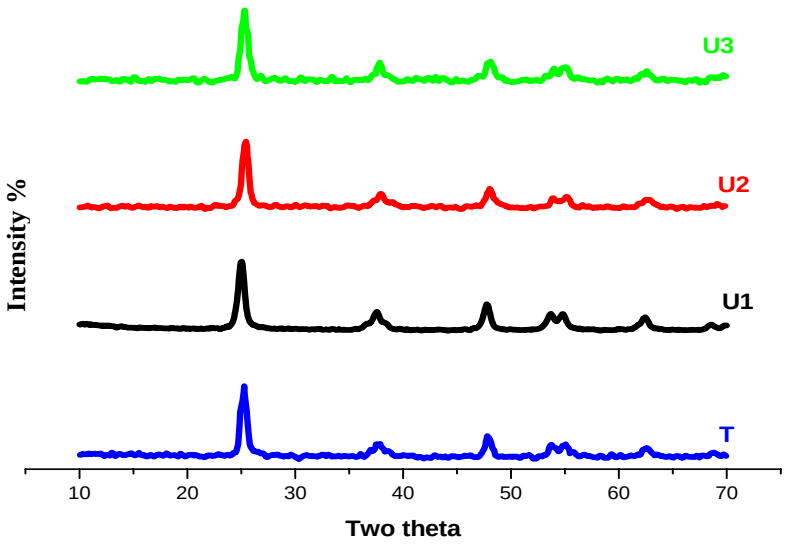

Fig.3.1 XRD spectra of N doped titania

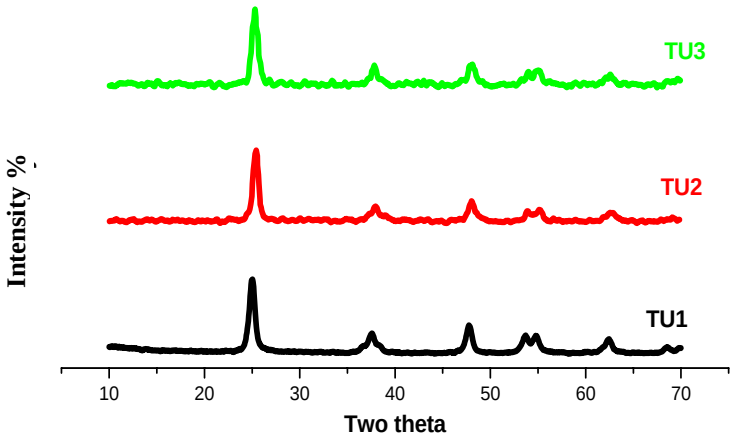

Fig.3.2 XRD spectra of N-S codoped titania

The diffraction peak at 25.4 [13-15] corresponds to anatase phase of titania. Usually amorphous–anatase transformation may complete in the temperature range 250-400^{o}C. The peak positions are same and no extra peaks except for anatase TiO_2 was observed, suggesting that the structure of TiO_2 is not changed. [16]. No peak was observed for dopants, may be due to the low amount of doped nitrogen and sulphur so that it cannot be detected by XRD. The materials show a very high degree of crystallinity of fully anatase phase.

The crystalline structure of the Mo-TiO_2 catalysts are shown in fig.3.3

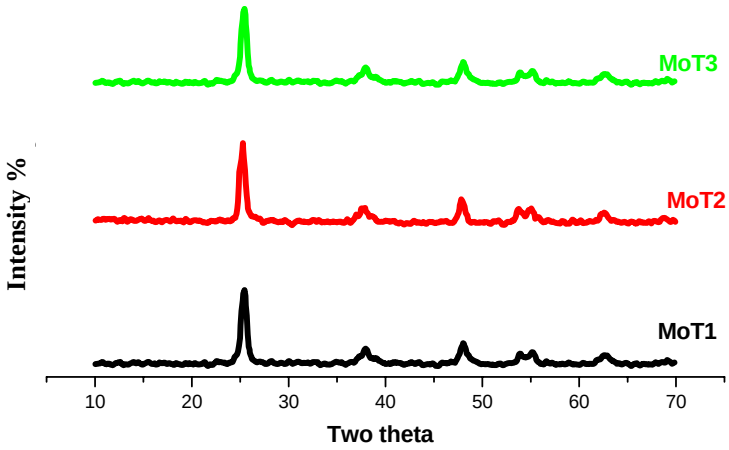

Fig.3.3 XRD spectra of Mo doped titania

The diffraction patterns of the doped materials calcined at 400^{o}C only exhibit peaks which correspond to the anatase phase .This result indicates that the structure is preserved by the incorporation of Mo to the lattice. It is reported that the doped TiO_2 with metal dopant concentration above 5 wt % can show a small peak attributed to a separate oxide phase in addition to the lines of anatase.

The XRD profile of Agdoped TiO_2 catalysts are shown in fig. 3.4

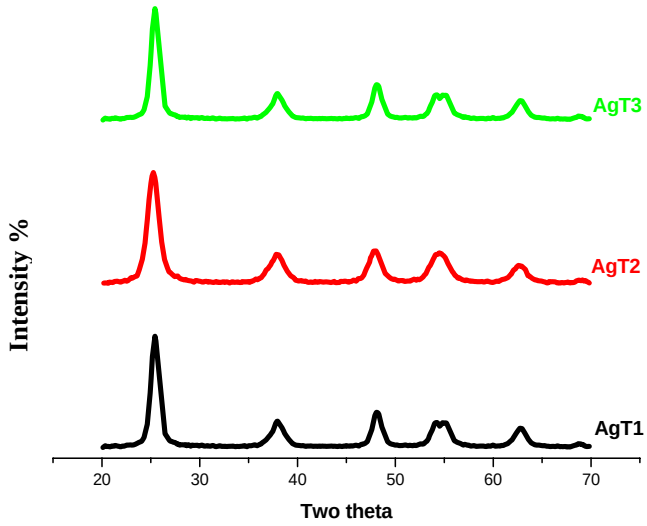

Fig.3.4 XRD spectra of Ag doped titania

The sharp peak of the anatase signal shows good crystallinity and complete transformation of the anatase phase. The size or ionic radius of the dopant ions, play a part in the choice of dopants. Evidently, the nearer the radius of a dopant ion is to the radius of the Ti^{4+} ion, the easier it is for the dopant to occupy substitutional lattice positions. The ionic radius of Ag^{+} ion is much larger than Ti^{4+}. In this research, however, doping with less than 3 % metal ions may have not distorted the crystal structure of anatase. Even though Ag^{+} have an ionic radius of 136 pm, the XRD peak observed for Ag^{+} doped TiO_2 was sharp. This is because during the catalyst preparation, Ag^{+} ions would not enter the lattice of anatase phase and during the calcinations process these uniformly dispersed Ag^{+} ions would gradually migrate from the volume of TiO_2 grains to the surface of TiO_2. This caused the TiO_2 host to have a more perfect anatase structure [4].

Crystallite size was determined by using Scherrer's equation:

$D=0.9\lambda /\beta(\Pi/180)\cos\theta$ .Where D is the crystallite size λ is the wavelength of X ray radiation , β is the fullwidth of half maximum and θ is the diffraction angle. The crystallite size of the sample are in arrange of 9-13, which is promising since nanocrystalline anatase is considered as the more photoactive form of titania [16,17].

3.4 BET Surface area

Specific surface area is one of the important properties of photocatalyst, a greater surface area is generally favourable to yield a higher photoactivity [17].

The BET surface area of powders was analaysed. The samples were activated at 90^{o}C for 30 minutes and degassed at 350^{o}C for 4 hours prior to the actual measurements. The surface area of doped samples is much higher than that of undoped one. The surface area of TU2 is 153 m^2/g which is double that of pure titania. For metal-doped TiO_2 samples, the surface areas increase with the increase of dopant concentration up to a maximum of 1 wt % and then decreases with the increase of dopant concentration. In case of non-metal doped catalysts also the surface area first increases with dopant concentration and then decreases. It can be concluded that the present sol gel method adopted is a good route for the preparation of photocatalyst with high surface area, which is favourable in enhancing the photoactivity of TiO_2 based photocatalyst.

The crystallite size and surface area of the catalysts are given in table 3.1

Table 3.1 Crystallite size and surface area of prepared catalysts

Catalyst	Crystallite size(nm)	BET surface area (m^2/g)
AgT1	8.9	108
AgT2	8.6	119
AgT3	8.3	86
MoT1	9.6	69
MoT2	9.4	91
MoT3	8.7	38
T	13.4	77
TU1	11	115
TU2	10.9	153
TU3	9.4	52
U1	12	91
U2	11.7	121
U3	11.6	46

3.5 UV-Vis. Diffuse Reflectance Spectroscopy (UV-Vis. DRS)

Extending the absorption edge of TiO_2 to the visible region is considered as one of the main objective in this study. The UV-Vis diffuse reflectance spectroscopy method was used to record absorbance capacity of the powders and to estimate band-gap energies of the prepared TiO_2 samples .The minimum wavelength required to promote an electron depends upon the band-gap energy, E_{bg}, of the photocatalyst and is given by $E_{bg} = 1240/\lambda$ where λ is the wavelength in nanometers [18]. The band gap of pure titania is 3.2eV (fig.3.5)corresponding to a wavelength of 389nm which falls in the UV region[11,17].

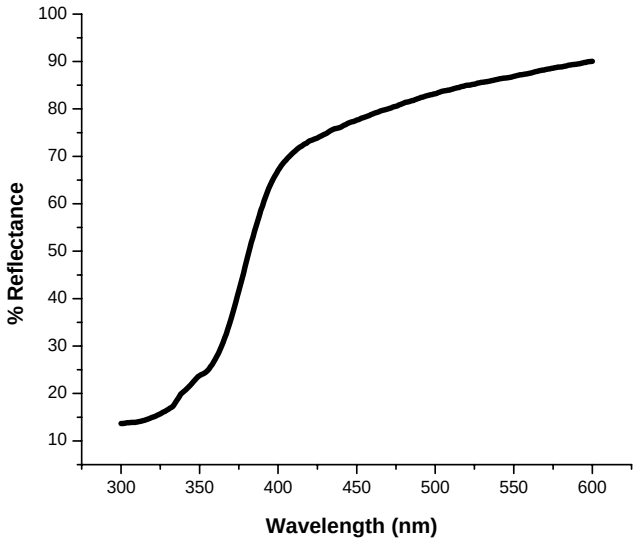

Fig. 3.5 UV-Vis.DRS of pure titania

The UV-vis.DRS of Mo doped TiO_2 samples are shown in fig.3.6

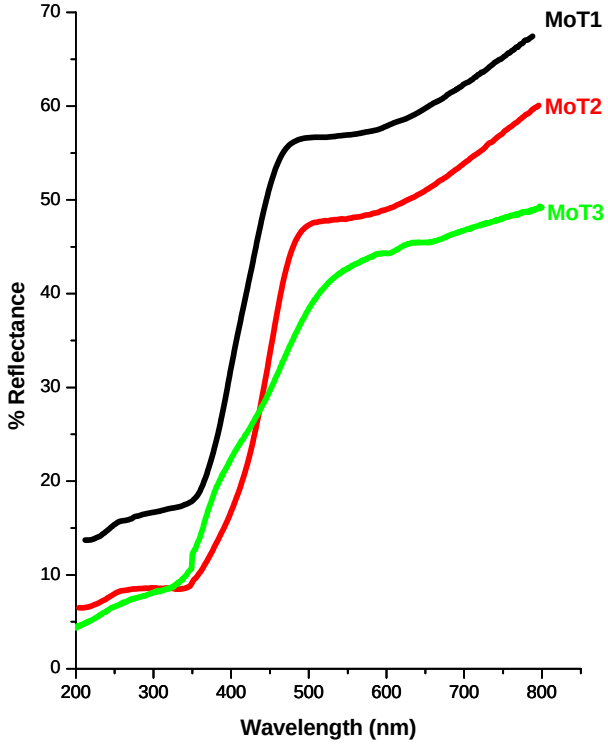

Fig.3.6 UV-Vis.DRS of Mo doped titania

The presence of a small amount of Mo in the catalyst gives rise to the red shift of its absorbance wavelength, decrease of its energy gap, and increase of the utility of visible light [3,19]. The absorption of visible light enhance along with the impurity concentration.

Increasing amounts of Ag also results in a higher visible absorbance capability of the materials (fig. 3.7).

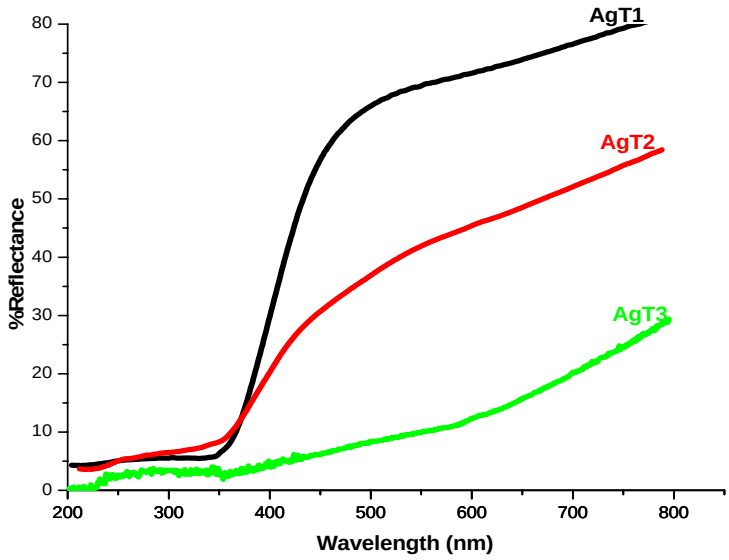

Fig.3.7 UV-Vis.DRS of Ag doped titania

The most pronounced effect occurred in the case of 3wt% Ag-doped TiO_2 sample. Increase in Ag concentration induces a shift in light absorption to the visible range for wavelengths up to 700 nm. The calculated values of band gap are listed in Table 3.2. In conclusion upon increasing the Ag doping content, it is possible to tune/change/decrease the band gap of TiO_2.

The UV DRS spectra were recorded for N and N-S codoped catalysts (fig.3.8 and 3.9) The doped samples are yellow in colour. The change in

colour of the nanoparticles upon N and S incorporation demonstrates a profound effect on their optical response in the visible wave length [13,14].

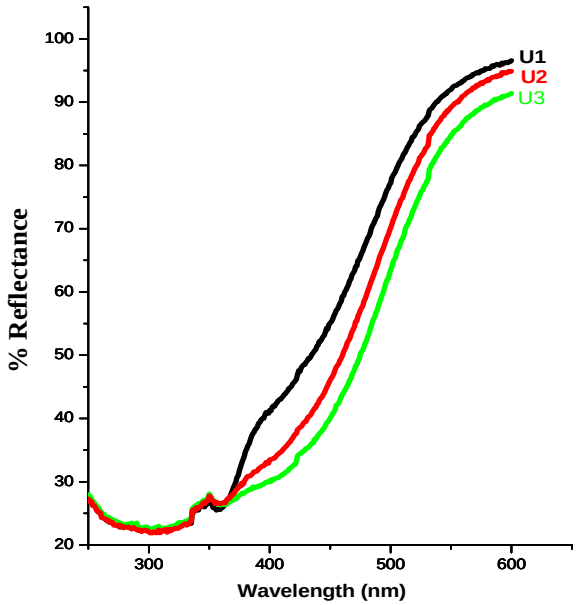

Fig.3.8 UV-Vis.DRS of N doped titania

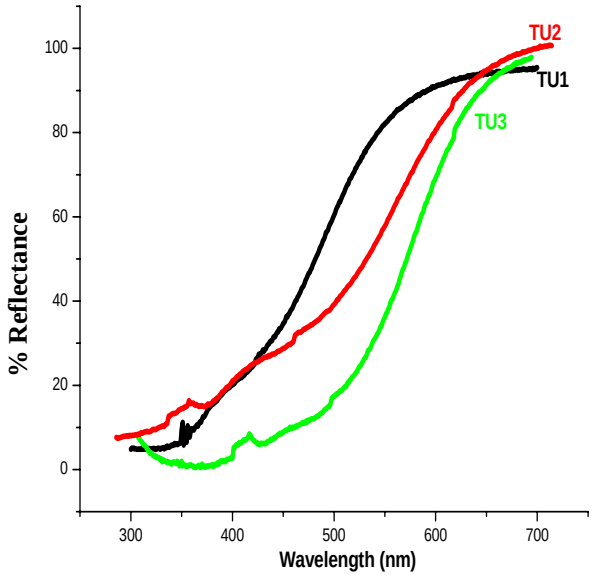

Fig.3.9 UV-Vis.DRS of N-S codoped titania

As shown in fig.3.8, N doping obviously affects light absorption characteristics of TiO_2. Unmodified TiO_2 nanoparticles hardly absorb visible light, while N-doped TiO_2 nanomaterials show a clear red shift towards visible light region, suggesting the formation of an energy level within the band gap. It can be seen from fig. 3.9 that the N-S codoping results in an intense increase in absorption in visible light region with a red shift in the absorption edge. Moreover, the absorption in this range increases with the increase of doped N and S content. This clearly indicates a decrease of the band gap energy of TiO_2. N doping can extend the wavelength response range to the visible region and increase the number of photogenerated electrons and holes to participate in the photocatalytic reaction, which would enhance the photocatalytic activity of TiO_2. However there is no direct relation between light absorption and photocatalytic activity of samples, that stronger absorption of visible light does not mean the higher degradation of pollutants [16,20].

Table 3.2 Band gap of doped and undoped TiO_2 catalysts

Catalyst	Band gap(eV)	Wavelength (nm)
AgT2	2.35	526
MoT2	2.57	482
U2	2.25	550
TU2	2.23	554
T	3.18	389

Various mechanisms have been proposed to explain the light absorption and photoactivity of N-doped TiO_2, researchers proposed that the introduction of nitrogen introduced new orbitals in between the valence band (which are comprised primarily of O-2p orbitals) and conduction band (which are

comprised primarily of Ti-3d orbitals). These N-2p orbitals acted as a step up for the electrons in the O-2p orbital, which once populated had now a much smaller jump to make to be promoted into the conduction band. Once this process occurs, electrons from the original valence band can migrate into the mid-band gap energy level, leaving a hole in the valence band, which reacts as described before. Di Valentin et al. provided theoretical evidence that [21] in the case of substitutional N-doped anatase TiO_2, the visible light response arises from occupied N 2p localized states slightly above the valence band edge [22].Hashimoto and co-workers [23,24] provided the explanation that a localized N 2p state formed above the valence band was the origin for the visible light response of the nitrogen-doped TiO_2[25-28].Yu et al. [29] found that sulphur doping can indeed create intraband gap state close to the conduction band edge, and thus induces visible-light absorption at the sub-band gap energy

3.6 CHNS Elemental Analysis (CHNS)

The presence of N and S in the doped catalysts was studied by CHNS analysis. The analysis was performed by a Elementar Vario EL III CHN analyzer.

Table 3.3 CHNS Elemental analysis of N doped and N-S codoped catalysts

Catalysts	%N	%S
U1	0.29	-
U2	0.48	-
U3	0.60	-
TU1	0.16	1.1
TU2	0.65	1.5
TU3	0.71	0.9

The results indicated that dopants N and S are incorporated in the catalysts. The percentage of N and S increases with increase of dopant source concentration.

3.7 Scanning Electron Microscopy (SEM)

The surface morphology was studied by SEM analysis. Fig. 3.10 shows the SEM image of undoped TiO_2. Fig. 3.11 and 3.12 show SEM images of TiO_2 doped with metals.

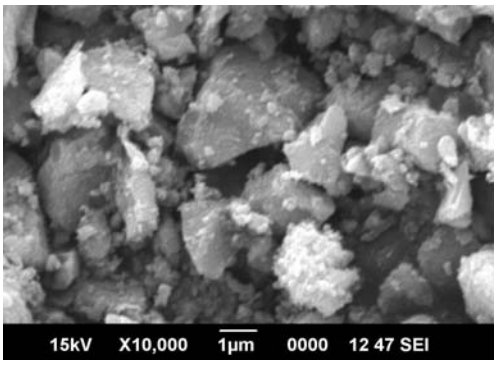

Fig.3.10 SEM image of undoped titania

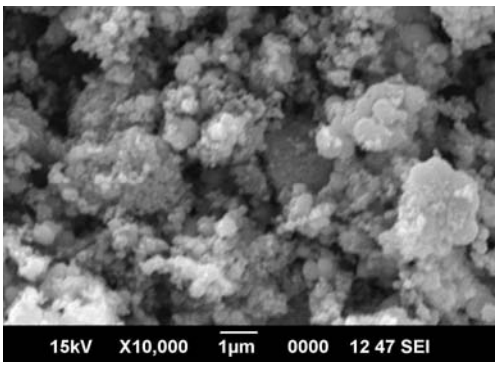

Fig.3.11 SEM image of MoT2

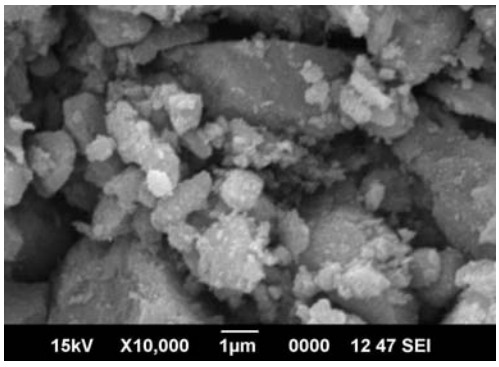

Fig.3.12 SEM image of AgT2

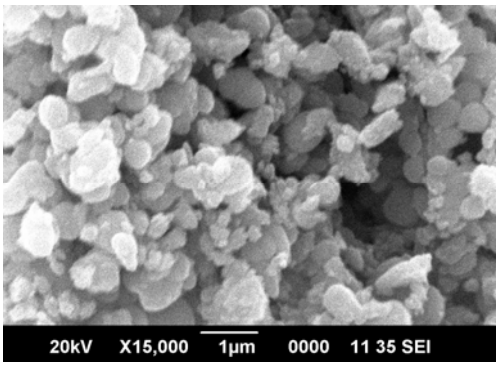

Fig.3.13 SEM image of U2

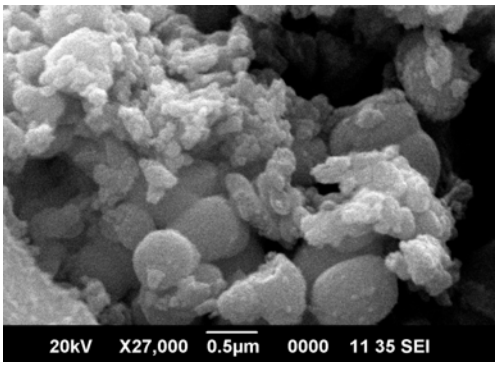

Fig.3.14 SEM image of TU2

Fig. 3.13 and 3.14 show the SEM images of N and N-S codoped catalysts.The images show that particles are somewhat spherical in nature. But most of them are in agglomerated form.

3.8 Energy Dispersive X-ray Analysis (EDX)

EDX is used to confirm the existence of dopants in the doped catalysts. EDX analysis gives both qualitative and quantitative information about the elemental composition in the catalysts.

The presence of dopants in all the catalyst samples was not detected by XRD, possibly due to the very small quantity of dopants in the catalysts. However, this is proven by elemental analysis conducted using EDX, which showed the existence of dopants in the catalysts. All dopants, which were not detectable in the XRD analysis, were observed by EDX .This is because the percentage amount of elements given in the EDX data represents the total amount of that individual element in the sample. No information on the type of species that a particular element formed can be extracted from the data.

Table 3.4 Elemental composition from EDX

Wt% of metal incorporated	catalysts	EDX values	
		Ag	Mo
0.5	AgT1	0.21	-
1	AgT2	0.33	-
3	AgT3	0.87	-
0.5	MoT1	-	0.1
1	MoT2	-	0.3
3	MoT3	-	1.14

3.9 Transmission Electron Microscopy (TEM)

The TEM images of MoT2 and AgT2 are shown in fig.3.15 and 3.16. The particles are either spherical or rectangular in shape but most of them are in agglomerated form. The particle size histogram of MoT2 and AgT2 are shown in fig.3.17 and 3.18 respectively the particle size are in a range of 7-16 nm

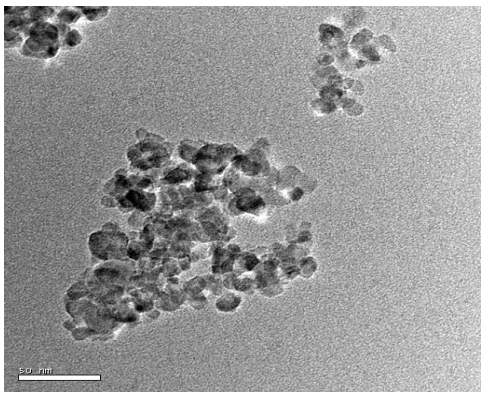

Fig. 3.15 TEM image of MoT2

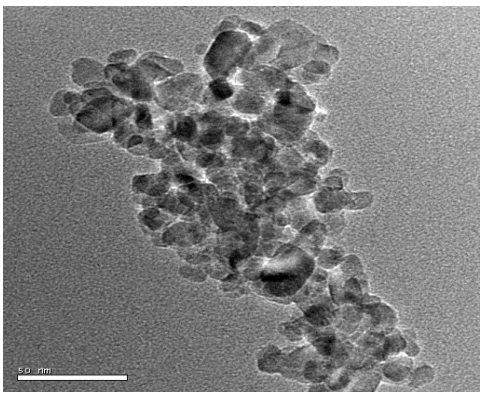

Fig. 3.16 TEM image of AgT2

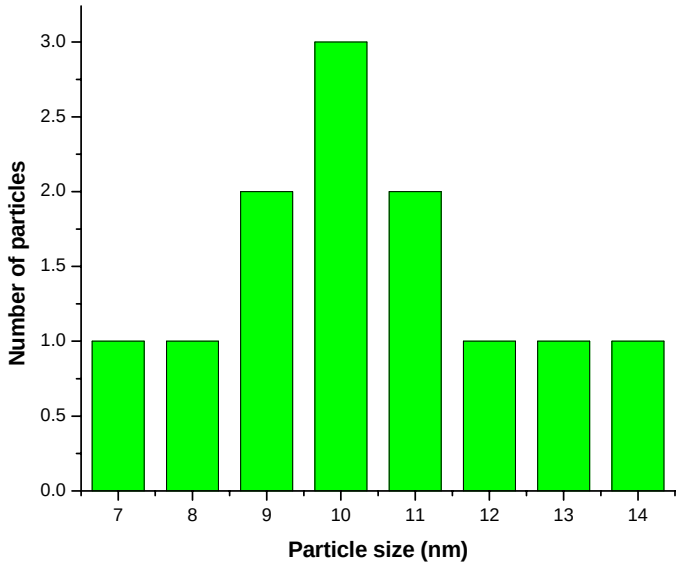

Fig.3.17 Particle size histogramof MoT2

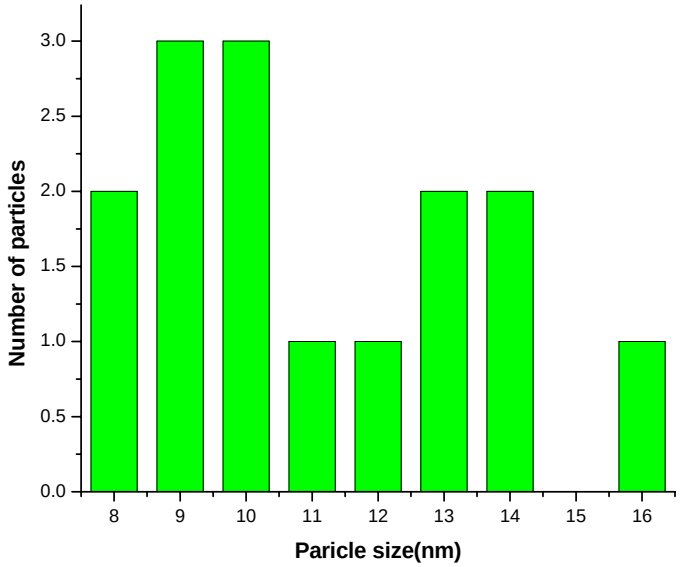

Fig.3.18 Particle size histogramof AgT2

The TEM images of U2 and TU2 are shown in fig.3.19 and 3.20.The particles are agglomerated and exhibit spherical or rectangular shape. The

particle size histogram of U2 and TU2 are shown in fig.3.21 and 3.22 respectively. The particle size is in a range of 7-15 nm.

The HRTEM images of bothU2 and TU2 are shown in fig.3.23 and 3.24. The images indicate that particles are well ordered and highly crystalline in nature. The catalysts give the same d value (0.352nm) which is in correlation with the d value obtained from XRD spectrum and corresponds to101 anatase planes. This again confirms the presence of anatase phase.

Fig.3.25 shows the selected area electron diffraction pattern of U2 catalyst. The electron diffraction image shows well distinct spots due to the high crystallinity of titania indicated as anatase phase with major 101 planes. The d value corresponding to each pattern can be calculated using the equation

$$d=Lh/R\sqrt{(2ME)}$$

L- camera const, h- planks const, E- energy of electron beam M- mass of electron R- radius of diffraction circle .The d value obtained from the main diffraction circle is approximately equal to 0.352nm. The results show that the prepared catalyst shows anatase phase with major 101 planes.

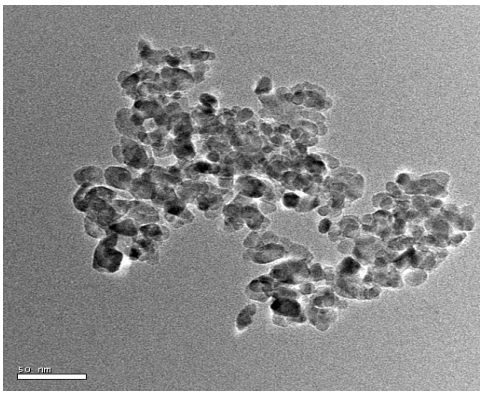

Fig.3.19 TEM image of U2

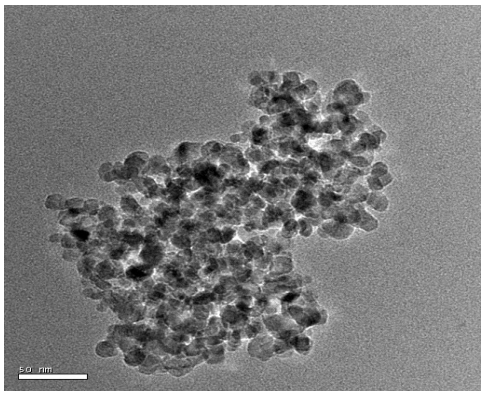

Fig. 3.20 TEM image of TU2

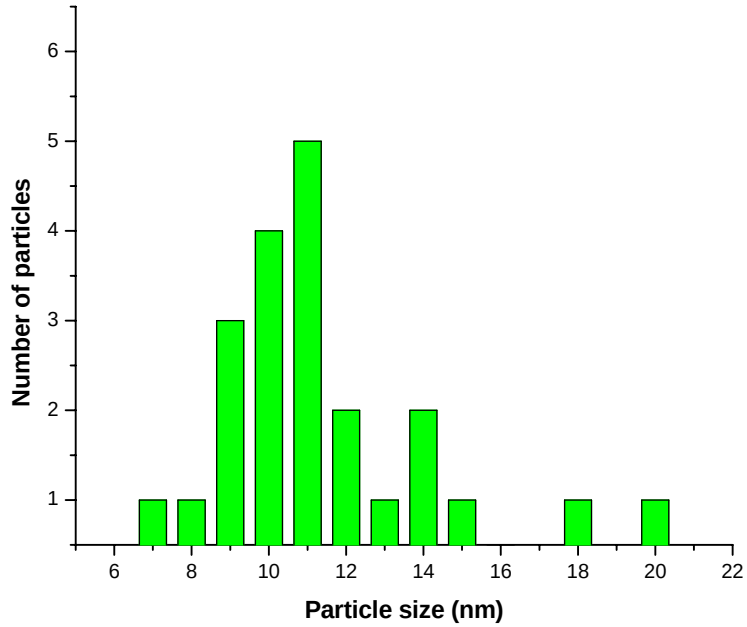

Fig. 3.21 Particle size histogramof U2

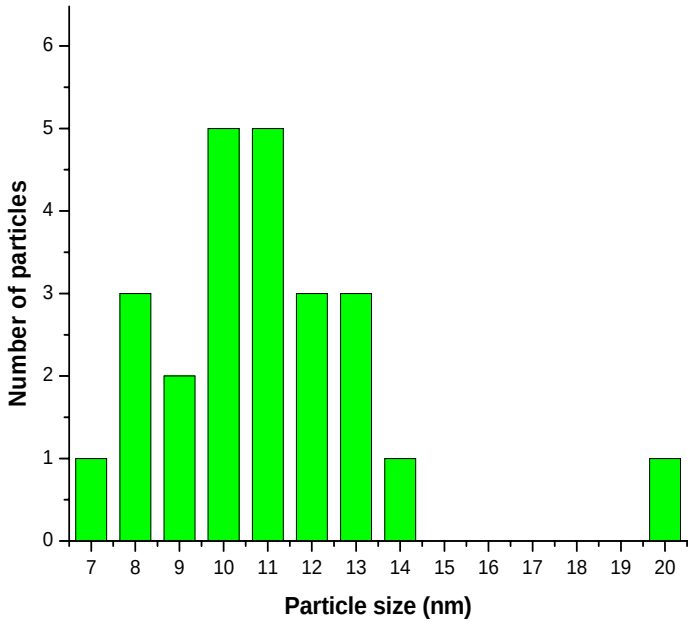

Fig.3.22 Particle size histogramof TU2

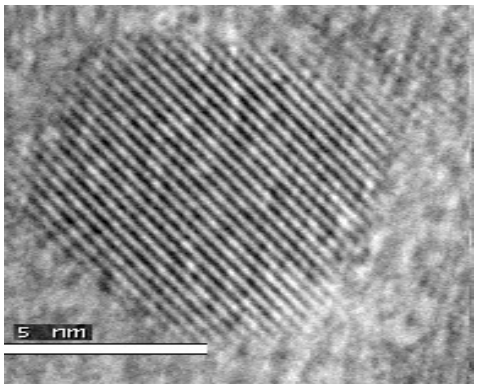

Fig.3.23 HRTEM image of U2

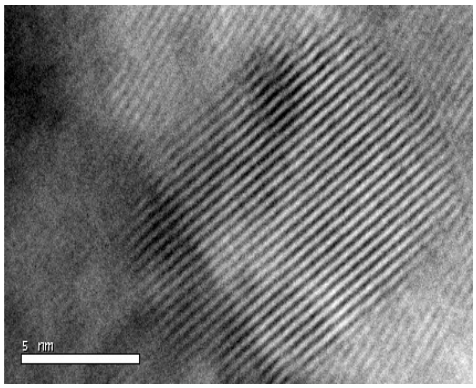

Fig.3.24 HRTEM image of TU2

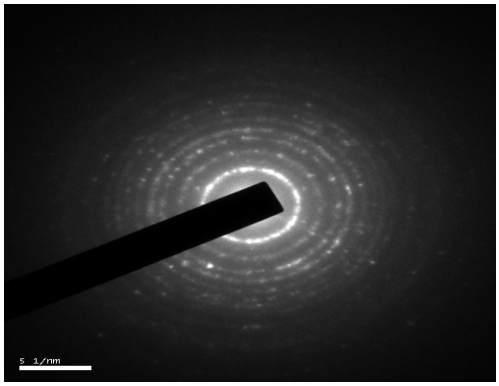

Fig.3.25 SAED image of U2

3.10 Fourier Transform Infrared Spectroscopy (FTIR)

The FT-IR spectra of Mo and Ag doped catalysts are shown in fig. 3.26 and 3.27 respectively

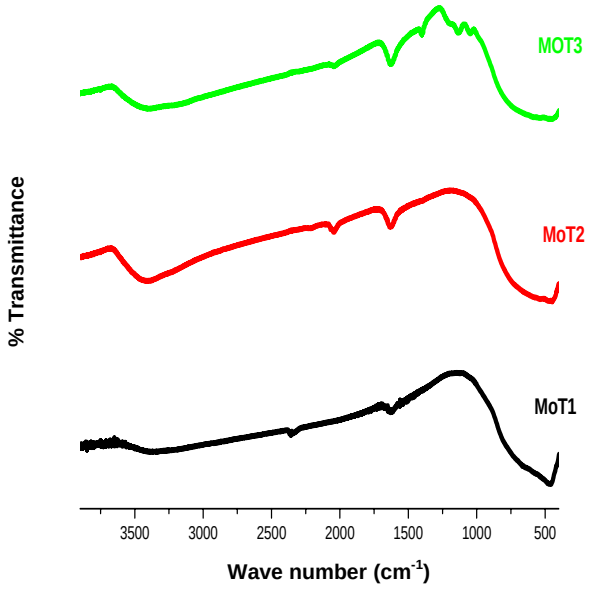

Fig.3.26 FTIR spectra of Mo doped titania

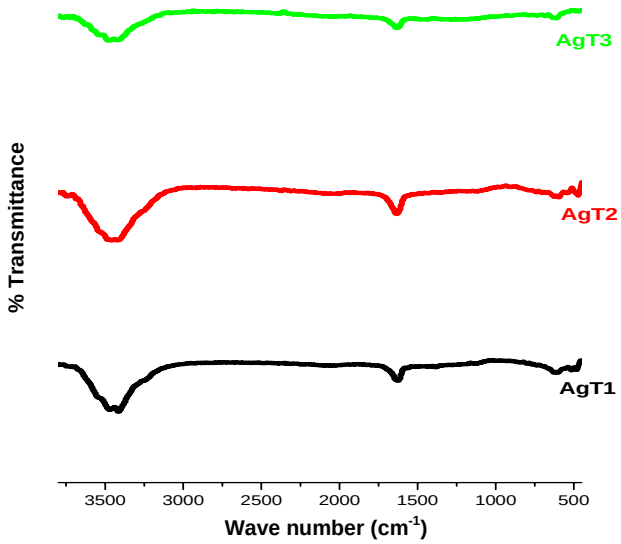

Fig.3.27 FTIR spectra of Ag doped titania

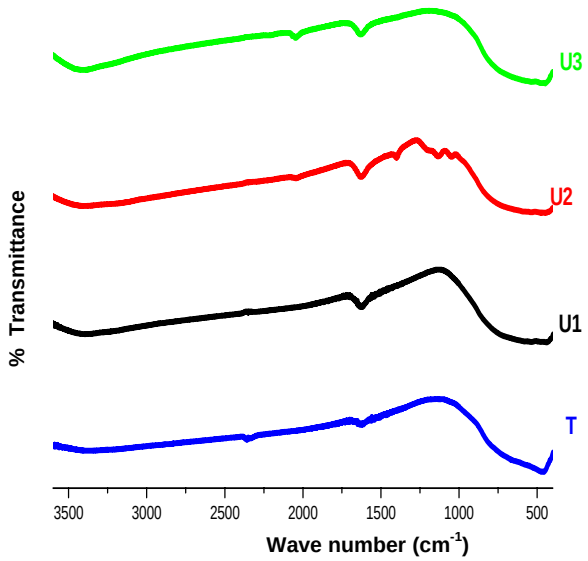

Fig.3.28 FTIR spectra of undoped and N doped titania

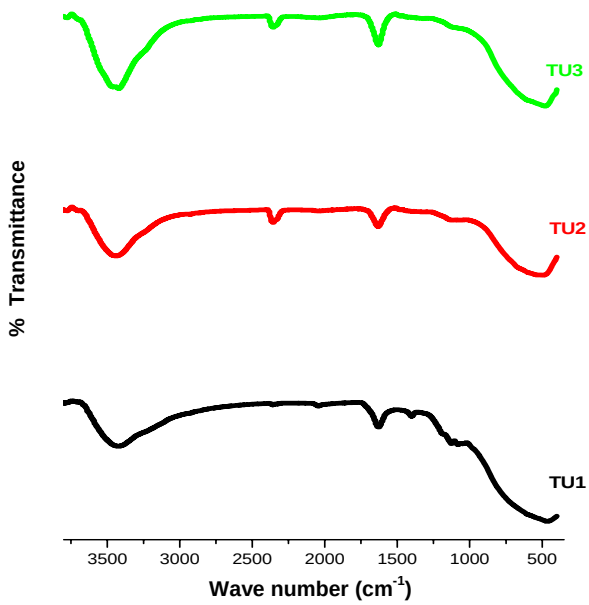

Fig.3.29 FTIR spectra of N-S codoped titania

The broad peak at 3450 cm^{-1} and the peak at 1650 cm^{-1} specifically correspond to the OH stretching and bending vibrations, respectively [13, 30-32]. This absorption band is due to surface-adsorbed water and hydroxyl groups, which are considered to play a key role in the photocatalytic reaction because the photoinduced holes can attack those surface hydroxyl groups and yield surface hydroxyl radicals with high oxidation capability[14,33,34].The bands below 500cm^{-1} are attributed to the anatase phase of TiO_2[22].

3.11 X-ray Photoelectron Spectroscopy (XPS)

XPS spectra were recorded in an indigenously developed electron spectrometer equipped with Thermo VG Clamp-2 Analyser and a Mg Kα X-ray source (1253.6 eV, 30mA × 8 kV). A thin sample wafer of 12 mm in diameter was used in these studies. As an internal reference for the absolute binding energy of C 1s peak at 284.6 eV was used. Table 3.5 presents the binding energy values derived from the XPS analysis of the sample.

Atomic concentration values derived from the XPS data are presented in Table 3.6.For oxygen the 1s XPS spectra was de-convoluted using Gaussian multi-peak fitting program and peak area of 529.3 eV peak was taken for atomic ratio calculation purpose. Area for corresponding peak was divided by the sensitivity factor in these calculations. The values of sensitivity factors used in these calculations are given in Table-3.7. C 1s peak with binding energy value of 284.8 eV is referred as standard value for the surface adventitious carbon.

Table 3.5 Binding energy values derived for nitrogen, titanium and oxygen from the XPS spectra of N doped titania sample

Sample Name	Details	Ti, $2p_{3/2}$, $2p_{1/2}$ eV	O, 1s eV	N, 1s eV
U2	High resolution	458.2(Ti^{4+}), 464.24	529.3 531	399.2

Table 3.6 Atomic ratios derived from the XPS data

Sample Name	Ti $2p_{3/2}$ peak			O 1s peak			N 1s peak			Ti:O:N
	B.E. (eV)	FWHM (eV)	Peak Area	B.E. (eV)	FWHM (eV)	Peak Area	B.E. (eV)	FWHM (eV)	Peak Area	
U2	458.2	1.06	3748.1	529.3	1.08	4232.4	399.2	2.2	220.3	1:2.07:0.17

Table3.7 Sensitivity Factors

Element	XPS peak	Sensitivity Factor
Ti	$2p_{3/2}$	5.22
O	1s	2.85
N	1s	1.74

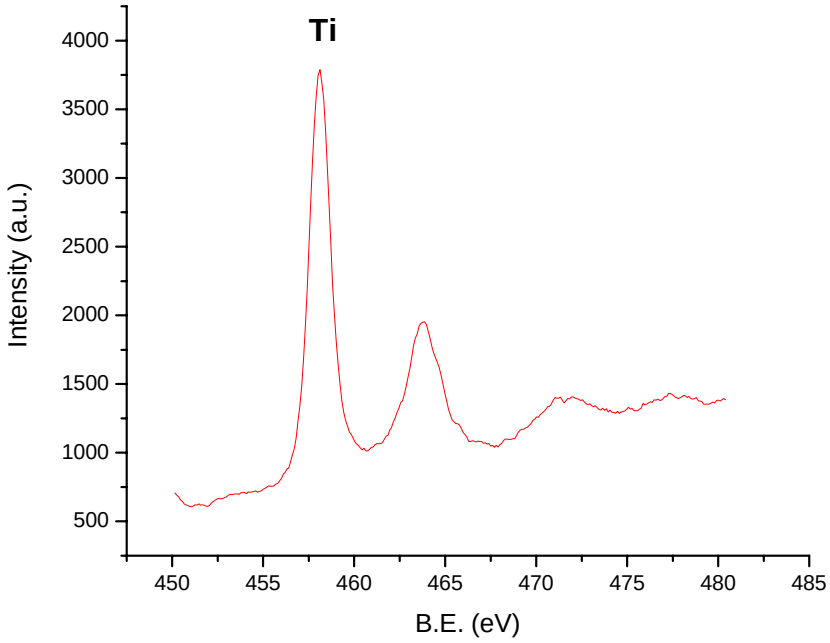

Fig.3.30 Ti 2p spectrum of sample U2

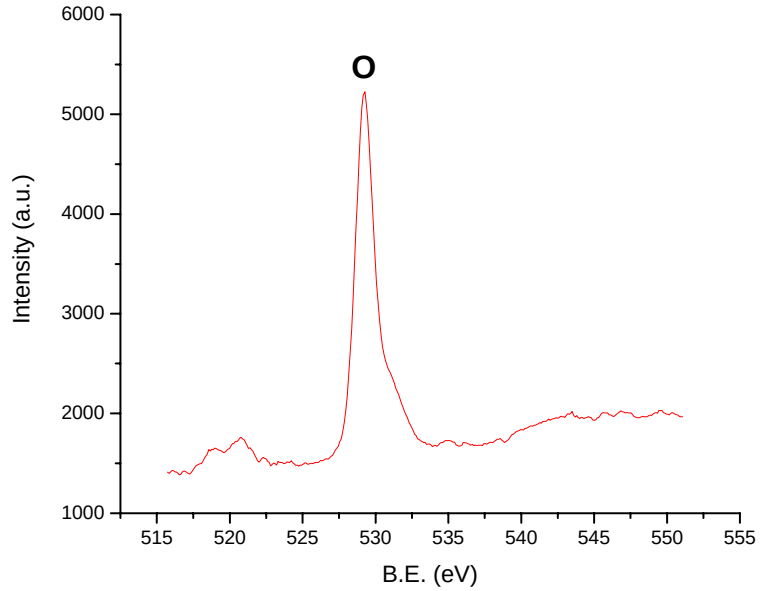

Fig. 3.31 O 1s spectrum of sample U2

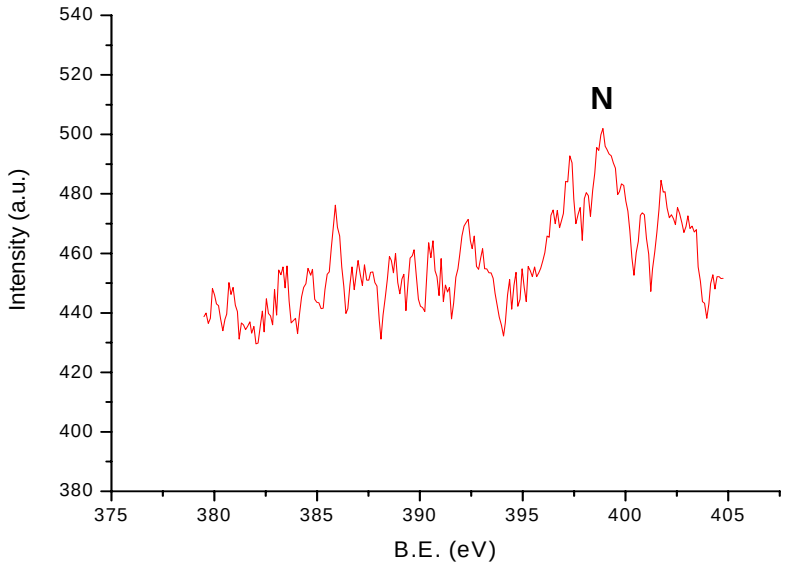

Fig. 3.32 N 1s spectrum of sample U2

There were two peaks for Ti 2p (fig.3.30) at 458.2 and 464.2 eV. According to the literatures [26–28], the peak at 458.2 eV was attributed to

$Ti2p_{3/2}$ and the peak at 464.2 eV was assigned to $Ti2p_{1/2}$, indicating that Ti remained in an octahedral environment [35]. Binding Energy values of Ti are attributed to its 4+ oxidation state.

A shoulder seen in O 1s spectrum at higher B.E at ~ 531 eV is associated with surface hydroxyl groups while the main peak at ~529. 3 is due to oxygen associated with titania[36].

Nitrogen 1s peak at ~ 399.2 eV appears to be very broad has relatively lower intensity.

The origin of the peak in the 396–403 eV region is still under debate and remains to be clearly understood. Some researchers [28] attributed the N 1s peaks at binding energies at 400 and 402 eV to molecularly adsorbed nitrogen species. Burda et al. [38] observed an N 1s core level at 401.3 eV in nitrogen-doped titania nanoparticles and suggested that it is attributed to the N atoms in the environment of O–Ti–N, based on the comparison with the N 1s electron binding energy of TiN (397.2 eV).

The XPS peak around 399.2 eV which is due to the formation of an O-Ti-N bond, suggesting that the nitrogen is doped in the lattice as an anion by the bond formation (O-Ti-N). This peak therefore can be attributed to the 1s electron binding energy of the N atom in the O-Ti-N environment [13,26] .This O-Ti-N bond formation occurs by the replacement of the lattice oxygen by nitrogen in $[TiO_6]^{2-}$ octahedra [34,38,39]

3.12 Thermogravimetric Analysis (TG)

In this technique the change in sample weight is measured while the sample is heated at a constant rate (or at constant temperature), under air (oxidative) or nitrogen (inert) atmosphere. In this study this technique is used

to determine the calcination temperature of the catalyst. The TG analysis were done on a Perkin Elmer Pyris Diamond thermogravimetric/differential thermal analyser by heating the samples at a rate of 10^{o}C /min from room temperature to 800^{o}C in nitrogen atmosphere with samples mounted on a platinum sample holder.

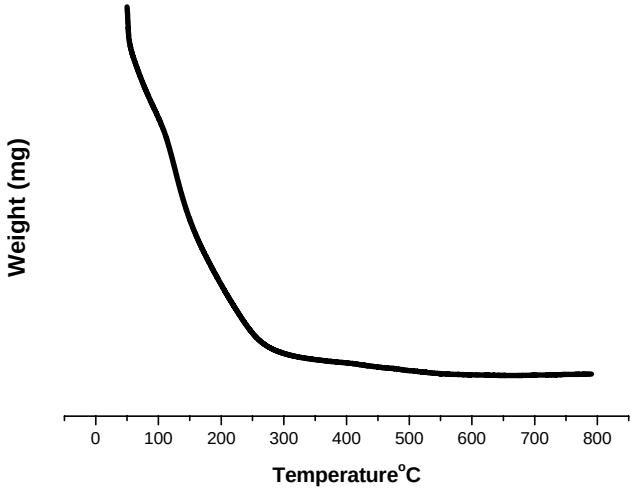

Fig.3.33 Thermogram of U2

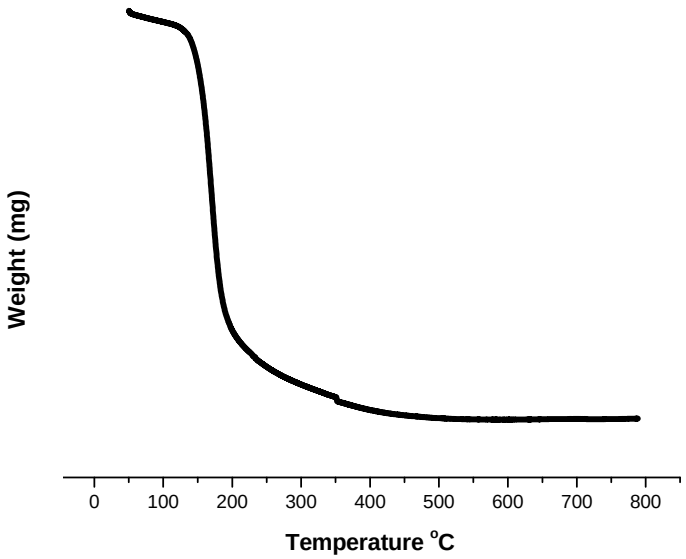

Fig.3.34 Thermogram of TU2

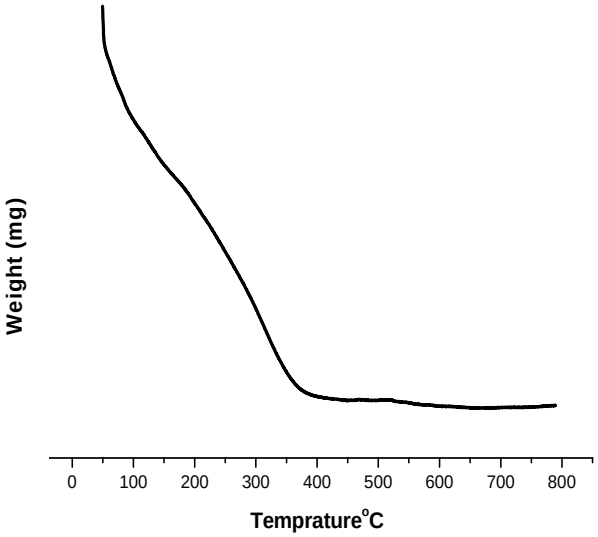

Fig.3.35 Thermogram of AgT2

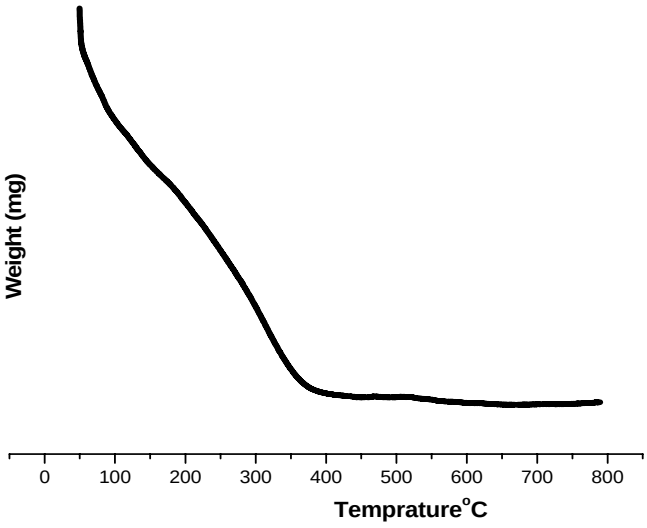

Fig.3.36 Thermogram of MoT2

Initially there is a weight loss due to the removal of water molecules. The carbonaceous species are burnt out by calcination at elevated temperature. Thermo-gravimetric analysis indicated that the weight loss of the prepared TiO_2 sample depended on the calcination temperature. The weight loss of the sample markedly decreases as the calcination temperature rose above 350°C, indicating that the residual organic substances may have been thoroughly eliminated by burning [40,41] therefore the prepared samples were calcined at 400^oC for 4hours.

References

[1] C. H. Liu, M. H. Hong, Y. Zhou, G. X. Chen, M. M. Saw, A. T. S. Hor, Phys. Scr. T.,129 (2007) 326.

[2] Hassan Ilyas, Ishtiaq A. Qazi, Wasim Asgar, M. Ali Awan, Zahir-ud-din Khan, Journal of Nanomaterials, 2011 (2011)1.

[3] Vaclav S tengl, Snejana Bakardjieva, J. Phys. Chem. C, 114 (2010) 19308.

[4] Michael K. Seery, Reenamole George, Patrick Floris, Suresh C. illai, Journal of Photochemistry and Photobiology A: Chemistry, 189 (2007) 258.

[5] A. Mills, R.H. Davies, D. Worsley, Chem. Soc.Rev., 22 (1993) 417.

[6] Xiaofeng Qiu, Clemens Burda, Chemical Physics, 339 (2007) 1.

[7] Marıa D. Hernandez-Alonso, Fernando Fresno, Silvia Suareza, Juan M. Coronado, Energy Environ. Sci., 2 (2009) 1231 .

[8] O. Carp, C. L. Huisman, A. Reller, Prog. Solid State Chem., 32 (2004) 33.

[9] Xiang Li, Rongchun Xiong, Gang Wei, Catal Lett., 125 (2008)104.

[10] D.M. Chen, D. Yang, Q. Wang, Z.Y. Jiang Chem Res., 45 (2006) 4110.

[11] Clemens Burda, Yongbing Lou, Xiaobo Chen, Anna C. S. Samia, John Stout, James L. Gole, Nanoletters, 3(2003)1049

[12] Di Paola, G. Marc, L. Palmisano, M. Schiavello, K. Uosaki, S. Ikeda, B. Ohtani J. Phys. Chem. B, 106(2002) 637.

[13] L. Lin, R. Y. Zheng, J. L. Xie, Y. X. Zhu, Y. C. Xie, Applied Catalysis B: Environmental, 76 (2007) 196.

[14] L. Lin, W. Lin, J. L. Xie, Y.X. Zhu, B. Y. Zhao, Y. C. Xie, Applied Catalysis B: Environmental, 75 (2007) 52.

[15] Horst Kisch, Shanmugasundaram Sakthivel, Marcin Janczarek, Dariusz Mitoraj, J. Phys. Chem. C, 111(2007)11445.

[16] Yi Xie, Qingam Zhao, Xiu Jian Zhao, Yuanzhi Li, Catal Lett., 118 (2007) 231.

[17] Jian Yuan, Mingxia Chen, Jianwei Shi, Wenfeng Shangguan, International Journal of Hydrogen Energy, 31 (2006) 1326.

[18] Shu Yin, Masakazu Komatsu, Qiwu Zhang, Fumio Saito, Tsugio Sato, J.Mater. Sci., 42 (2007) 2399.

[19] J. Zhang, Q. Li, W. Cao, J. Environ. Sci., 17 (2005) 350.

[20] Rocıo Silveyra, Luis De La Torre Saenz, Wilber Antunez Flores, V. Collins Martınez, A. Aguilar Elguezabal ,Catalysis Today ,107–108 (2005) 602.

[21] C. Di Valentin, G. Pacchioni, A. Selloni, S. Livraghi, E. Giamello, J. Phys. Chem. B, 109 (2005) 11414.

[22] Feng Peng, Lingfeng Cai, Hao Yu, Hongjuan Wang, Jian Yang, Journal of Solid State Chemistry, 181 (2008) 130 .

[23] H. Irie, S. Washizuka, N. Yoshino, K. Hashimoto, Chem.Commun.,11 (2003) 1298.

[24] H. Irie, Y .Watanabe, K .Hashimoto, J. Phys. Chem. B, 107 (2003) 5483.

[25] Aditi R. Gandhe, Julio B. Fernandes. Journal of Solid State Chemistry, 178 (2005) 2953.

[26] Y. Aita, M. Komatsu, S. Yin, T. Sato, J. Solid State Chem., 177 (2004) 3235.

[27] T. Morikawa, R. Asahi, T. Ohwaki, K. Aoki, Y. Taga, Jpn.J. Appl. Phys. 40 (2001) L561.

[28] R. Asahi, T. Morikawa, T. Ohwaki, K. Aoki, Y. Taga, Science, 293 (2001) 269.

[29] J. C. Yu, W.K. Ho, J. G. Yu, H .Yip, P. K .Wong, J. C. Zhao, Environ Sci Technol., 39(2005)1175.

[30] J. G. Yu, H. G. Yu, B. Cheng, X. J. Zhao, J. C. Yu, W. K. Ho, J. Phys. Chem. B, 107 (2003) 13871.

[31] D. S. Warren, A. J. Mc Quillan, J. Phys. Chem. B,108 (2004) 19373.

[32] S. K. Samantaray, K.M. Parida, J. Mater. Sci.,38 (2003) 1835.

[33] M. Hamadanian, A. Reisi-Vanani, A. Majedi, Material Chemistry and Physics, 116 (2009)376 .

[34] Pradeepan Periyat, Declan E. McCormack, Steven J. Hinder, Suresh C. Pillai, J. Phys. Chem. C, 113 (2009) 3246 .

[35] Xiang-Zhong Shen, Jun Guo, Zhi-Cheng Liu, Shan-Mei Xie, Applied Surface Science, 254 (2008) 4726.

[36] Haimei Liu, Wensheng Yang, Ying Ma, Yaan Cao, Jiannian Yao,New J. Chem., 26 (2002) 975.

[37] X. Chen, C. Burda, J. Phys. Chem. B, 108 (2004) 15446.

[38] X. Chen, C.Burda, J. Phys. Chem. B, 107(2004**)** 5483.

[39] Mingyang Xing, Jinlong Zhang, Feng Chen, Applied Catalysis B: Environmental, 89(2009)563.

[40] Shu Yin, Hiroshi Yamaki, Masakazu Komatsu, Qiwu Zhang, Jinshu Wang, Qing Tang, Fumio Saito, Tsugio Sato, J. Mater. Chem., 13(2003) 2996.

[41] R. S. Sonawane, M. K. Dongare, Journal of Molecular Catalysis A: Chemical, 243 (2006) 68.

.....ഠാര.....

Chapter 4

Photocatalytic Degradation of Dyes

Contents

Toxic dyes are very important in the viewpoint of environmental protection because they produce toxic aromatic amines and have other harmful environmental effects. They are widely used and many of dye molecules are resistant to biological degradation. Advanced oxidation processes are good alternatives for conventional methods. The photocatalytic degradation of some of the dyes Methylene Blue, Acid Orange 7, Acid Red1, Crystal Violet and Acid Blue 25 have been studied using prepared catalysts in aqueous solution under visible and UV irradiation. The effects of operational parameters, such as time, dye concentration, catalyst concentration, light source and dopant concentration on the degradation of aqueous dye solutions is examined. In the presence dopants the activity of catalyst is significantly improved.

4.1 Introduction

A dye is a colored substance that has an affinity to the substrate to which it is being applied. The dye is generally applied in an aqueous solution, and requires a mordant to improve the fastness of the dye on the fiber. Unlike most organic compounds, dyes possess colour because they absorb light in the visible spectrum (400–700 nm), have at least one chromophore (colour-bearing group), have a conjugated system, and exhibit resonance of electrons, which is a stabilizing force in organic compounds. When any one of these features is lacking from the molecular structure the colour is lost. In addition to chromophores, most dyes also contain groups known as auxochromes. By the nature of their chromophore, dyes are divided into: Acridine dyes, Xanthene dyes Anthraquinone dyes, Arylmethane dyes, Azo dyes, Diazonium dyes, Nitro dyes, Nitroso dyes, Rhodamine dyes etc [1].

The dyes may be divided into water soluble cationic and anionic dyes and water insoluble dyes. Methylene Blue and Crystal Violet are cationic dyes. Acid Red 1 and Acid Orange 7 are anionic dyes.

Textile dyes and other industrial dyestuffs constitute one of the largest groups of organic compounds that represent an increasing environmental danger. About 1–20% of the total world production of dyes is lost during the dying process and is released in the textile effluents [2–4]. The release of those colored waste waters in the environment is a considerable source of pollution and can originate dangerous by products through oxidation, hydrolysis, or other chemical reactions taking place in the wastewater phase [5–8]. The large amount of waste water generated in textile manufacturing processes represents an increasing environmental danger due to the refractory carcinogenic nature of the dyes. Decolorization of dye effluents has therefore received increasing attention.

For the removal of dye pollutants, traditional physical techniques (adsorption on activated carbon, ultrafiltration, reverse osmosis, coagulation by chemical agents, ion exchange on synthetic adsorbent resins etc.) can generally be used efficiently [9–12]. Nevertheless, they are non-destructive, since they just transfer organic compounds from water to another phase, thus causing secondary pollution. Consequently, regeneration of the adsorbent materials and post-treatment of solid-wastes, which are expensive operations, are needed [12,13]. Due to the large degree of aromatics present in dye molecules and the stability of modern dyes, conventional biological treatment methods are ineffective for decolorization and degradation [14–17]. Furthermore, the majority of dyes is only adsorbed on the sludge and is not degraded [18]. Chlorination and ozonation are also being used for the removal of certain dyes but at slower rates as they have often high operating costs and limited effect on carbon content [12, 19–22].

Advanced Oxidation Processes (AOPs) have been growing during the last decade since they are able to deal with the problem of dye destruction in aqueous systems. AOPs were based on the generation of very reactive species such as hydroxyl radicals (•OH) that oxidize a broad range of pollutants quickly and non selectively.

Among AOPs, heterogeneous photocatalysis using TiO_2 as photocatalyst appears as the most emerging destructive technology [4, 23-28]. The key advantage is its inherent destructive nature. It does not involve mass transfer, it can be carried out under ambient conditions (atmospheric oxygen is used as oxidant) and may lead to complete mineralisation of organic carbon into CO_2. Moreover, TiO_2 photocatalyst is largely available, inexpensive, non-toxic and show relatively high chemical stability. Finally, TiO_2 photocatalytic process is receiving increasing attention because of its low cost when using sunlight as the source of irradiation.

Heterogeneous photocatalysis is based on the irradiation of a photocatalyst, usually a semiconductor such as TiO_2, with light energy equal to or greater than the band gap energy. This causes a valence-band electron to be excited to the conduction band, causing charge separation. The conduction band electrons and valence band holes can then migrate to the surface and participate in interfacial oxidation–reduction reactions. The oxidative degradation of an organic pollutant is attributed to reaction at the positive hole where adsorbed water or hydroxyl groups are oxidized to hydroxyl radicals ($^{\bullet}OH$), which then react with the pollutant molecule [29-31].

The utilization of combined photocatalysis and solar technologies may be developed to a useful process for the reduction of water pollution by dying because of the mild conditions required and their efficiency in the mineralisation [7, 32-35].

The aim of the present study is to investigate the photocatalytic degradation of some dyes over semiconductive, TiO_2-based photocatalysts irradiated with a150W Xe lamp. The experiment was carried out using an Oriel Uniform Illuminator 150 W Xe ozone free lamp with filters. Dichoric mirror of wavelength, 280-420nm (for UV light), and 420-630nm dichoric mirror (cold mirror) for visible irradiation were used. Dyes -Acid Orange 7, Acid Red1, Methylene Blue, Crystal Violet and Acid Blue 25 were selected for the photocatalytic degradation. The degradation of dyes using different prepared catalysts was studied.

Samples were withdrawn at different time intervals during the photodegradation inorder to measure the absorbance. The absorbance of samples was measured spectrophotometrically (SPECTRASCAN UV 2600 DOUBLEBEAM UV VIS spectrophotometer).The concentration of dye was

determined by the employment of a calibration curve of absorbance (at maximum wavelength) vs.dye concentration obtained by spectrophotometric measurements. The percentage degradation of dye was calculated using the equation: $X=(C_o- C_t /C_o) \times 100$ in which X is the percentage degradation, C_t is dye concentration at time t and C_o is initial dye concentration.

The effect of operational parameters, such as time, dye concentration, catalyst concentration, light source and dopant concentration on the degradation of aqueous dye solutions is examined. The mineralisation was studied by using TOC analysis. Total organic carbon (TOC) of dye solution was measured using a Elemental Vario TOC analyser.

4.2 Azo Dyes

Azo dyes are a class of colored organic compounds that have been extensively used in both industry, such as textiles, papers, cosmetics, and in analytical chemistry. About a half of global production of synthetic textile dye is classified to azo compounds that have the chromophore of −N=N− unit in their molecular structure. These azo dyes are known to be largely nonbiodegradable in aerobic conditions and known to be reduced to more hazardous intermediates in anaerobic conditions. Of the dyes available on the market today, approximately 50–70% are azo compounds followed by the anthraquinone group. Some azo dyes and their dye precursors have been shown to be or are suspected to be human carcinogens as they form toxic aromatic amines [36-38]. Therefore azo dyes are pollutants of high environmental impact and were selected as the most relevant group of dyes concerning their degradation using TiO_2 assisted photocatalysis. In this study the degradation two azo dyes, Acid Orange7 and Acid Red1 was studied using the doped catalysts and pure titania [31].

Acid Orange7

Acid Orange 7 is a popular water-soluble dye that is used for dyeing a variety of materials such as nylon, aluminum, detergents, cosmetics, wool, and silk. It is highly toxic, and its ingestion can cause eye, skin, mucous membrane, and upper respiratory tract irritation, severe headaches, nausea, water-borne diseases such as dermatitis and loss of bone marrow leading to anemia. Its consumption can also prove fatal, as it is carcinogenic in nature and can lead to tumors [39].

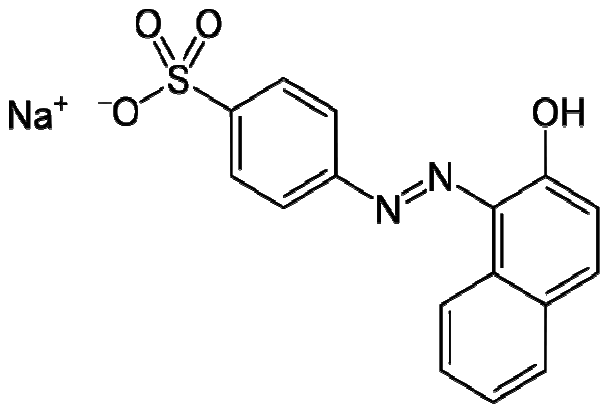

Fig. 4.1 Structure of Acid Orange7

Acid Red 1

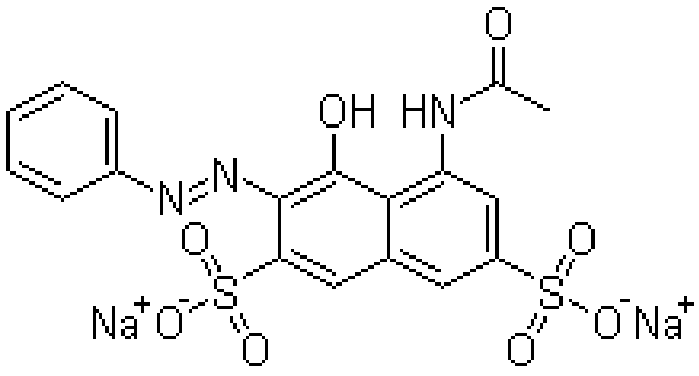

Fig. 4.2 Structure of Acid Red1

4.2.1 Effect of time

The effect of time on the photocatalytic degradation of Acid orange 7 and Acid Red 1 was studied using TU2, U2 and T as catalysts. For this 10ml of 10^{-4}M dye solution and 1g/L of catalyst was used. Prior to irradiation, the solution was magnetically stirred in the dark for 30 minutes to ensure the establishment of an adsorption/desorption equilibrium. Irradiations were carried out under visible light using 150W Xe lamp.

The percentage degradation was studied for a time range of 15 to 60 minutes. After photodegradation, the solution was centrifuged and recorded the absorbance using spectrophotometer. In the case of Acid Orange 7 the absorbance was taken at the wavelength 483 nm and for Acid Red 1 at 530nm.

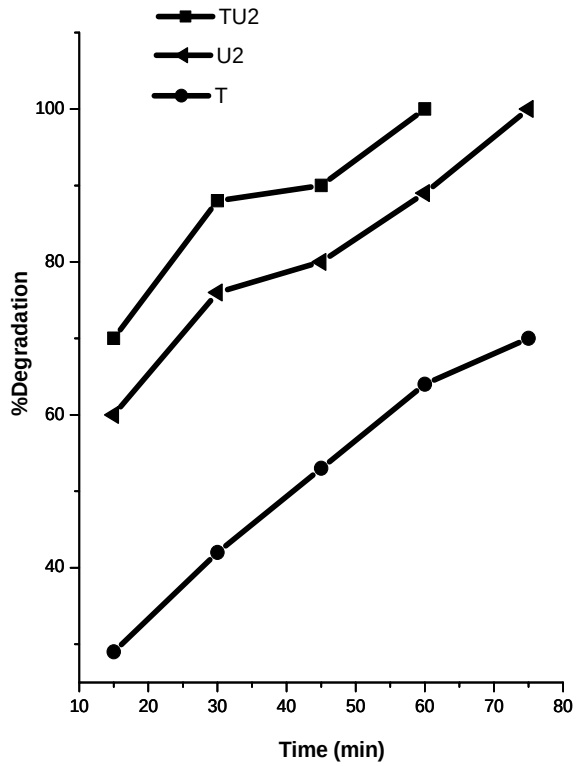

Fig. 4.3 %Degradation of Acid Orange 7 against time
Amount of catalyst 1g/L; Dye concentration 10ml of 10^{-4}M

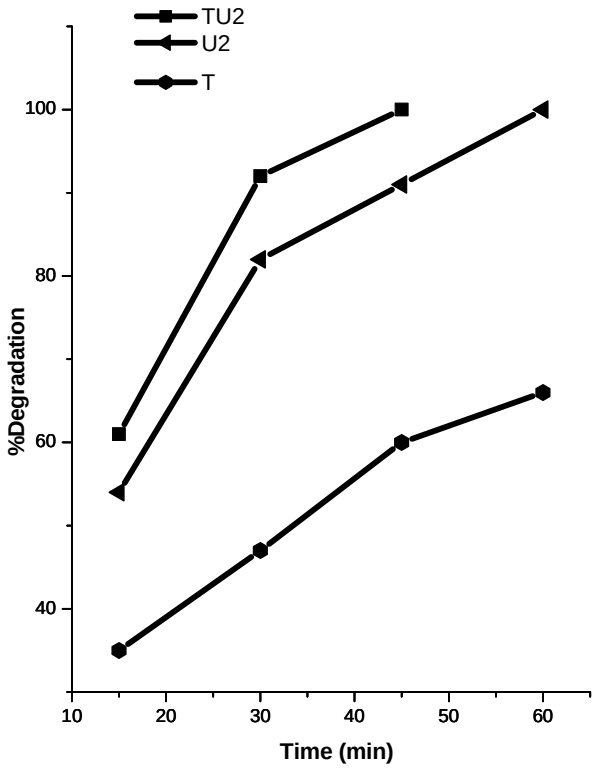

Fig. 4.4 %Degradation of Acid Red 1 against time
Amount of catalyst 1g/L; Dye concentration 10ml 10^{-4}M

Results (fig.4.3 and 4.4) show that as time increase the percentage degradation increases. The doped photocatalyst showed higher photoactivity than the undoped titania for the degradation of both these dyes. In the case of Acid Orange7, 88% degradation was achieved with in 30 minutes whereas complete degradation was achieved in 1hour when TU2 was used as photocatalyst. 64% degradation was achieved after 1hour using undoped titania.

In the case of Acid Red 1 complete degradation was achieved after 45 minutes of irradiation using TU2 as catalyst. 66% degradation was achieved after 1hour using pure titania. The results indicate that as time increases the amount of light falling on the catalyst surface increases which increases the formation of photoexcited species thereby enhances the photocatalytic activity.

4.2.2 Effect of catalyst concentration

The effect of catalyst concentration on the photodegradation of Acid Orange7 and Acid Red1 was investigated by employing different concentrations of TU2 catalyst varying from 0.5 to 3 g/L. 10ml of 10^{-4}M of dye solution was used in all cases and it was irradiated for 30 minutes using visible light.

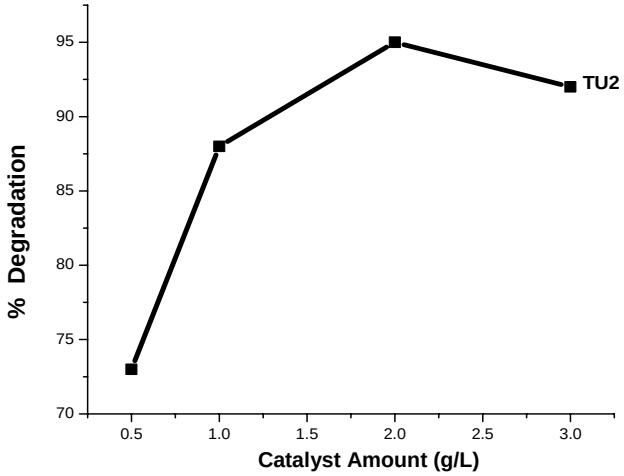

Fig. 4.5 % Degradation of Acid Orange 7against amount of catalyst Irradiation time 30 minutes; Dye concentration 10ml 10^{-4}M

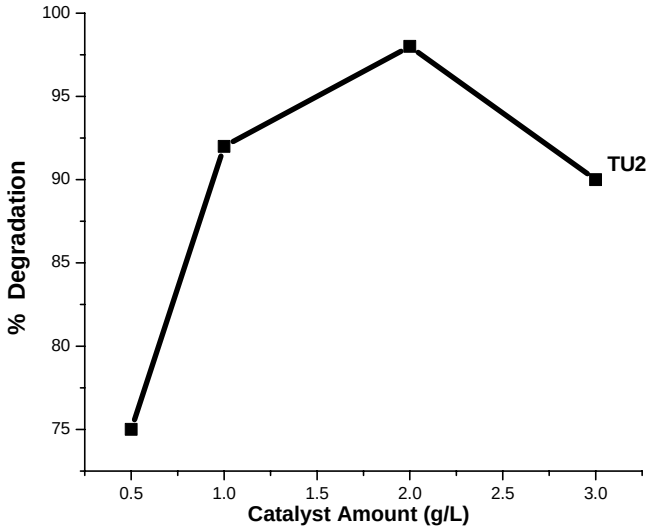

Fig. 4.6 % Degradation of Acid Red1 against amount of catalyst Irradiation time 30 minutes; Dye concentration 10ml of 10^{-4}M

The percentage degradation of the dyes was found to increase, then decrease with the increase in the catalyst concentration (fig.4.5, 4.6). This can be rationalized in terms of availability of active sites on TiO_2 surface. The availability of active sites increases with the increase of catalyst loading. The decrease in the percentage of degradation at higher catalyst loading may be due to agglomeration of particles. In such a condition, part of the catalyst surface probably became unavailable for photon absorption and dye adsorption, thus decreasing the catalytic reaction [31, 40].

4.2.3 Effect of dye concentration

The effect of initial dye concentration was studied by employing different concentration of dye varying between $0.8x10^{-4}$M to $3x10^{-4}$M and in each case 10ml of dye solution was taken and 1g/L of TU2 catalyst was used. The solution was irradiated for a time of 30 minutes using visible light.

Results presented in table 4.1 clearly show that the time required for complete decolorization of aqueous solutions of dyes strongly depends on the initial concentration of the dye. The time required for complete decoloristion of Acid Orange 7 and Acid Red1 increases with increase of dye concentration. At very low concentration especially at 10^{-5} M solution 100% decolorisation of both dyes takes place within 10 minutes whereas for 10^{-4} M solution complete decolorisation was achieved after 60 minutes for Acid Orange 7 and after 45 minutes for Acid Red1 when TU2 was used as photocatalyst.

Table 4.1 Time for complete degradation of Acid Orange 7 and Acid Red 1 at different dye concentrations; Amount of TU2 catalyst 1g/L

Dye concentration (M)	Time for complete decolourisation (min)	
	Acid Orange7	Acid Red 1
10^{-5}	10	10
10^{-4}	60	45

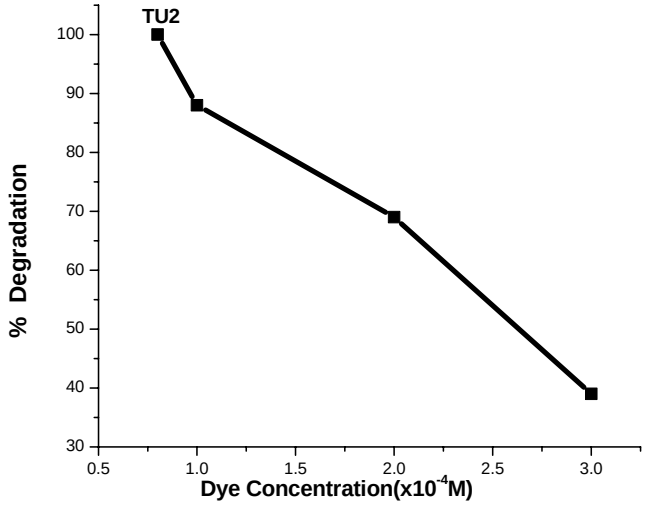

Fig. 4.7 % Degradation of Acid Orange 7 against dye concentration Irradiation time 30 minutes; Amount of catalyst 1g/L

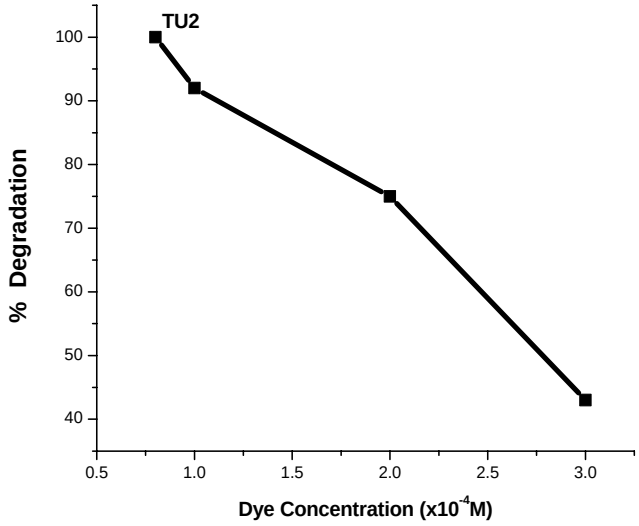

Fig. 4.8 % Degradation of Acid Red1 against dye concentration Irradiation time 30 minutes; Amount of catalyst 1g/L

It can be seen that as the dye concentration increase the percentage degradation decreases rapidly (fig. 4.7 and 4.8). The presumed reason is that at high dye concentrations the generation of •OH radicals on the surface of catalyst are reduced since the active sites are covered by dye ions. Another

possible cause for such results is the light screening effect of the dye itself. At high dye concentration, a significant amount of light may be absorbed by the dye molecules rather than the TiO_2 particles and that reduces the efficiency of the catalytic reaction because the concentrations of •OH decreases [31,41-47].The degradation is quite fast at low initial dye concentration. Hence, it is concluded that as initial concentration of the dye increases, the requirement of catalyst surface needed for the degradation also increases [7].

4.2.4 Effect of dopants

The photocatalytic degradation of dye was studied using doped samples with different concentration of dopants. The line diagram represents the percentage degradation of Acid Orange 7 using all ratios of metal and non metal doped catalyst within a time of 30 minutes under visible light irradiation.

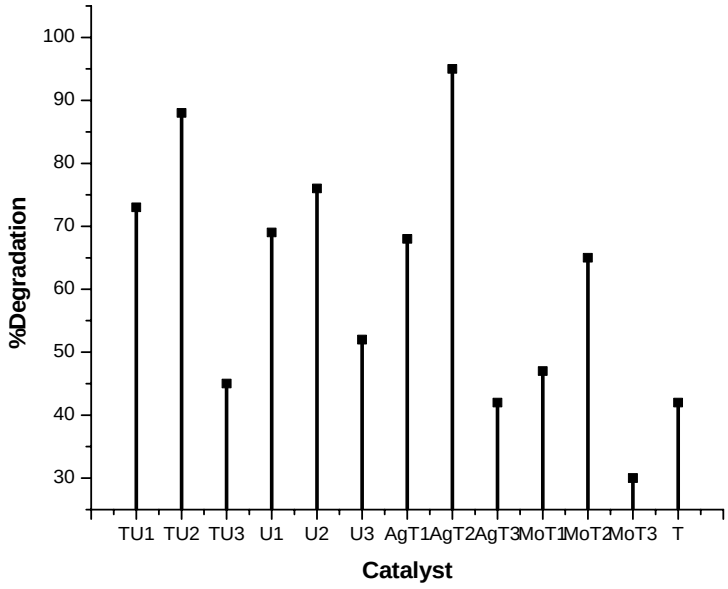

Fig. 4.9 % Degradation of Acid orange 7 using different catalysts Irradiation time 30 minutes; Amount of catalyst 1g/L; Dye concentration 10ml of 10^{-4}M

It shows an interesting trend, where, for all dopants, there appears to be an optimal dopant concentration above which, the observed photoreactivity

decreases. In the case of N and N-S doped catalysts high activity was observed with catalysts prepared in 1:5 mole ratio of TTIP and urea/thiourea (TU2 and U2 respectively). In the case of metal doped TiO_2 catalysts high activity was observed for 1wt% metal doped TiO_2 (AgT2 andMoT2).

The observed optimum dopant concentration can be related to the charge transfer process involved in the photocatalytic mechanisms. Once excitation occurs in the semiconductor, the created electron-hole pair can undergo charge transfer to adsorbed species on the semiconductor surface. The addition of dopant can promote interfacial charge transfer process.

At lower concentration below the optimal value, photoactivity increases with increase of dopant concentration because there are fewer trapping sites available at low concentration of dopant and the number of trapping sites increases with concentration of dopant. This means that the number of trapped carriers in doped TiO_2 is the highest at the optimum ratio for which the highest activity was observed.

However, when the concentrations of dopant ions are above the optimum ratio, the dopant atoms become the recombination centres [48]. This can be seen from the reduced photocatalytic efficiency of the catalyst with doping ratio above the optimum value.

The existence of the optimum value can also be associated with the amount of active sites on TiO_2. These active sites however will be easily blocked if the amount of dopants is too high or above the optimum value. The blocking process will reduce the probability of further charge transfer process and consequently decrease the amount of photocatalytic reaction.

The photo activities of doped TiO_2 are widely dependent upon the specific dopant also as shown in fig. 4.10. The figure represents the effect of different dopants on the percentage degradation of Acid Red1.

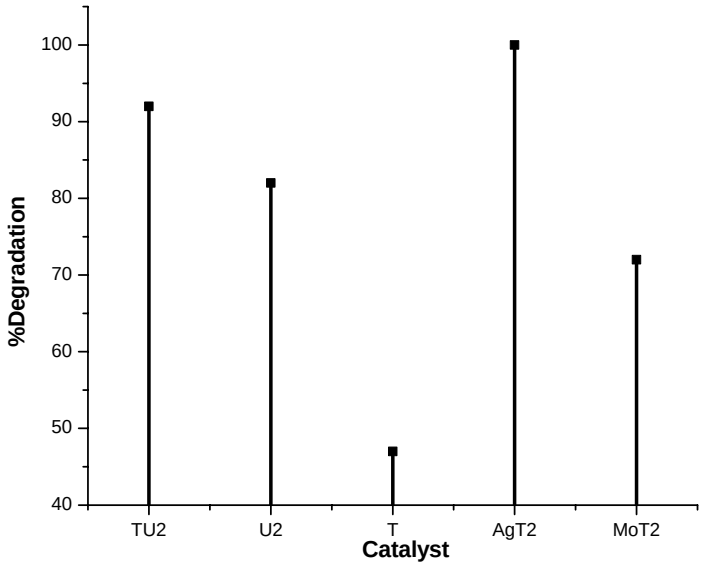

Fig. 4.10 % Degradation of Acid Red 1 using different catalysts Irradiation time 30 minutes; Amount of catalyst 1g/L; Dye concentration 10ml of 10^{-4}M

It can be seen that doping with N, N-S, Ag, Mo enhance the photoactivity of TiO_2 in Acid Orange 7 and Acid Red1 while pure titania shows very low activity at visible light. The different activities exhibited by different doped catalysts could be attributed to the efficiency of the dopants in trapping charge carriers. In addition, the absorbance in visible-light region of catalysts was also an important factor to influence the visible-light activity of catalysts.

4.2.5 Effect of light source

Experiments were conducted using visible light, UV light and under dark condition.150W Xe lamp was used as source of light. Dichoric mirror of wavelength, 280-420 nm (for UV light), and 420-630 nm dichoric mirror(for

visible light) were used. 10ml 10^{-4}M dye solution and 1g/L of catalyst was used for the studies and the solution was irradiated for 30 minutes. Catalysts TU2, AgT2 and T were used for the studies. A blank experiment was also carried out in the absence of catalyst. Table 4.2 shows the effect of light source of different wavelength on the photodegradation of dyes using undoped and doped TiO_2.

Table 4.2 % Degradation of Acid Orange 7 and Acid Red1 against light source

Light	% degradation of Acid Orange 7			% degradation of Acid Red1		
	TU2	AgT2	T	TU2	AgT2	T
Visible light (420-630 nm)	88	95	42	92	100	47
UV light (280- 400nm)	70	76	58	74	80	65

Table 4.3 % Degradation of Acid Orange 7 and Acid Red 1 in absence of light/catalyst

studies	% degradation of Acid Orange 7	% degradation of Acid Red1
Without catalyst	3	4
Without light	5	6

The doped catalysts shows higher degradation in visible light compared to undoped titania. This result clearly shows that doping increase the photoactivity of TiO_2 in visible light and also shows the possibility of utilizing sunlight for photodegradation. It was also observed that no decolorization of the solution was achieved in the absence of light, indicating that the decolorization process is photo-induced. It is obvious that the degradation is achieved by using UV and visible light in the presence of catalysts and fastest degradation was achieved by using radiation which contains visible light with doped catalysts.

The blank experiments conducted in the absence of photocatalyst, did not result in any measurable degradation of Acid Orange7 and Acid Red1. So effective destruction of these dyes are possible in the presence of light and catalysts suggesting that the degradation occurs through photocatalytic mechanism [31, 48] .

4.3 Methylene Blue

Methylene blue is a heterocyclic aromatic chemical compound with the molecular formula $C_{16}H_{18}N_3SCl$. It has many uses in a range of different fields, such as biology and chemistry.

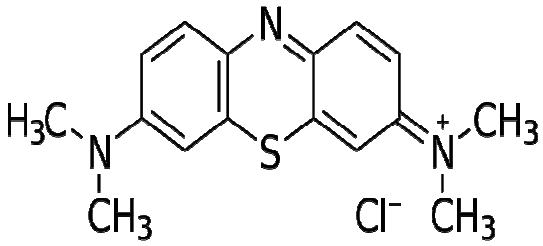

Fig.4.11 Structure of Methylene Blue

The reason for choosing methylene blue dye is due to its wider applications that include coloring paper, temporary hair colorant, dyeing cottons, wools and coating for paper stock and thus acute exposure to methylene blue will cause health problems such as increased heart rate, vomiting, shock, heinz body formation, cyanosis and tissue necrosis in humans [49].

4.3.1 Effect of time

Effect of time on photocatlytic degradation of methylene blue was studied using TU2, U2 and T as catalysts. Experiments were carried out using 1g/L of catalyst and 10ml of 10^{-4}M dye solution. Prior to irradiation, the solution was magnetically stirred in the dark for 30 minutes to ensure the

establishment of an adsorption/desorption equilibrium. Irradiations were carried out under visible light using 150W Xe lamp. After irradiation the solution was centrifuged to remove the catalyst and the absorbance was measured at 653nm.

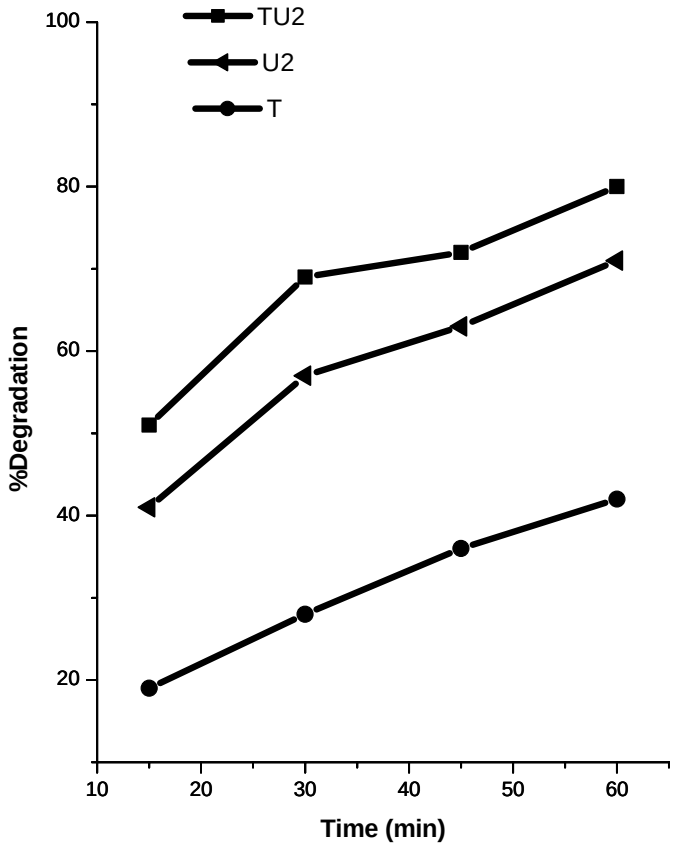

Fig. 4.12 % Degradation of Methylene Blue against time
Amount of catalyst 1g/L; Dye concentration 10ml of 10^{-4}M

Fig.4.12 shows the percent degradation of Methylene Blue against the irradiation time using undoped and doped TiO_2. The percentage degradation increases with increase in irradiation time. The photodegradation of Methylene Blue was significantly high with doped catalyst where 88% of dye was

degraded with TU2 catalyst in visible light irradiation within one hour where as only 42% degradation was achieved when pure titania was used as catalyst.

The changes of the UV-Vis. spectra during the photocatalytic degradation process of the methylene blue dye in the aqueous solution using TU2 photocatalyst under visible irradiation are shown in fig.4.13

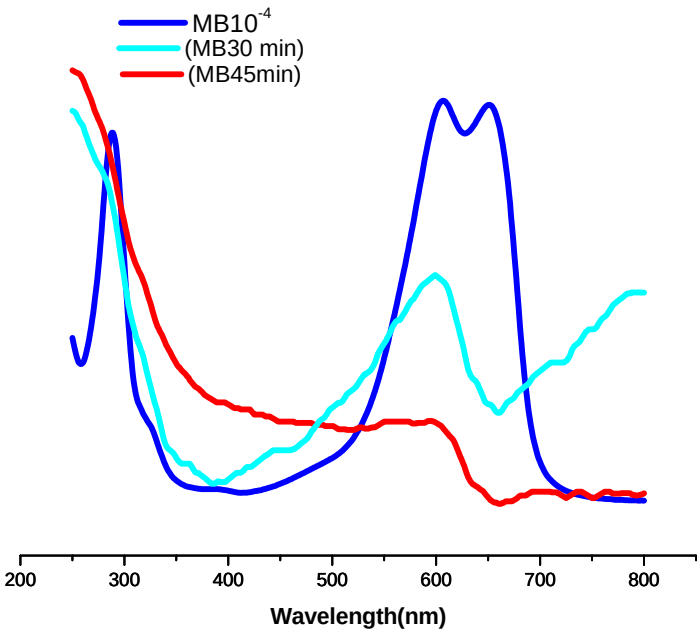

Fig.4.13 Absorbance spectra of Methylene Blue after phtocatalytic treatmement for 30 and 45 minutes

During light irradiation with catalyst, the characteristic absorption band of the dye around 653 nm decreased rapidly.

4.3.2 Effect of catalyst concentration

The effect of catalyst concentration on the degradation of Methylene Blue was investigated by employing different concentrations of TU2 catalyst varying from 0.5 to 3 g/L. 10ml of 10^{-4}M of dye solution was used and it was irradiated for 30 minutes using visible light.

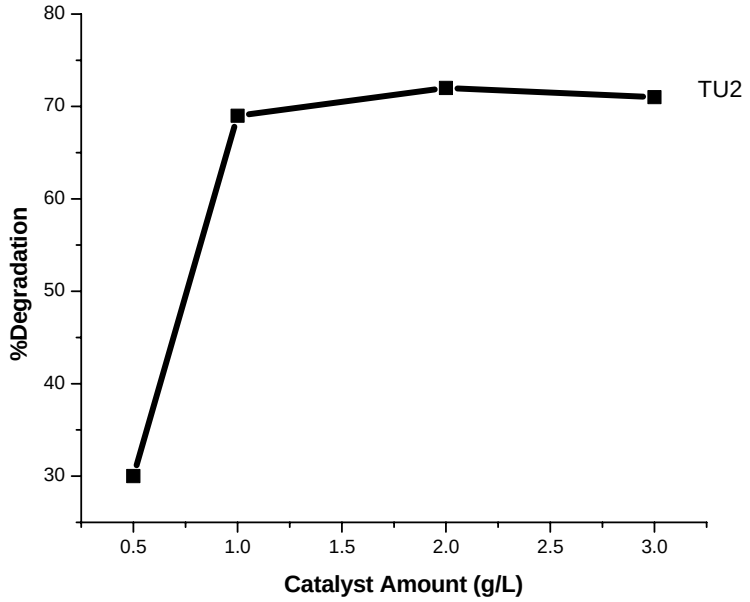

Fig. 4.14 % Degradation of Methylene Blue against amount of catalyst Irradiation time 30 minutes; Dye concentration 10ml of 10^{-4}M

The percentage degradation of Methylene Blue increases with the increase in catalyst concentration from 0.5 to 2 g /L and a further increase in catalyst concentration leads to a decrease in degradation (fig.4.14). At high TiO_2 concentrations, particles aggregate which in turn reduces the interfacial area between the reaction solution and the photocatalyst. Thus, the number of active sites on the catalyst surface is decreased. The increase in opacity and light scattering by the particle may be the other reasons for the decrease in the degradation at higher catalyst concentration [50].

4.3.3 Effect of dye concentration

The initial dye concentration was varied between $0.8x10^{-4}$M to $3x10^{-4}$M and 1g/L of TU2 catalyst was used and solution was irradiated for 30 minutes under visible light. The influence of the initial dye concentration on the decolorisation of Methylene Blue is presented in fig. 4.15.

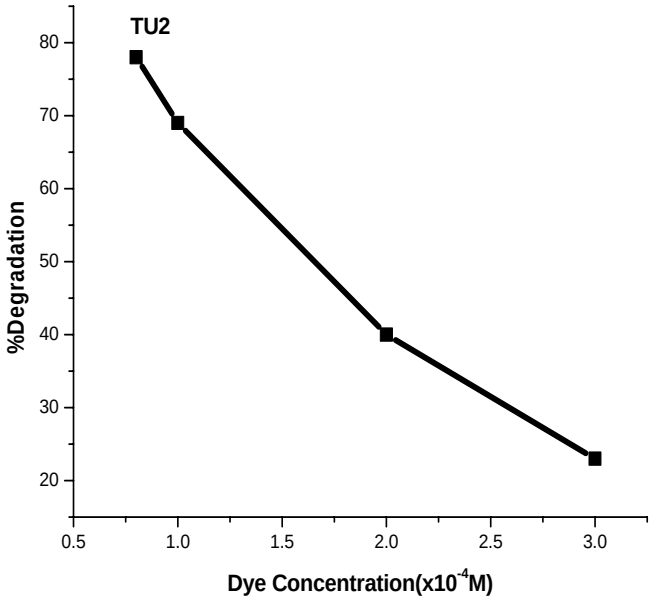

Fig. 4.15 % Degradation of Methylene Blue against dye concentration Irradiation time 30 minutes; Amount of catalyst 1g/L

Table 4.4 Time for complete decolorisation of Methylene Blue at different dye concentration; Amount of TU2 catalyst 1g/L

Dye concentration (M)	Time for complete decolourisation (min)
10^{-5}	10
10^{-4}	80

Table 4.4 shows the time required for the complete decolorisation of Methylene Blue at low and high concentration. It is clearly observed that the time required for the decolorization of Methylene Blue solutions depend significantly on the initial dye concentration. At low dye concentration complete decolorization of the solutions takes place in less than 15 minutes whereas for 10^{-4}M concentration complete decolorisation was achieved after 80 minutes.

This is an obvious observation where the amount of dye degraded depend on the amount of hydroxyl radicals on the catalyst, which in turn

depend on the number of holes generated on the catalyst. Therefore with a lower concentration of dye the hydroxyl radicals generated by the holes is sufficient enough to degrade the low quantity of Methylene Blue. But with the higher dye concentration the amounts of the radicals is insufficient to degrade the dye [30, 31].

4.3.4 Effect of dopants

The effect of dopants on the photocatalytic degradation of dye was studied using undoped titania (T) and all catalysts with optimal concentration of dopants (TU2, U2, AgT2, MoT2). The line diagram represents the percentage degradation of Methylene Blue using metal and non metal doped catalyst within a time of 30 minutes. The experiment was carried out using 10ml of 10^{-4}M dye solution and1g/L of catalyst under visible light irradiation.

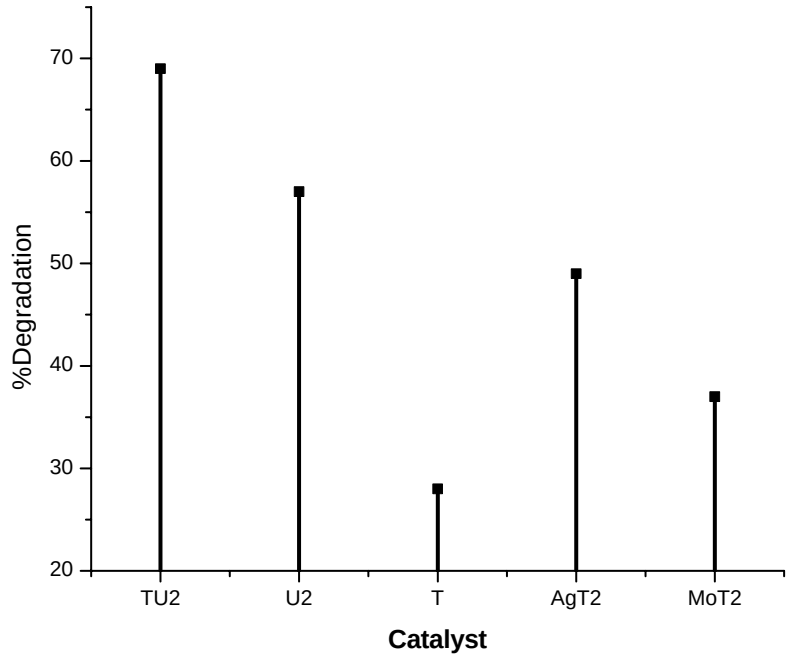

Fig. 4.16 % Degradation of Methylene Blue using different catalysts Irradiation time 30 minutes; Amount of catalyst 1g/L; Dye concentration 10ml of 10^{-4}M

It can be seen that all the doped catalysts show a higher degradation compared to undoped titania. The highest degradation was observed when TU2 was used as catalyst. The larger specific surface area induced by doping would enhance the adsorption capacity of doped titania for organic substrates, which is of benefit to the photocatalytic reaction. In addition, absorbance in visible-light region of catalysts was also an important factor to influence the visible-light activity of catalysts.

4.3.5 Effect of light source

Experiments were conducted using visible light, UV light and under dark condition.150W Xe lamp was used as source of light. Dichoric mirror of wavelength, 280-420 nm (for UV light), and 420-630 nm dichoric mirror (for visiblelight) were used. 10ml 10^{-4}M dye solution and 1g/L of catalyst was used for the studies and the solution was irradiated for 30 minutes. Catalysts TU2, AgT2 and T were used for the studies. A blank experiment was also carried out in the absence of catalyst.

Table 4.5 shows the effect of light source of different wavelength on the photodegradation of dyes using undoped and doped TiO_2.

Table 4.5 % Degradation of Methylene Blue against light source

Light	% degradation		
	TU2	AgT2	T
Visible light (420-630 nm)	69	49	28
UV light (280- 400nm)	52	39	38

Table 4.6 % Degradation of Methylene Blue in absence of light/catalyst

studies	% degradation
Without catalyst	--
Without light	5

The results clearly indicate the applicability of the photocatalytic method for the degradation of aqueous solutions of Methylene Blue. Under this condition, the process is quite fast, especially for low initial dye concentrations. Under identical experimental conditions but in the dark, there is no change in the concentration of the dye with time, indicating that the observed changes are due to a photo-induced process. In addition, blank experiments conducted in the presence of visible radiation but in the absence of photocatalyst did not result in any measurable degradation of Methylene Blue. The doped catalysts show higher degradation in visible light region compared to undoped titania. The superior activity of doped photocatalysts could be attributed to the improved visible light absorption [51].

4.3.6 Reusability of catalysts

During photocatalytic treatment catalyst recycling is one of the major challenges towards large scale application. Catalyst fouling and loss of catalyst during filtration is major cause behind drop in efficiency of the catalyst. The reusability test was carried out using TU2 and U2 catalysts. 10ml of 10^{-4}M dye solution and 1g/L of catalyst were used and it was irradiated with visible light for 30 minutes. During our studies the catalyst was effectively recycled for two times but with reduction in the degradation efficiency. After each run the catalyst was filtered using a whatmann filter paper and catalyst was activated at 150^{o}C.

Table 4.7 Reusablity of catalyst
Irradiation time 30 minutes; Amount of catalyst 1g/L; Dye concentration 10 ml of 10^{-4}M

cycle	% degradation of Methylene Blue (30 min)	
	TU2	U2
1st cycle	69	57
2nd cycle	67	56
3rd cycle	59	47

The observed decrease of photocatalyst activity was attributed to the decrease of active surface sites. After long and repeated use of the catalyst, the reaction residues and intermediates generated during the decomposition of dye was accumulated and adsorbed strongly on the catalyst surface. This will reduce the number of active sites and led to the reduced photocatalytic activity of the catalyst.

4.4 Crystal Violet

Crystal Violet is a triphenyl methane dye. Triphenylmethane dyes are used extensively in textile industry for dyeing nylon, wool, cotton, and silk, as well as for coloring of oil, fats, waxes, varnish, and plastics. Paper, leather, cosmetic, and food industries consume a high quantity of triphenylmethane dyes in various kinds. However, there is a great concern about the thyroid peroxidase-catalyzed oxidation of the triphenylmethane class of dyes because the reactions might form various N-de-alkylated primary and secondary aromatic amines, whose structures are similar to aromatic amine carcinogens [40].Chemical structure of the Crystal Violet is shown in fig. 4.17.

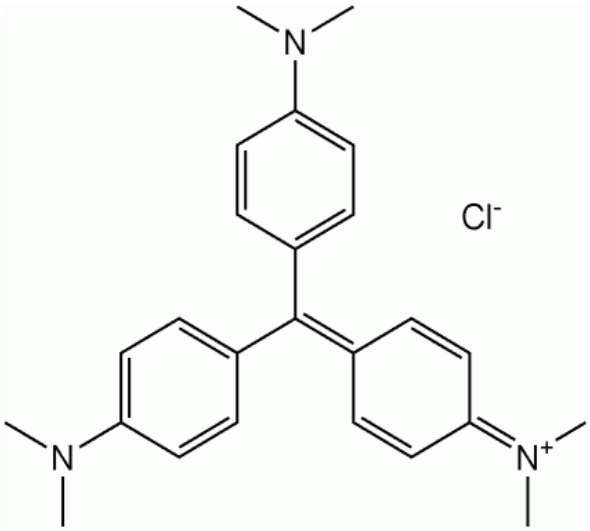

Fig.4.17 Structure of Crystal Violet

4.4.1 Effect of time

Effect of time on photocatalytic degradation of Crystal Violet was studied using TU2, U2 and T as catalysts. Experiments were carried out using 1g/L of catalyst and 10ml of 10^{-4}M dye soslution. Prior to irradiation, the solution was magnetically stirred in the dark for 30 minutes to ensure the establishment of an adsorption/desorption equilibrium. Irradiations were carried out under visible light using 150W Xe lamp. After irradiation the solution centrifuged to remove the catalyst and the absorbance was measured at 583 nm.

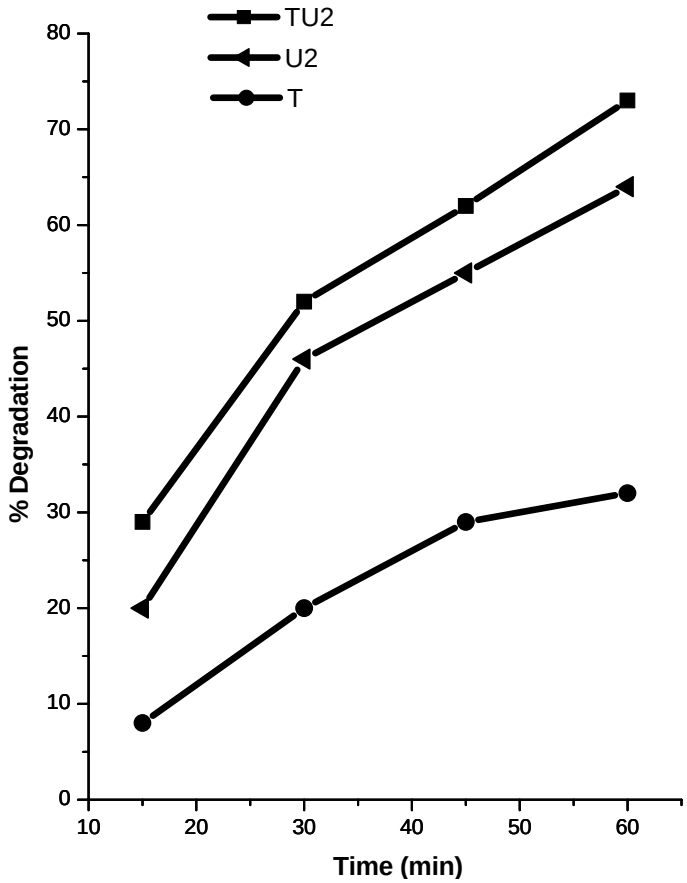

Fig. 4.18 %Degradation of Crystal Violet against time
Amount of catalyst 1g/L; Dye concentration 10ml 10^{-4}M

Fig.4.18 shows the percentage degradation of Crystal Violet against the irradiation time using undoped and doped TiO_2. The percentage degradation increases with increase in irradiation time. The doped photocatalyst showed higher photocatalytic activity than undoped titania for the degradation of Crystal Violet. 73 % of dye was degraded with TU2 catalyst in visible light irradiation within one hour where as 32% degradation was achieved with pure titania. In all the following experiments TU2 was used since it showed better activity.

4.4.2 Effect of catalyst concentration

The effect of catalyst concentration on the degradation of Crystal Violet was investigated by employing different concentrations of TU2 catalyst varying from 0.5 to 3 g/L. 10ml of 10^{-4}M of dye solution was used in all cases and the solution was irradiated for 30 minutes using visible light.

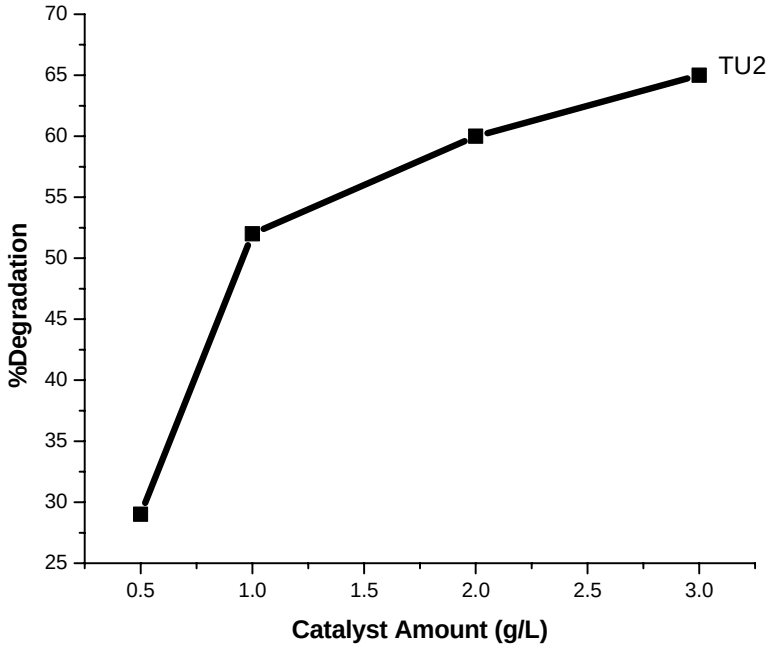

Fig.4.19 % Degradation of Crystal Violet against amount of catalyst Irradiation time 30 minutes; Dye concentration 10ml of 10^{-4}M

The photodegradation of Crystal Violet was found to increase with the increase in the catalyst concentration (fig.4.19)which is a general characteristic of heterogeneous photocatalyst [40,52].

4.4.3 Effect of dye concentration

The initial dye concentration was varied between $0.8x10^{-4}$M to $3x10^{-4}$M and 1g/L of TU2 catalyst was used and solution was irradiated for 30 minutes under visible light.

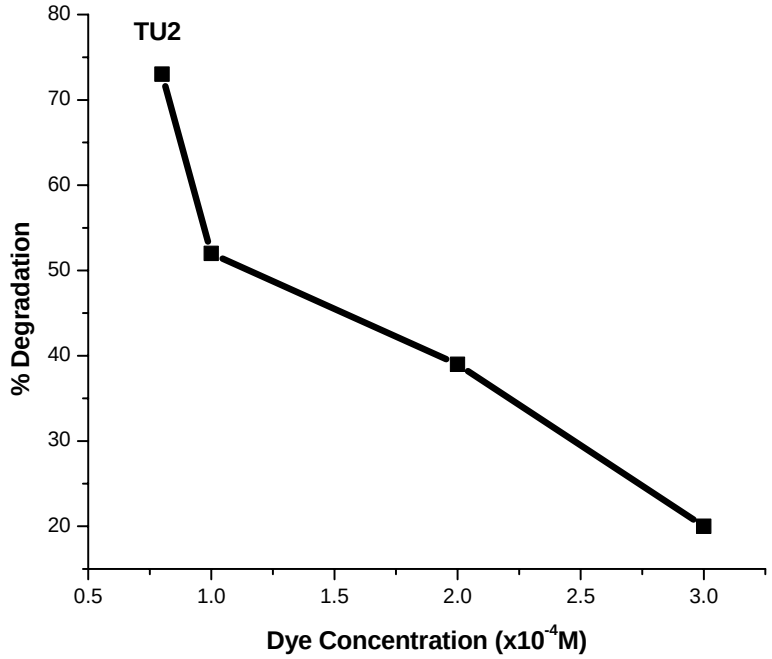

Fig.4.20 % Degradation of Crystal Violet against dye concentration Irradiation time 30 minutes; Amount of catalyst 1g/L

Table 4.8 Time for complete decolorisation of Crystal Violet at different dye concentration

Dye concentration M	Time for complete decolourisation (min)
10^{-5}	15
10^{-4}	90

It is clearly observed that the time required for the decolorization of Crystal Violet depend significantly on the initial dye concentration. At low dye concentration complete decolorization of the solution takes place in 15 minutes whereas for 10^{-4}M concentration complete decolorisation was achieved after 90 minutes.

With a lower concentration of dye the hydroxyl radicals generated by the holes is sufficiently high enough to degrade the low quantity of dye. But with the higher dye concentration the amount of the radicals is insufficient to degrade Crystal Violet [30, 31].

In addition, it should be taken into account that the incident photons can be absorbed either by the TiO_2 or by dye molecules present in the solution. Increasing dye concentration leads to an increase of the amount of photons which are absorbed by the dye molecules and never reach the photocatalyst surface.

4.4.4 Effect of dopants

The effect of dopants on the photocatalytic degradation of dye was studied using undoped titania (T) and all samples with optimal concentration of dopants (TU2, U2, AgT2, MoT2). The line diagram represents the percentage degradation of Crystal Violet using metal and non metal doped catalyst within a time of 30 minutes. The experiment was carried out using 10ml of 10^{-4}M dye solution and1g/L of catalyst under visible light irradiation.

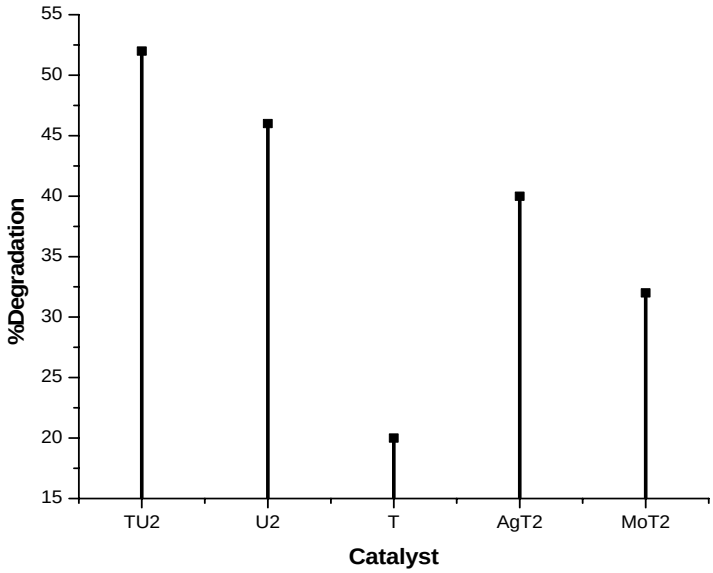

Fig.4.21 % Degradation of Crystal Violet using different catalysts Irradiation time 30 minutes; Amount of catalyst 1g/L; Dye concentration 10ml of 10^{-4}M

It can be seen that all the doped catalysts show a higher degradation compared to undoped titania. The highest degradation was observed when TU2 was used as catalyst. The superior photocatalytic activity of doped photocatalysts could be attributed to the smaller grain size and improved visible light absorption [51]. Also the presence of dopants increases the charge separation efficiency or prevents the recombination of electrons and holes.

4.4.5 Effect of light source

Experiments were conducted using visible light, UV light and under dark condition.150W Xe lamp was used as source of light. Dichoric mirror of wavelength, 280-420 nm (for UV light), and 420-630 nm dichoric mirror (for visible light) were used. 10ml 10^{-4}M dye solution and 1g/L of catalyst was used for the studies and the solution was irradiated for 30minutes. Catalysts TU2, AgT2 and T were used for the studies. A blank experiment was also carried out in the absence of catalyst under visible light.

Table 4.9 % Degradation of Crystal Violet against light source

Light	% degradation		
	TU2	AgT2	T
Visible light (420-630 nm)	52	40	20
UV light (280- 400nm)	41	31	32

Table 4.10 % Degradation of Crystal Violet in absence of light/catalyst

studies	% degradation
Without catalyst	--
Without light	4

It is observed that no decolorization of the solution is achieved in the absence of light, indicating that the decolorization process is photo-induced. It is obvious that the fastest degradation is achieved by using radiation which contains visible light, and doped catalysts where complete disappearance of the dye is achieved after at 90 minutes of irradiation. When only UV light is used, degradation takes place slowly. The blank experiments conducted in the presence of light, but in the absence of photocatalyst, did not result in any measurable degradation of Crystal Violet.

4.5 Acid Blue 25

Acid Blue25 is an anthraquinone dye with molecular formula $C_{20}H_{13}N_2NaO_5S$. The structure of Acid Blue 25 is given in fig. 4.22

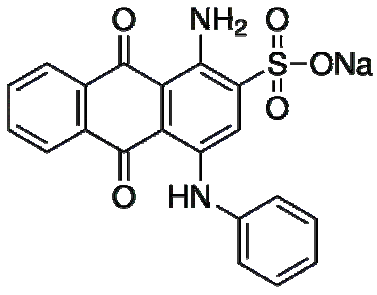

Fig. 4.22 Structure of Acid Blue 25

The photocatalytic degradation of Acid Blue 25 was studied. The effect of dopants, time and catalyst concentration was studied. Blank experiments were also carried out in dark, and in absence of catalyst.

4.5.1 Effect of time

The effect of time on the photocatalytic degradation of dyes was studied using TU2 as catalyst. For this 10ml of 10^{-4}M dye solution and 1g/L of catalyst was used. Prior to irradiation, the solution was magnetically stirred in the dark for 30 minutes to ensure the establishment of an adsorption/desorption equilibrium. Irradiations were carried out under visible light using 150W Xe lamp.

The percentage degradation was studied for a time range of 15 to 60 minutes. After photodegradation, the solution was centrifuged and recorded the absorbance using spectrophotometer. In the case of Acid Blue 25 the absorbance was taken at the wavelength 602 nm.

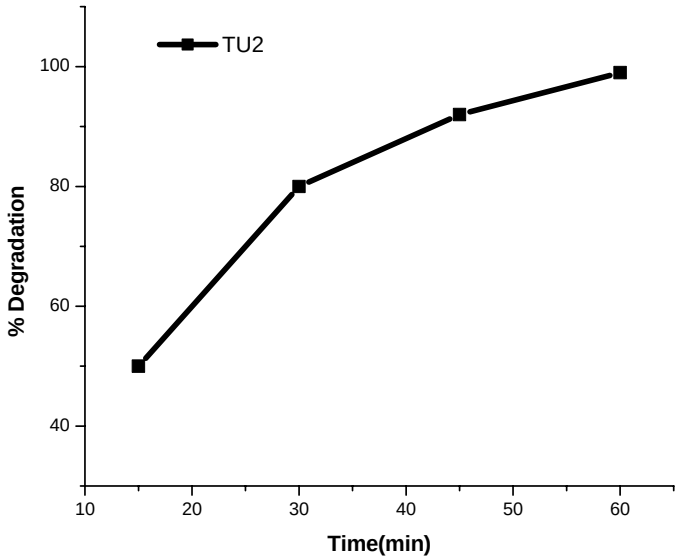

Fig.4.23 %Degradation of Acid Blue 25 against time
Amount of catalyst 1g/L; Dye concentration 10ml 10^{-4}M

The photocatalytic degradation of Acid Blue 25 against irradiation time is shown here. The percentage degradation increases with increase of irradiation time. As time increases more and more light energy falls on the catalyst which causes the generation of higher amount of photoexcited species. 99% degradation was achieved after 60 minutes irradiation in presence of TU2 catalyst.

4.5.2 Effect of catalyst concentration

The effect of catalyst concentration on the photodegradation Acid Blue25 was investigated by employing different concentrations of TU2 catalyst varying from 0.5 to 3 g/L. 10ml of 10^{-4}M of dye solution was used and the solution was irradiated for 30 minutes under visible light.

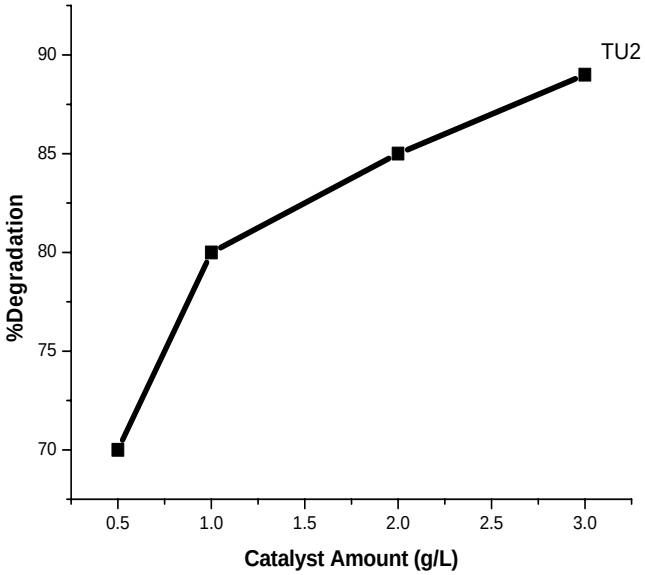

Fig.4.24 % Degradation of Acid Blue 25 against amount of catalyst Irradiation time 30 minutes; Dye concentration 10ml of 10^{-4}M

The photodegradation of the dyes was found to increase, with the catalyst concentration (fig.4.24) which is a general characteristic of heterogeneous

photocatalyst. This can be rationalized in terms of availability of active sites on TiO_2 surface. The availability of active sites increases with the increase of catalyst loading.

4.5.3 Effect of dopants

The effect of dopants on the photocatalytic degradation of dye was studied using undoped titania (T) and all samples with optimal concentration of dopants (TU2, U2, AgT2, MoT2). The line diagram represents the percentage degradation of Acid Blue 25 using metal and non metal doped catalyst within a time of 30 minutes. The experiment was carried out using 10ml of 10^{-4}M dye solution and1g/L of catalyst under visible light irradiation.

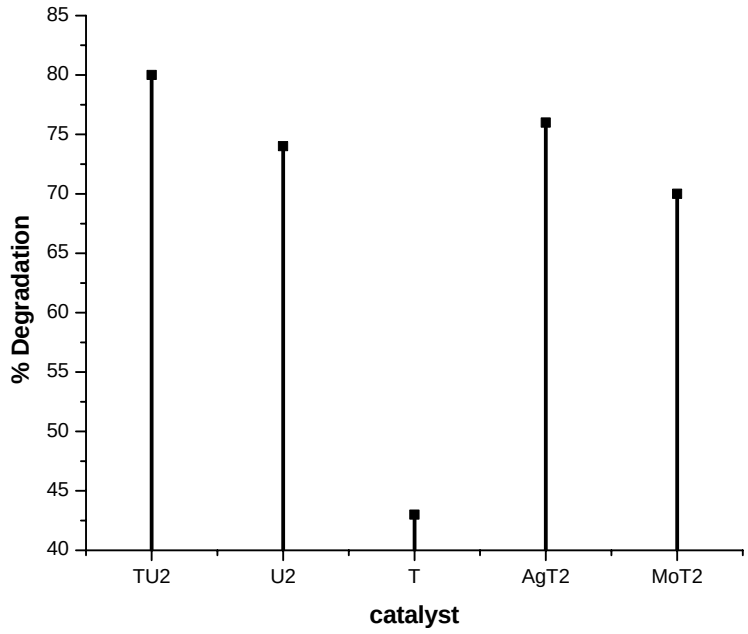

Fig.4.25 % Degradation of Acid Blue 25 using different catalysts Irradiation time 30 minutes; Amount of catalyst 1g/L; Dye concentration 10ml of 10^{-4}M

It can be seen that all the doped catalysts show a higher degradation compared to undoped titania. The highest degradation was observed when

TU2 was used as catalyst. All the doped catalysts showed greater than 70% degradation of Acid Blue 25 within 30 minutes where as pure titania shows only 43 % degradation .

4.5.4 Effect of light source

Experiments were conducted in dark condition and also in the absence of catalysts

Table 4.11 % Degradation of Acid Blue 25 in absence of light/catalyst

studies	% degradation
Without catalyst	2
Without light	3

Neglgible degradation was observed under dark condition. It should also be noted here that blank experiments conducted in the presence of light, but in the absence of photocatalyst, did not result in any measurable degradation of the dye. Results discussed so far clearly indicate the applicability of the photocatalytic method for the degradation of aqueous solutions of Acid Blue 25.

Effective destruction of all dyes are possible by photocatalysis in presence of doped catalysts and visible light.

4.6 TOC Analysis

Reaction intermediates are known sometimes to be formed by the oxidation of organic dyes and some may be longer-lived and even more toxic to aquatic animals and human beings than parent compounds. Although identifying the intermediates is very important in determining the reaction path this investigation more strongly focuses on the extent of mineralization. The removal of TOC is commonly used in the industrial treatment of wastewater to

determine this extent of mineralization. Therefore, this study addresses the removal of TOC from dye solution, rather than on identifying reaction intermediates [53].

The mineralisation of Acid Orange 7 was studied at different time intervals using TU2 as catalyst. 1g/L of catalyst and 20ml 10^{-4} M dye solution was used. Prior to irradiation, the solution was magnetically stirred in the dark for 30 minutes to ensure the establishment of an adsorption/desorption equilibrium. Irradiations were carried out under visible light using 150W Xe lamp.

The percentage TOC removal was studied for a time range of 1 to 3hours. After photodegradation, the solution was centrifuged and TOC was analysed using an Elemental Vario TOC analyser.

The percentage mineralisation= $(TOC_o - TOC_t / TOC_o) \times 100$ where TOC_o is the value of TOC for initial solution TOC_t is the value after time t.

Table 4.12 % Mineralisation of Acid Orange 7 against time

Time (hour)	%TOC removal
1	58
2	66
3	84

Decolourization of aqueous solutions of Acid Orange7 is much faster than TOC removal due to the formation of uncolored intermediates. 88% mineralisation was achieved after 3hours using TU2catalyst and visible light radiation. Complete mineralization is achievable under prolonged exposure. The results show that the catalyst does not only promote degradation but also does mineralisation of dyes.

References

[1] http://en.wikipedia.org

[2] J. Weber, V.C. Stickney, Wat. Res., 27 (1993) 63.

[3] C. Ràfols, D. Barceló, J. Chromatogr. A, 777 (1997) 177.

[4] A.Houas, H. Lachheb, M. Ksibi, E. Elaloui, C. Guillard, J.M.Hermann, Appl. Catal. B: Environ., 31 (2001) 145.

[5] U. Pagga, D. Bruan, Chemosphere, 15 (1986) 479.

[6] Bianco-Prevot, C. Baiocchi, M.C. Brussino, E. Pramauro, P. Savarino, V. Augugliaro, G. Marci, L. Palmisano, Environ. Sci. Technol., 35 (2001) 971.

[7] B. Neppolian, H. C.Choi, S. Sakthivel, B. Arabindoo, V. Murugesan, Chemosphere, 46(2002) 1173.

[8] M. Saquib, M. Muneer, Dyes Pigments ,56 (2003) 37.

[9] W.Z. Tang, H. An, Chemosphere, 31 (1995) 4157.

[10] V. Meshko, L. Markovska, M. Mincheva, A.E. Rodrigues, Wat. Res., 35 (2001) 3357.

[11] W.S. Kuo, P.H. Ho, Chemosphere ,45 (2001) 77.

[12] C. Galindo, P. Jacques, A. Kalt, Chemosphere, 45 (2001) 997.

[13] P. Cooper, J. Soc. Dyers. Colour., 109 (1993) 97.

[14] S.S. Patil, V.M. Shinde, Environ. Sci. Technol., 22 (1988) 1160.

[15] A.T. More, A. Vira, S. Fogel, Environ. Sci. Technol., 23 (1989) 403.

[16] M.C. Venceslau, S. Tom, J.J. Simon, Environ. Technol., 15 (1994) 917.

[17] I. Arslan, I. A. Balcioglou, Dyes Pigments, 43 (1999) 95.

[18] U. Pagga, K. Taeger, Wat. Res., 28 (1994) 1051.

[19] H. L. Sheng, M. L. Chi, Wat. Res., 27 (1993) 1743.

[20] S. H. Lin, W. Y. Liu, J. Environ. Eng., 120 (1994) 437.

[21] F. Strickland, S. Perkins, Text. Chem. Color., 5 (1995) 11.

[22] Y. M. Slokar, A. M. Le Marechal, Dyes Pigments, 37 (1998) 335.

[23] G. Liu, T. Wu, J. Zhao, H. Hidaka, N. Serpone, Environ. Sci. Technol., 33 (1999) 2081.

[24] J. Zhao, T. Wu, K. Wu, K. Oikawa, H. Hidaka, N. Serpone, Environ. Sci. Technol., 32 (1998) 2394.

[25] M. R. Hoffmann, S. T. Martin, W. Choi, D. W. Bahnemann, Chem. Rev., 95 (1995) 69.

[26] I. K. Konstantinou, T. A. Albanis, Appl. Catal. B: Environ., 42 (2003)319.

[27] A. L. Linsebigler, L. Guangquan, J. T. Yates, Chem. Rev., 95 (1995)735.

[28] P. Reeves, R. Ohlhausen, D. Sloan, K. Pamplin, T. Scoggins, Solar Energy, 48 (1992) 413

[29] C. S. Turchi, D. F. Ollis, J. Catal., 122 (1990) 178.

[30] Fotini Kiriakidou, Dimitris I. Kondarides, Xenophon E. Verykios, Catalysis Today 54 (1999) 119.

[31] Ioannis K. Konstantinou*, Triantafyllos A. Albanis,Applied Catalysis B: Environmental, 49 (2004) 1.

[32] X.Z. Li, M. Zang, Wat. Sci. Technol., 34 (1996) 49.

[33] Y. Wang, Wat. Res., 34 (2000) 990.

[34] S. Sakthivel, B. Neppolian, M. V. Shankar, B. Arabindoo, M. Palanichamy, V. Murugesan, Solar Energy Mater. Solar Cells, 77(2003) 65.

[35] V. Augugliaro, C. Baiocchi, A. Bianco-Prevot, E. Garcia-Lopez, V. Loddo, S. Malato, G. Marci, L. Palmisano, M. Pazzi, E. Pramauro, Chemosphere, 49 (2002) 1223.

[36] M. Stylidi, D. I. Kondarides, X. E. Verykios, Appl. Catal. B: Environ., 40 (2003) 271.

[37] C. Gomes da Silva, J. L. Faria, J. Photochem. Photobiol. A: Chem., 155 (2003) 133.

[38] M.A. Brown, S.C. De Vito, Crit. Rev. Environ. Sci. Technol., 23(1993) 249.

[39] V. K. Gupta, Alok Mittal, Vibha Gajbe, Jyoti Mittal, Ind. Eng. Chem. Res., 45(2006) 1446.

[40] Chiing-Chang Chen, Fu-Der Mai, Kung-Tung Chen, Chia-Wei Wu, Chung-Shin Lu Dyes and Pigments, 75 (2007) 434.

[41] W.Z. Tang, H. An, Chemosphere, 31 (1995) 4157.

[42] C.M. So, M.Y. Cheng, J.C. Yu, P.K. Wong, Chemosphere, 46 (2002)905.

[43] J. Grzechulska, A.W. Morawski, Appl. Catal. B: Environ., 36 (2002)45

[44] N. Daneshvar, D. Salari, A.R. Khataee, J. Photochem. Photobiol.A: Chem., 15(2003)111.

[45] L.B. Reutergarth, M. Iangphasuk, Chemosphere, 35 (1997) 585.

[46] A.Mills, R.H. Davis, D. Worsley, Chem. Soc. Rev., 22 (1993) 417.

[47] I. Poulios, I. Aetopoulou, Environ. Technol., 20 (1999) 479.

[48] Hao-Li Qin, Guo-Bang Gu, Song Liu, C.R. Chimie, 11 (2008) 95.

[49] Mohamed Mokhtar Mohameda, Mater M. Al-Esaimi, Journal of Molecular Catalysis A: Chemical, 255 (2006) 53.

[50] M. Faisal, M. Abu Tariq, M. Muneer Dyes and Pigments, 72 (2007) 233.

[51] Y. Liu, X.Chen, J. Li, C. Burda, Chemosphere, 61(2005)11.

[52] Saquib M, Muneer M. Dyes Pigments, 56(2003)37.

[53] Chan-Li Hsueh, Yao-Hui Huanga, Cheng-Chien Wang, Chuh-Yung Chena, Journal of Molecular Catalysis A: Chemical, 245 (2006) 78.

.....ൠ.....

Chapter

5

Photocatalytic Degradation of Pesticides

Contents

The photocatalytic degradation of some herbicides and insecticides has been investigated in aqueous suspension of TiO_2 under different conditions. The mineralization was studied by depletion in total organic carbon (TOC).The effect of operational parameters i.e., time, catalyst concentration, dopants, light source on the degradation of pesticides has been examined. Results show that the employment of efficient photocatalysts at optimal operational conditions may lead to degradation of pesticides.

5.1 Introduction

The term "pesticide" is a composite term that includes all chemicals that are used to kill or control pests. Pesticides are cause of pollution, affecting land and water in particular. The problem is huge and growing. Pesticides decrease biodiversity in soil because they do not just kill the intended pest; they often kill many other small organisms present.

The pesticide has a broader meaning, and includes many different kinds. The classification of pesticides is often based on the type of organism they target to control or kill. Pesticides can be insecticides, herbicides or fungicides.

5.1.1 Pesticide pollution

The problem of the pesticide pollution is increasing day by day due to its maximum use in the agricultural field and also pesticide contaminated water if taken above the permissible limits may lead to the serious health problems such as vomiting, nausea, diarrhea, hypertension and many others health related problems. Pesticide is a general term for substances, which are used to poison pests (weeds, insects, rodents etc). Synthetic pesticides have been popular with farmers, because of their widespread availability, simplicity in application, efficiency and economic returns. But they also have huge environmental costs. The heavy use of these chemicals has already caused grave damage to health, ecosystems and ground water.

The use of pesticides in agriculture contributes to environmental pollution. Pesticides are used to control the growth of insects, weeds, and fungi, which compete with humans in the consumption of crops. The different types of pesticides are bactericides (for the control of bacteria), fungicides

(for the control of fungi), herbicides (for the control of weeds), insecticides (for the control of insects) and virucides (for the control of viruses).

The water solubility of a pesticide determines how easily it goes into solution with water. When these compounds go into solution with water they can travel with it as it runs off the land or leaches through the soil. The control of organic pollutants in water is an important measure in environmental protection. A wide variety of pesticides are applied on agricultural sites which due to their chemical stability, resistance to biodegradation and sufficient water solubility penetrate into ground water. Their toxicity, stability to natural decomposition and persistence in environment has been cause of much environmental concern [1].

Development of appropriate methods for the degradation of contaminated water containing toxic compounds is necessary. Among many processes proposed for the degradation of organic contaminants, biodegradation has received the greatest attention. However many organic chemicals, especially those are toxic are nonamendable to microbial degradation. Recently considerable attention has been focused on the use of semiconductor as a means to oxidise toxic organic chemicals [2-5]. Photocatalytic oxidation processes are included within group of Advanced Oxidation Technologies. The process is extensively studied and developed today to the degradation of various organic compounds and pollutants in water [6].

The photocatalysed degradation of various organics employing irradiated TiO_2 is well documented in literature. In the case of heterogeneous photocatalysis, the interaction of a photon produces the appearance of electron/hole pairs, the catalyst being a semiconductor. Heterogeneous photocatalysis is a good method for the degradation of a number of pesticides in aqueous systems under non-

expensive solar irradiation. The initial step in TiO_2 mediated photocatalysed degradation is proposed to involve the generation of (e-/h+) pair leading to the formation of hydroxyl radical and superoxide radical anion. It has been suggested that the hydroxyl radicals are the primary oxidizing species in photocatalytic oxidation processes. The oxidative reaction would result in degradation of pollutant.

This present work focuses on the photocatalytic properties of prepared catalysts. We have selected a few pesticides for our study that have been used in agricultural field for better quality and quantity of crops. The selected pesticides are 2,4-D, 2,4,5-T, Monolinuron, Dazomet and Phosphamidon. The influence of the dopant content on the photocatalytic activity, have been investigated. The irradiation experiments were carried out with a light source of 150 W Xe lamp in visible region. The concentration of pesticide solution was 10^{-4} M and 20ml of solution was used for experiment. The concentration of TiO_2 was set as 1g/L.

Samples were withdrawn at different time intervals during the photodegradation and centrifuged immediately and percentage mineralisation was studied using TOC analysis. Total organic carbon (TOC) of the solution was measured using an Elemental Vario TOC analyser. The effects of operational parameters, such as time, catalyst concentration, light source, dopants were examined.

5.2 2,4-Dichlorophenoxy acetic acid(2,4-D) and 2,4,5 –Trichlrophenoxy acetic acid (2,4,5-T)

Phenoxy alkanolic acid herbicides are used extensively throughout the world to control weeds. They are used in lakes, ponds and ditches for aquatic weed control. 2,4-D and 2,4,5-T are most frequently used herbicides in this

group[7].The increasing contamination of our environment with chloro organic compounds is certainly one of the greatest problems for human future.

The structure of 2,4-D as follows

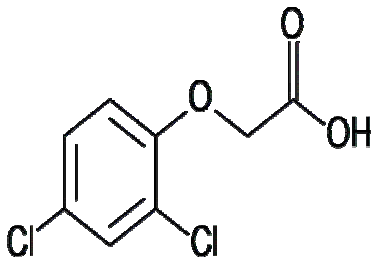

Fig.5.1 Structure of 2,4-D

There are approximately 1500 registered products that contain 2,4-D in their composition [8]. 2,4-D is one of the most commonly used herbicide in controlling broad leaf weeds and other vegetation. The widespread use of 2,4-D leads to a certain environmental impact, because this pesticides easily spread within the environment [9].

It is a pollutant of great environmental concern because of its relatively high solubility in water [7,10]. After its application to crops, the unused portions can leach below the root zone or be washed out during precipitation and contaminate nearby water sources. In addition various amounts of 2,4-D have been detected in surface water and in ground water not only during application but also after a long period of use. The degradation of these compounds is possible via chemical, photochemical, and biological processes, but most of them require long treatment periods and in practise are often difficult to apply in the disposal of waste waters. Photocatalysis is a subject of increasing interest as a method of waste water treatment. In these processes, the oxidation occurs through an attack by $OH^{\cdot}$ [11]. The oxidative photocatalytic

degradation of many chlorinated organic compounds by semiconductor particles, such as TiO_2 has been widely recommended as a promising method of water and waste water treatment processes [7,12,13]. 2,4,5-T is used in foerestry and in agriculture as a systematic herbicide. The amine salt of 2,4,5-Trichlorophenoxy acetic acid are extensively used for the control of dicotyledonous weeds in ceral crops. It has been used on wheat, barley, oats, and rice to kill weeds. There are about 400 products which contain 2,4,5-T. It considerably irritates eyes and skin. Chronic exposure causes impairement of liver function, changes in behaviour and nerve damages [1,14,15].

The structure of 2,4,5-T as follows

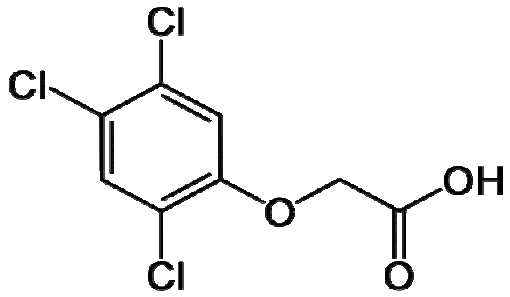

Fig. 5.2 Structure of 2,4,5–T

The photocatalytic degradation of 2,4-D and 2,4,5-T were studied using the prepared catalysts. Samples were withdrawn at different time intervals during the photodegradation and centrifuged immediately and percentage mineralization was studied using TOC analysis. The effects of operational parameters, such as time, catalyst concentration, light source, dopants were examined.

5.2.1 Effect of time

The effect of time on the photocatalytic degradation of pesticides was studied using TU2, U2 and T as catalysts. For this 20ml of10^{-4}M pesticide solution and 1g/L of catalyst was used. Prior to irradiation, the solution was magnetically stirred in the dark for 30 minutes to ensure the establishment of an adsorption/desorption equilibrium. Irradiation was carried out under visible light using 150W Xe lamp.

The effect of time on the degradation of 2,4-D and 2,4,5-T was examined in the reaction time ranging from 30 to 180 minutes. Samples were withdrawn at different time intervals during the photodegradation and centrifuged immediately and percentage mineralisation was studied using TOC analysis. The results of percentage mineralisation at different times are shown in fig. 5.3 and 5.4

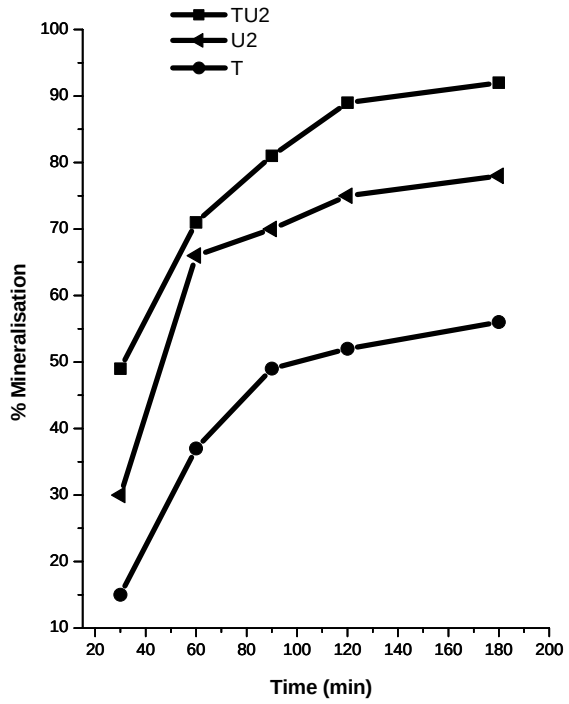

Fig.5.3 % Mineralisation of 2,4-D against time
Amount of catalyst 1g/L; Pesticide concentration 20ml of 10^{-4}M

It was found that 92% TOC was removed after 3 hours when TU2 was used as catalyst where as only 56% TOC was removed when undoped titania was used as catalyst.

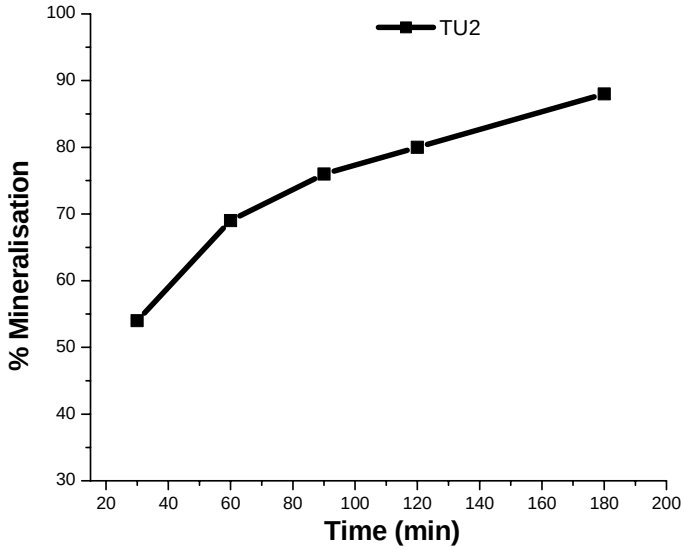

Fig.5.4 % Mineralisation of 2,4,5-T against time
Amount of catalyst 1g/L; Pesticide concentration 20ml 10^{-4}M

For studying the effect of time on photocatalytic degradation of 2,4,5-T only TU2 was used since it shows better photocatalytic activity. In the case of 2,4,5-T, 88% of TOC was removed after 3 hours suggesting that the catalyst is good for the photocatalytic degradation of 2,4-D and 2,4,5-T. After long time irradiation, these compounds may be completely mineralised.

From previous studies it was known that the photocatalytic degradation is through the attack of $OH^{\cdot}$ on the substrate [11,16].The attack of $OH^{\cdot}$ radical on the aromatic ring produces hydroxylated aromatic compounds. After the attachment of two OH groups the aromatic ring breaks and the subsequent products oxidised to CO_2 and water. In this study we concentrated more on

mineralization rather than studying the mechanism. Results show that as time increases the percentage mineralisation increases.

5.2.2 Effect of catalyst concentration

The effect of photocatalyst concentration on the degradation of 2,4-D was investigated by employing different concentrations of TU2 catalyst varying from 0.5 to 3 g/L. 20ml of 10^{-4}M of pesticide solution was used and the solution was irradiated for 1 hour using visible light. It is interesting to note that the percentage mineralisation increases with the increase in catalyst concentration from 0.5 to 2g /L and a further increase in catalyst concentration leads to a decrease in degradation.

As the catalyst loading is increased, there is an increase of surface area of the catalyst available for adsorption and degradation [11,17]. The increase in opacity and light scattering by particle are the reasons for the decrease in degradation at higher catalyst loading.

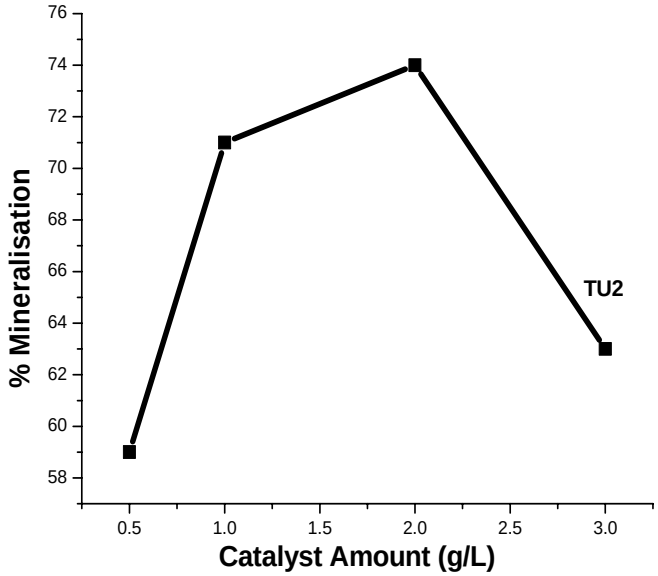

Fig.5.5 % Mineralisation of 2,4-D against amount of catalyst Irradiation time 1 hour; Pesticide concentration 20ml 10^{-4}M

5.2.3 Effect of dopants

The effect of dopants on the photocatalytic degradation of pesticide was studied using undoped titania (T) and all samples with optimal concentration of dopants (TU2, U2, AgT2, MoT2). The line diagram represents the percentage degradation of 2,4-D and 2,4,5-T using metal and non metal doped catalyst within a time of 1 hour. The experiment was carried out using 20ml of 10^{-4}M pesticide solution and 1g/L of catalyst under visible light irradiation.

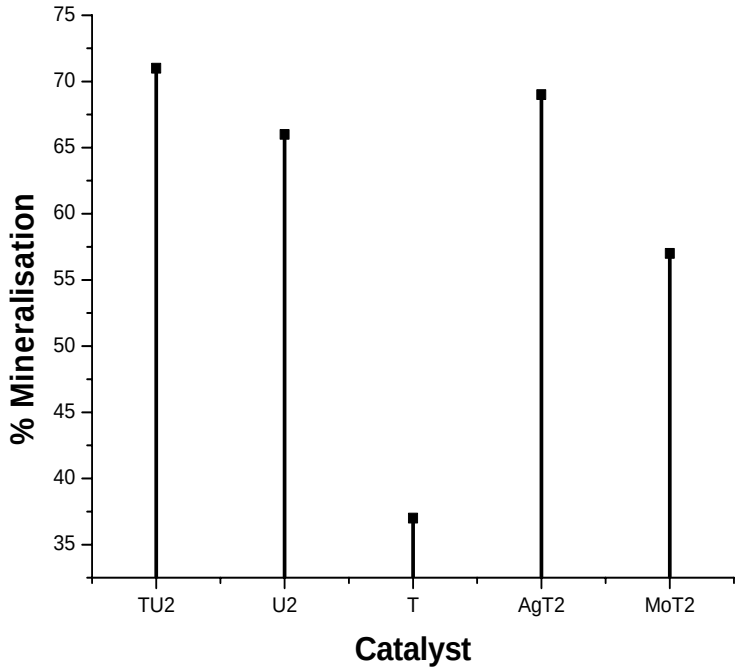

Fig. 5.6 % Mineralisation of 2,4-D using different catalysts Irradiation time 1hour; Amount of catalyst 1g/L; Pesticide concentration 20ml of 10^{-4}M

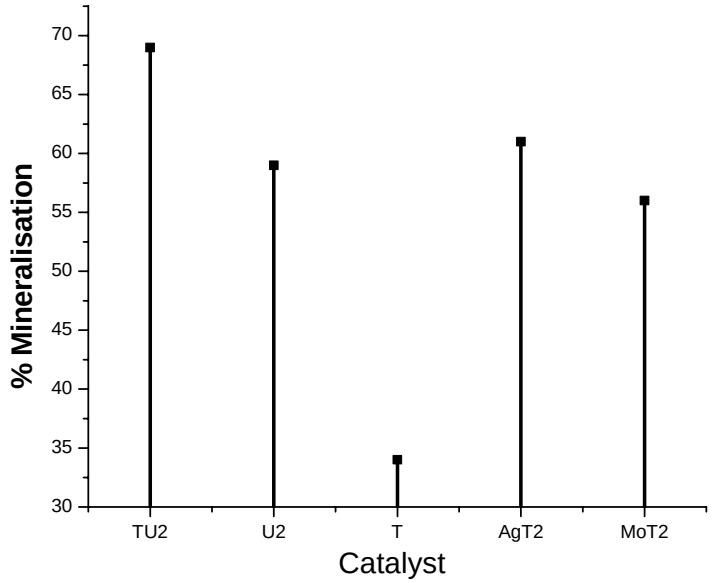

Fig. 5.7 % Mineralisation of 2,4,5-T using different catalysts Irradiation time 1hour; Amount of catalyst 1g/L; Pesticide concentration 20ml of 10^{-4}M

It has been observed that the mineralisation of these compounds proceeds much more rapidly in the presence of doped catalysts in visible light. Highest percentage mineralization of the pesticides was observed with TU2 catalyst. The reason for better photoactivity could be attributed to the fact that these catalysts are composed of nanocrystalline anatase form. The bandgap energy is lower than that of pure titania, it shows a stronger absorption in visible light region and the presence of dopants prevents the recombination of photogenerated electrons and holes leading to better photocatalytic activity.

5.2.4 Effect of light source

Experiments were conducted using visible light, UV light and under dark condition.150W Xe lamp was used as source of light. Dichoric mirror of wavelength, 280-420nm (for UV light), and 420-630nm dichoric mirror (cold mirror) for visible irradiation were used. 20ml of 10^{-4}M pesticide solution and

1g/L of catalyst was used for the studies and the solution was irradiated for 1hour. Catalysts TU2, AgT2 and T were used for the studies. Table 5.1 shows the effect of light source of different wavelength on the photodegradation of 2,4-D using undoped and doped TiO_2.

Table 5.1 %Mineralisation of 2,4-D against light source

Light	% mineralisation		
	TU2	AgT2	T
Visible light (420-630 nm)	71	69	37
UV light (280- 400nm)	58	49	48

When only UV light is used, degradation takes place slowly using the doped catalysts. Negligible degradation was observed in the absence of light. Control experiments were also carried out employing unirradiated solution. Negligible mineralisation was observed when irradiation was carried out in absence of photocatalyst. All these results suggest that mineralization of these compounds takes place through photocatalytic mechanism.

Table 5.2 % Mineralisation of 2,4-D and 2,4,5-T in absence of light/catalyst

studies	% mineralisation	
	2,4-D	2,4,5-T
Without catalyst	3	----
Without light	5	2

5.3 Monolinuron

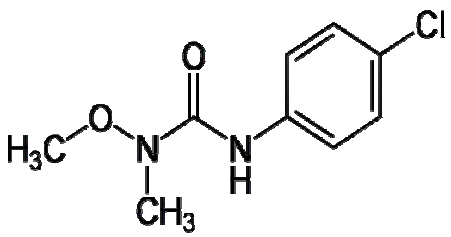

Fig. 5.8 Structure of Monolinuron

Monolinuron is a phenyl urea herbicide. Phenylurea herbicides were introduced in the 1950's and their use has considerably increased. Phenylurea herbicides have been used worldwide as photosynthesis inhibitors. Due to their relatively high water solubility, a significant amount of the applied herbicides can be washed out in the aquatic environment. As a result, it damages the nontarget aquatic primary producer which in turn alters the ecosystem equilibrium [18]. Indeed, several pesticides of this chemical group have been detected in different aquatic environments [19-22].

The photocatalytic degradation of Monolinuron was studied using the prepared catalysts.

5.3.1 Effect of time

The effect of time on the photocatalytic degradation of pesticide was studied. For this 20ml of 10^{-4}M dye solution and 1g/L of catalyst were used. Prior to irradiation, the solution was magnetically stirred in the dark for 30 minutes to ensure the establishment of an adsorption/desorption equilibrium. Irradiations were carried out under visible light using 150W Xe lamp. The effect of time was studied within a time range of 30 to 120 minutes. After irradiation the absorbance was measured spectrophotometrically.

The changes of the UV-Vis.spectra of monolinuron during the photocatalytic degradation process in the aqueous solution using TU2 photocatalyst under visible irradiation are illustrated in fig.5.9. During light irradiation with catalyst, the absorption band of monolinuron around 244 nm decreased rapidly.

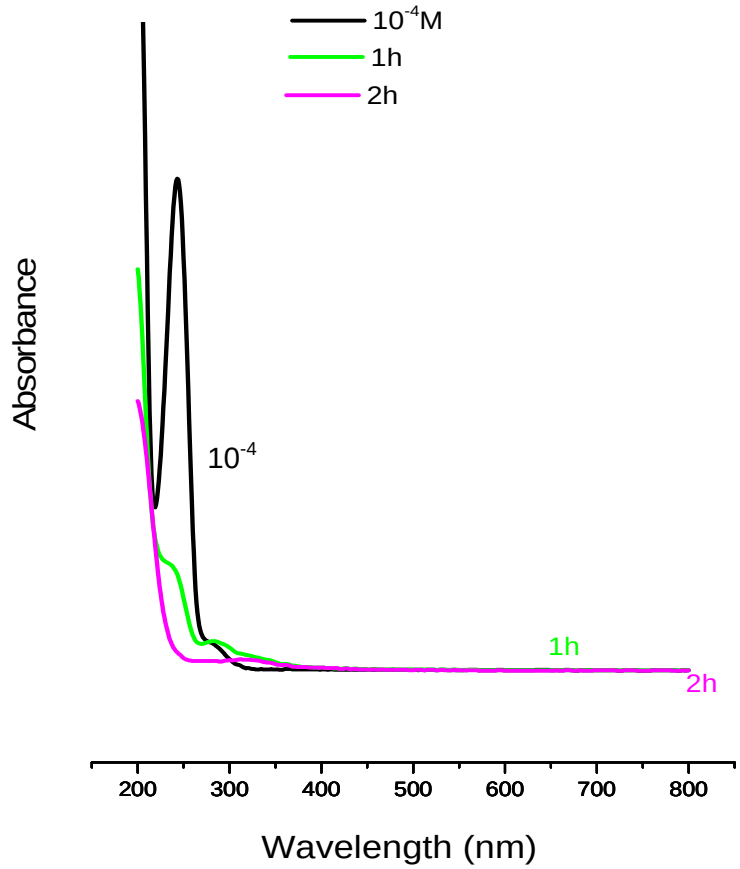

Fig.5.9. Absorbance spectra of Monolinuron after phtocatalytic treatment for 1 and 2 hours

Phenylurea herbicides are not very toxic compounds. However, products resulting from their photo- or bio-transformation may be more toxic. It can be deduced that disappearance of the herbicide is not necessarily accompanied by a decrease in toxicity. Photocatalysis may be sufficient to achieve the total mineralisation of the substrate [23]. Here the photocatalytic mineralisation of monolinuron at different time intervals was studied using TU2, U2 and T as catalysts.

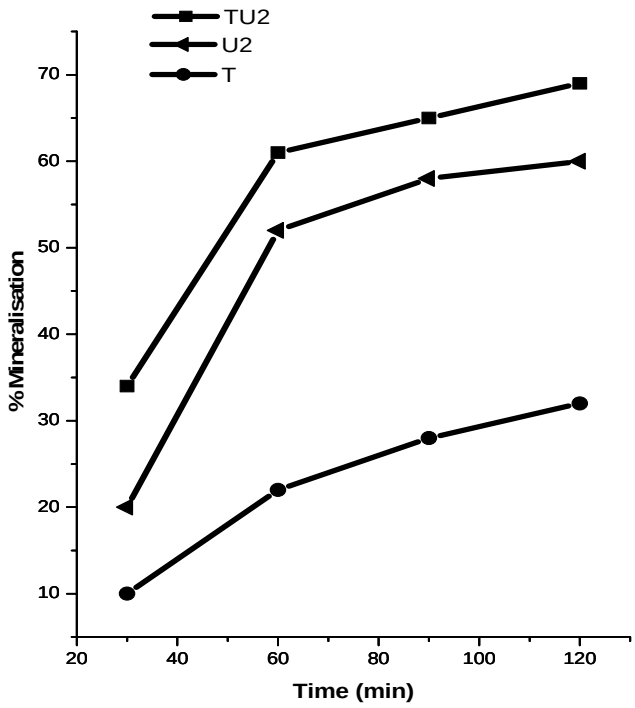

Fig.5.10 % Mineralisation of Monolinuron against time
Amount of catalyst 1g/L; Pesticide concentration 20ml 10^{-4}M

The percentage mineralisation increases with increase of time. Several studies on the transformation of phenylureas induced by irradiation of semiconductor (mainly TiO_2) suspensions have been reported [24-28]. This process is well known to generate very powerful oxidising species, such as $OH^{\cdot}$ radicals and positive holes (h^{+}) on the semiconductor surface. The reaction of these species with organic matter is fast and nonselective, intermediate photoproducts do not accumulate much and the process usually leads to the total mineralisation of the herbicide [23]. In this study 69% mineralisation was achieved with TU2 catalyst after 2 hours and 32% mineralisation was achieved with undoped titania.

.

5.3.2 Effect of catalyst concentration

In order to study the effect of catalyst concentration a series of experiments were carried out by employing different catalyst concentration varying from 0.5g/L to 3g/L. 20ml of 10^{-4}M pesticide solution was used in all cases and the solution was irradiated for 1 hour using visible light.

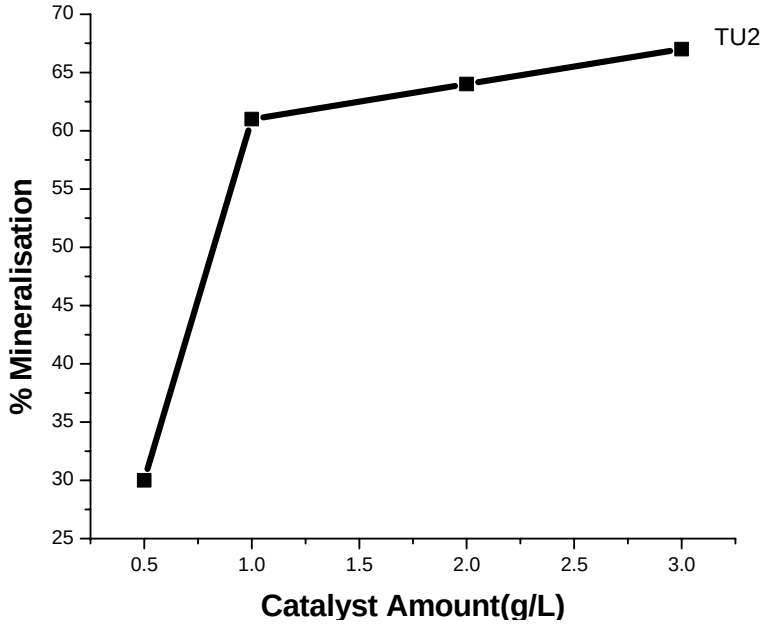

Fig.5.11 % Mineralisation of Monolinuron against amount of catalyst Irradiation time 1 hour; Pesticide concentration 20ml of 10^{-4}M

5.3.3 Effect of dopants

The effect of dopants on the photocatalytic degradation of pesticide was studied using undoped titania (T) and samples with optimal concentration of dopants (TU2, U2, AgT2, MoT2). The line diagram represents the percentage degradation of monolinuron using metal and non metal doped catalyst within a time of 1 hour. The experiment was carried out using 20ml of 10^{-4}M pesticide solution and1g/L of catalyst under visible light irradiation.

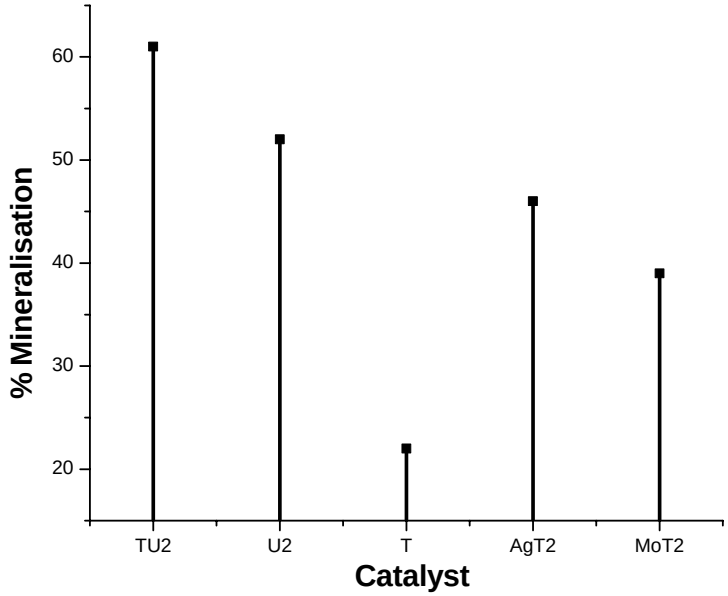

Fig. 5.12 % Mineralisation of Monolinuron using different catalysts Irradiation time 1hour; Amount of catalyst 1g/L; Pesticide concentration 20ml of 10^{-4}M

It has been observed that the mineralisation of these compounds proceeds much more rapidly in the presence of doped catalysts in visible light. Highest percentage mineralisationof monolinuron was observed when TU2 was used as catalyst, where 61% TOC was removed after one hour. The results indicate that doping is an effective way to improve the visible light activity of titania. The photocatalytic activity of catalysts under visible light is in this order TU2 > U2 > AgT2 > MoT2 > T.

5.3.4 Effect of light source

Experiments were conducted using visible light, UV light, under dark condition and without catalyst. 150W Xe lamp was used as source of light. Dichoric mirror of wavelength, 280-420nm (for UV light), and 420-630nm dichoric mirror (cold mirror) for visible irradiation were used. 20ml of 10^{-4}M pesticide solution and 1g/L of catalyst was used for the studies and the solution

was irradiated for 1 hour. Catalysts TU2, AgT2 and T were used for the studies. Table 5.3 shows the effect of light source of different wavelength on the photodegradation of pesticide using undoped and doped TiO_2

Table 5.3 % Mineralisation of Monolinuron against light source

	% mineralisation		
	TU2	**AgT2**	**T**
Visible light (420-630 nm)	61	46	22
UV light (280- 400nm)	50	34	32

Table 5.4 % Mineralisation of Monolinuron in absence of light/catalyst

Catalyst	% mineralisation(time 1h)
Without Catalyst	6
Without Light	5

In the absence of TiO_2, no significant decrease in the concentration of this herbicide was observed under visible light irradiation for one hour. In this case, the percentage mineralisation is 6% using a 150W Xe lamp. The result shows good photo stability of the pesticide under light irradiation, which implies that these compounds would be removed very slowly by direct photolysis. In presence of TiO_2, the percentage mineralisation in the dark is 5%. Thus degradation of these herbicides is exclusively due to photocatalytic processes via the formation of hydroxyl radicals generated at the surface of the semiconductor [29,30].

5.4 Dazomet

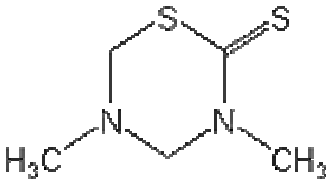

Fig. 5.13 Structure of Dazomet

Dazomet $C_5H_{10}N_2S_2$ is viable alternative to methyl bromide to control weeds, plant diseases, and insects. Because of the low cost and effectiveness in controlling soil pests, the use of these products increased about two-fold from 1992 to 2003. These agents are corrosive, damage skin, induce allergic reactions and fatal if swallowed [31-33]. The photocatalytic degradation of dazomet was studied using the prepared catalysts.

5.4.1 Effect of time

The effect of time on the photocatalytic degradation of pesticide was studied. For this 20ml of10^{-4}M pesticide solution and 1g/L of catalyst was used. Prior to irradiation, the solution was magnetically stirred in the dark for 30 minutes to ensure the establishment of an adsorption/desorption equilibrium. Irradiations were carried out under visible light using 150W Xe lamp. The effect of reaction time on the degradation of dazomet was examined in the reaction time ranging from 30 to 120 minutes. Samples were withdrawn at different time intervals after photodegradation and centrifuged immediately and percentage mineralisation was studied using TOC analysis. The results of percentage TOC removal at different times are shown in fig. 5.14

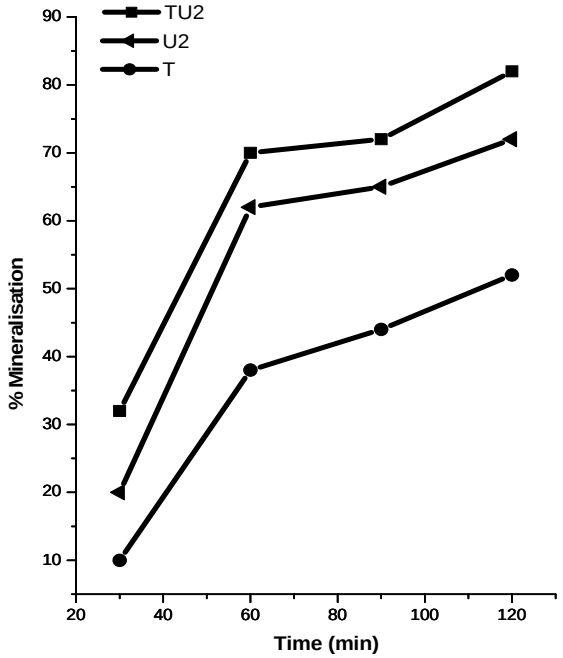

Fig.5.14 % Mineralisation of Dazomet against time
Amount of catalyst 1g/L; Pesticide concentration 20ml 10^{-4}M

It is noted that the percentage mineralisation increases with increase of irradiation time and 82% mineralisation was achieved after 2 hours when TU2 was used as catalyst. When time increases more and more light energy falls on the catalyst which causes the generation of higher amount of photoexcited species. As the number of photoexcited species increases, it causes an increase in reactive oxygen species responsible for the degradation of adsorbed species.

5.4.2 Effect of catalyst concentration

In order to study the effect of catalyst concentration a series of experiments were carried out by employing different catalyst concentration varying from 0.5g/L to 3g/L. 20ml of 10^{-4}M of pesticide solution was used and the solution was irradiated for 1 hour using visible light.

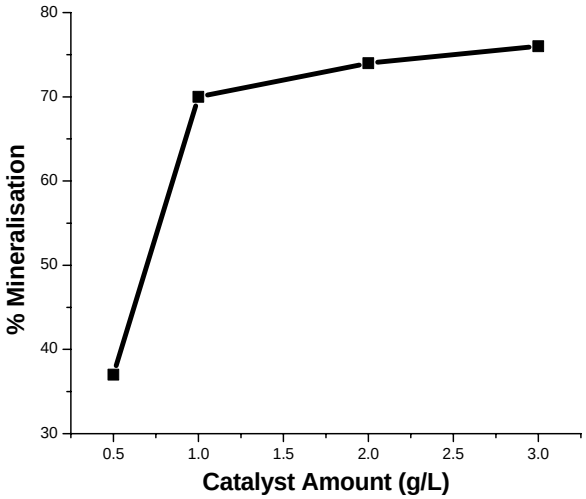

Fig.5.15 % Mineralisation of Dazomet against amount of catalyst Irradiation time 1 hour ; Pesticide concentration 20ml 10^{-4}M

It is interesting to note that the percentage mineralisation increases with the increase in catalyst concentration and then decreases. As the catalyst concentration increases the number of active sites increase and the effective surface area increase so more and more pesticide molecules are adsorbed by these particles. The increase in opacity and light scattering by particle are the reasons for the decrease in degradation at higher catalyst loading

5.4.3 Effect of dopants

The effect of dopants on the photocatalytic degradation of pesticide was studied using undoped titania (T) and all samples with optimal concentration of dopants (TU2, U2, AgT2, MoT2). The line diagram represents the percentage degradation of dazomet using metal and non metal doped catalyst within a time of 1 hour. The experiment was carried out using 20ml of 10^{-4}M pesticide solution and1g/L of catalyst under visible light irradiation.

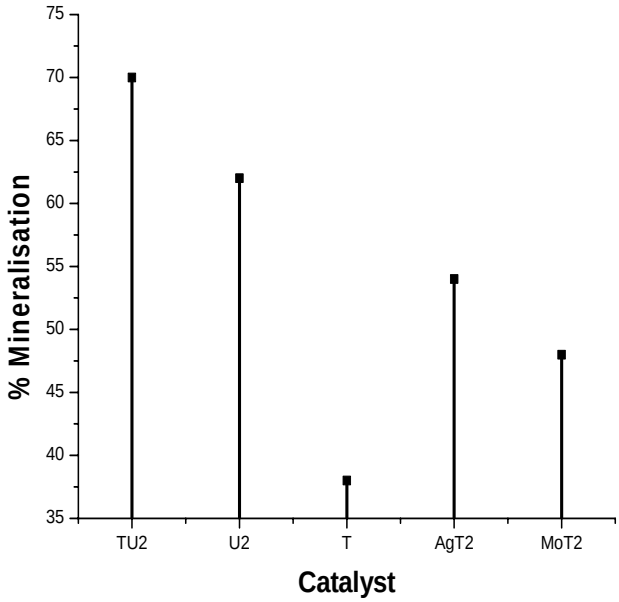

Fig. 5.16 % Mineralisation of Dazomet using different catalysts Irradiation time 1hour; Amount of catalyst 1g/L; Pesticide concentration 20ml of 10^{-4}M

It has been observed that the mineralisation of these compounds proceeds much more rapidly in the presence of doped catalysts in visible light. Highest percentage mineralisation was observed when TU2 was used as catalyst, where 70% TOC was removed after one hour.

5.4.4 Effect of light source

Experiments were conducted using visible light, UV light and under dark condition.150W Xe lamp was used as source of light. Dichoric mirror of wavelength, 280-420nm (for UV light), and 420-630nm dichoric mirror (cold mirror) for visible irradiation were used. 20 ml of 10^{-4}M pesticide solution and 1g/L of catalyst was used for the studies and the solution was irradiated for 1 hour. Catalysts TU2, AgT2 and T were used for the studies. Table 5.5 shows the effect of light source of different wavelength on the photodegradation of pesticide using undoped and doped TiO_2.

Table 5.5 %Mineralisation of Dazomet against light source

Light source	% mineralisation		
	TU2	AgT2	T
Visible light (420-630 nm)	70	54	38
UV light (280- 400nm)	60	47	49

Table 5.6 % Mineralisation of Dazomet in absence of light/catalyst

Studies	% mineralisation(time 1h)
Without Catalyst	5
Without Light	4

In the absence of TiO_2, no significant decrease in the concentration of this pesticide was observed under visible light irradiation for one hour. In this case, the percentage mineralisation is 5% using a 150W Xe lamp. In presence of TiO_2, the percentage mineralisation in the dark is 4%. The results show that though using light irradiation mineralisation of pesticide takes place in presence of photocatalyst.

5.5 Phosphamidon

Phosphamidon is a organophosphate insecticide. It is marketed under the trade name dimecron.

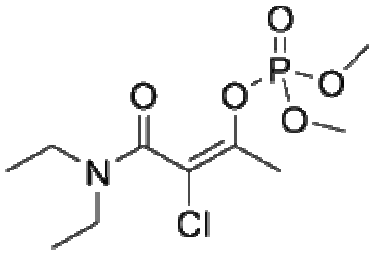

Fig.5.17 Structure of Phoshamidon

Organophosphates are important group of pesticides which act as insecticides. They are often detected in waters [34] due to agricultural runoff,

possessing a possible threat for human health and aquatic organisms. Organophosphorous pesticides are considered to be highly toxic, even at low concentrations, due to their cholinesterase inhibition effect which may lead to additive toxicity [21,35,36].

5.5.1 Effect of time

The effect of time on the photocatalytic degradation of pesticides was studied using TU2 as catalyst. For this 20ml of 10^{-4}M pesticide solution and 1g/L of catalyst was used. Prior to irradiation, the solution was magnetically stirred in the dark for 30 minutes to ensure the establishment of an adsorption/desorption equilibrium. Irradiations were carried out under visible light using 150W Xe lamp.

The effect of reaction time on the degradation of phosphamidon was examined in the reaction time range of 30 to 180 minutes. Samples were withdrawn at different time intervals during the photodegradation and centrifuged immediately and percentage mineralisation was studied using TOC analysis. The percentage TOC removal at different time is shown in fig. 5.18.

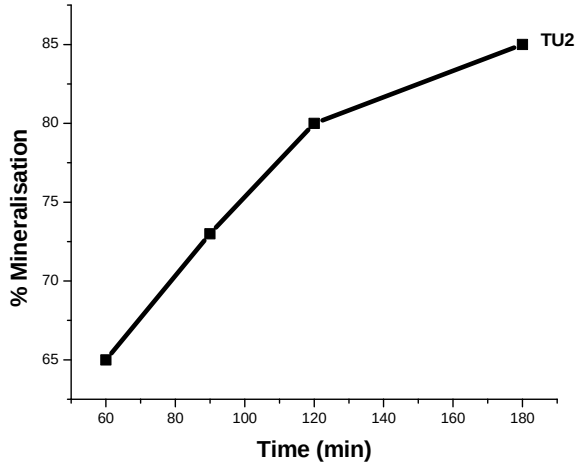

Fig.5. 18 % Mineralisation of Phosphamidon against time
Amount of catalyst 1g/L; Pesticide concentration 20ml of 10^{-4}M

Results show that as time increase the percentage degradation increases. In this case 65% mineralisation was achieved in 1hour and 85% degradation was achieved with in 3hours using TU2 as catalyst.

The results indicate that as time increases the amount of light falling on the catalyst surface increases which increases the formation of photoexcited species thereby enhances the photocatalytic activity.

5.5.2 Effect of dopants

The effect of dopants on the photocatalytic degradation of pesticide was studied using undoped titania (T) and all samples with optimal concentration of dopants (TU2, U2, AgT2, MoT2). The line diagram represents the percentage degradation of dazomet using metal and non metal doped catalyst within a time of 1 hour .The experiment was carried out using 20ml of 10^{-4}M pesticide solution and1g/L of catalyst under visible light irradiation.

The photo activities of doped TiO_2 are widely dependent upon the specific dopant as shown in fig.5.19. The figure represents the effect of different dopants on the percentage degradation of phoshamidon.

It can be seen that doping with N, N-S, Ag, Mo enhance the photoactivity of TiO_2 while pure titania shows very low activity at visible light. The different photoreactivities exhibited by different dopant catalysts could be attributed to the efficiencies of the dopants in trapping charge carriers. In addition, optical absorbance intensity in visible-light region of catalysts was also an important factor to influence the visible-light activity of catalysts.

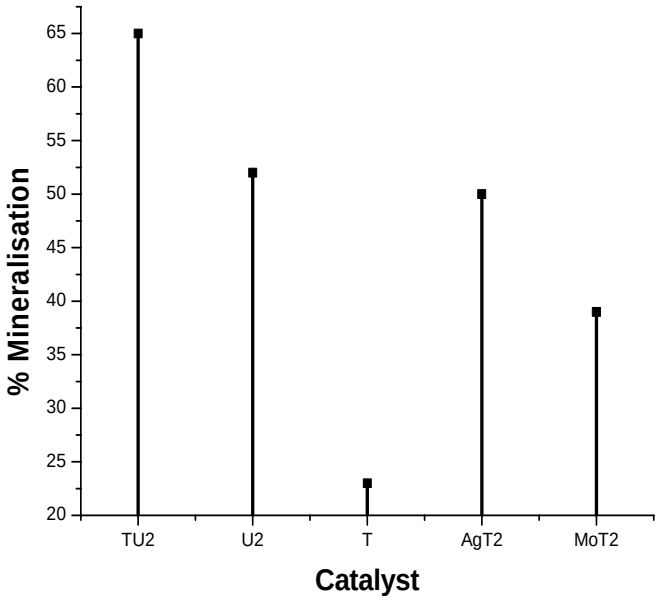

Fig. 5.19 % Mineralisation of Phosphamidon using different catalysts Irradiation time 1hour; Amount of catalyst 1g/L; Pesticide concentration 20ml of 10^{-4}M

5.5.3 Effect of light source

Experiments were conducted using visible light, UV light and under dark condition.150W Xe lamp was used as source of light. Dichoric mirror of wavelength, 280-420nm (for UV light), and 420-630nm dichoric mirror (cold mirror) for visible irradiation were used. 20ml 10^{-4}M pesticide solution and 1g/L of catalyst was used for the studies and the solution was irradiated for 1hour. Catalysts TU2, AgT2 and T were used for the studies. Table 5.7 shows the effect of light source of different wavelength on the photodegradation of pesticide using undoped and doped TiO_2

Table5.7 %Mineralisation of Phosphamidon against light source

Light	% mineralisation		
	TU2	AgT2	T
Visible light (420-630 nm)	65	50	23
UV light (280- 400nm)	47	39	35

Table 5.8 %Mineralisation of Phosphamidon in the absence of light/catalyst

Studies	% mineralisation(time 1h)
Without Catalyst	8
Without Light	6

In the absence of TiO_2, no significant decrease in the concentration of this herbicide was observed under visible light irradiation for one hour. In this case, the percentage mineralisation is 8% using a 150W Xe lamp

In presence of TiO_2, the percentage mineralisation in the dark is 6%. Thus degradation of these pesticides is exclusively due to photocatalytic processes via the formation of hydroxyl radicals generated at the surface of the semiconductor.

References

[1] W. Bahnemann, M. Muneer, M. M Haque, Catalysis Today, 124(2007) 133.

[2] A. Agudach, S.Brosillon, J.Morvan, E. K. Lhadi, Appl.Catal.B: Environ., 57 (2005) 55.

[3] M. M. Haque, M. Muneer, Ind. J. Chem. Technol., 2 (2005) 68.

[4] J. Lee, W. Choi, J. Yoon, Environ. Sci. Technol., 39 (2005) 6800.

[5] M.M. Haque, M. Muneer, D.W. Bahnemann, Environ. Sci. Technol., 40 (2006) 4765.

[6] Eusio Choi, Hyoung Cho, Jaehong Park, Journal of Environmental Science and Health Part B: Pesticides, Food Contaminants and Agricultural WastesB, 39 (2004) 53.

[7] K. Djeebar, A. Zertal, T. Sehli, Environmental Technology, 27(2006)1191.

[8] M. Trillas, J. Pearl, X. Domenech, Appl. Catal. B:Environ., 5(1995)377.

[9] M. Trillas, J. Pearl, X. Domenech, J. Chem. Technol. Biotechnol., 67(1996) 237.

[10] C.Y. Kwan, W. Chu, Water Res., 37 (2003) 4405.

[11] Sanjay P. Kamble, Sudhir P. Deosarkar, Sudir B. Sawant, Jacob A.Moulijn, Viswas G. Pangarkar, Ind. Eng.Chem. Res., 43 (2004) 8178.

[12] V. Laszlo, J. K .Terence, J. Photochem. Photobiol. A:Chem., 87 (1995) 257.

[13] W. H. Iaze, J. F. Kennebe, J. L. Ferry, Environ .Sci Tech., 27 (1993)177.

[14] H. K. Singh, M. Saquib, M. M. Haaque, M. Muneer, D. W. Bahnemann, J. Hazard. Mater., 142(2007)374.

[15] www.wikipedia .org

[16] D. S. Bhatkhande, V. G. Pangarkar, J. Chem. Technol. Biotechnol., 77 (2002) 102.

[17] D. S. Bhatkhande, V. G. Pangarkar, Water. Res., 37(2003) 1223.

[18] S. N. Lieu, L. Kerhoas, M. Sarakha, J. Einhorn, Environ Chem Lett., 2 (2004)83.

[19] A. Kotrikla, G. Gatidou, T. D. Lekkas, J. Environ.Sci.Health B, 41(2006)135.

[20] G . Gatidou, N. S. Thomaidis, J .L. Zhou, Environ. Int ., 33 (2007) 70.

[21] Georgia Gatidou, Evaggelia Iatrou, Environ Sci Pollut Res.,18 (2011)949.

[22] A. S. Stasinakis, S. Kotsifa, G. Gatidou, D. Mamais, Water Res., 43(2009) 1471.

[23] Amina Amine Khodja, Abdelaziz Boulkamh, PierreBoule, Photochem. Photobiol.Sci., 3(2004)145.

[24] C. Richard, S. Bengana, Chemosphere, 33(1996)635.

[25] S. Parra, J. Olivero, C. Pulgarin, Appl. Catal. B, 36(2002) 75.

[26] S. Parra, V. Sarria, S. Malato, P. Péringer, C. Pulgarin, Appl. Catal., B, 27 (2000) 153.

[27] Amine-Khodja, B. Lavédrine, C. Richard, T. Sehili, Int. J. Photoenergy, 4 (2002) 147.

[28] E. Pramauro, M. Vincenti, V. Augugliaro, L. Palmisano, Environ. Sci. Technol., 27(1993) 1790.

[29] Razika Zouaghi, Abdennour Zertal, Journal of Water Science, 20(2007)163

[30] M .Nargiello, T. Herz, Elsevier Sci., (1993) 801.

[31] Health And Safety Report By Rais Akanda, (2007)California Environmental Protection Agency.

[32] www.pesticideinfo.org

[33] www.alanwood.net/pesticides

[34] K. Werimo, A. A. Bergwerff, W. Seinen, Aquat Ecosyst Health Manage, 12 (2009) 337.

[35] H. K. Rotich, Z. Zhang, Y. Zhao, J. Lia., Int J Environ Anal Chem., 84 (2004) 289.

[36] S. Gitelson, J. T. Davidson, A. Werczbergerbrit, J. Industr.Med., 22 (1965) 236.

.....ꕥ.....

Chapter

6

Photocatalytic Degradation of 4-Nitrophenol

Contents

The photocatalytic degradation of 4-nitrophenol (4-NP) assisted by titanium dioxide (TiO_2) was investigated in aqueous solution under visible light irradiation. The effect of different dopants on TiO_2 on the photocatalytic degradation of 4-NP has been studied. TiO_2 with all dopants exhibits good efficiency for 4-NP degradation and was better than pure TiO_2.

6.1 Introduction

Nitrophenols are some of the most refractory pollutants, which can be present in industrial waste water. Among them, 4-nitrophenol (4-NP) is environmentally important for several reasons. Owing to high toxicity and carcinogenic character, 4-NP is characterized as environmentally hazardous material. This toxic pollutant is used in the production of pesticides, insecticides and herbicides [1] and many synthetic dyes [2]. Therefore, 4-NP and its derivatives are common pollutants in many natural water and wastewater systems. The removal of pollutants from wastewater is of great concern, because their complete biodegradation requires several days or weeks. Advanced oxidation processes (AOPs) are efficient treatment methods owing to their ability of complete degradation of wide range of organic pollutants. Titanium dioxide (TiO_2) assisted photocatalysis is a well known emerging AOP for the removal of organic pollutants in water and air [3-5]. TiO_2 is of great interest due to its non-toxic nature, photochemical stability and low cost, particularly when sunlight is used as the source of irradiation [6,7]. However, shortcoming of using TiO_2 in photocatalytic processes is its rapid aggregation in a suspension resulting in decrease of effective surface area in addition to recombination of generated electron-hole pairs [8].

The photocatalytic degradation rate of the different nitrophenols depends on various parameters, such as temperature, pH, initial concentration of the pollutant [9-10], and light intensity. Advanced oxidation processes (AOPs) have been proposed as an alternative for the treatment of wastewater containing nitrophenols. A lot of studies focused on these processes [11-14] have pointed out that, although the reacting systems were different they are all characterized by the same chemical feature, that is, the production of $OH^{\cdot}$ radicals, which as the second best

oxidant after fluorine, is the active species responsible for the destruction of organic pollutants [15-18].

The photocatalytic degradation of 4-nitrophenol was studied using the prepared catalysts. Samples were withdrawn at different time intervals during the photodegradation and centrifuged immediately and percentage mineralization was studied using TOC analysis. The effect of operational parameters, such as time, catalyst concentration, light source, dopants was examined. The structure of 4-Nitrophenol as follows

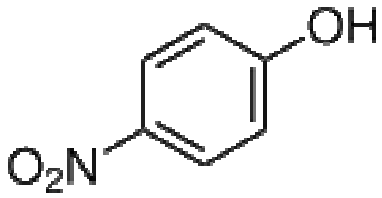

Fig.6.1 Structure of 4-Nitrophenol

6.2 Activity studies

6.2.1 Effect of time

One of the very important parameters that was studied for the photocatalytic degradation of *4*-nitrophenol was time of degradation. The effect of time on the photocatalytic degradation of 4-Nitrophenol was studied using TU2 as catalyst. For this, 20ml of 10^{-4}M solution and 1g/L of catalyst was used. Prior to irradiation, the solution was magnetically stirred in the dark for 30 minutes to ensure the establishment of an adsorption/desorption equilibrium. Irradiation was carried out under visible light using 150W Xe lamp. The percentage degradation was studied for a time range of 15 to 60 minutes. After photodegradation, the solution was centrifuged and recorded the absorbance using spectrophotometer at

a wavelength of 315nm [8]. The percentage degradation increased with increase in irradiation time as shown in fig. 6.2

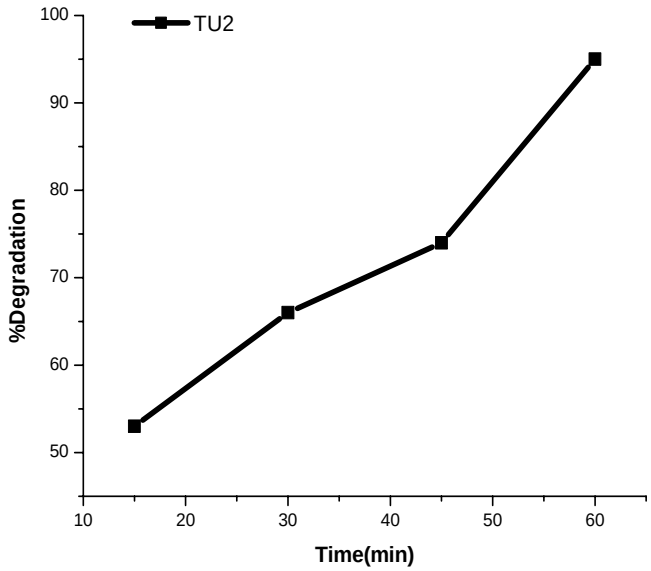

Fig.6.2 % Degradation of 4-NP against time
Amount of catalyst 1g/L; 4-NP concentration 20ml of 10^{-4}M

In the experimental work, photocatalytic degradation of 4-nitrophenol was primarily monitored using absorption spectroscopy. This, however, does not indicate the degree of mineralization of the organic compounds. Following the earlier study the oxidative mineralization was therefore examined by measuring the Total Organic Carbon (TOC) in the solution [19, 20]. The mineralisation was studied within a time period of 30 minutes to 3 hours. The percentage mineralisation of 4-NP was calculated by the following formula: Percentage mineralisation = $(TOC_o - TOC_t / TOC_o) \times 100$. Fig. 6.3 gives the results of the TOC experiments indicating that 80% mineralization was achieved within the period of 180 minutes. The results suggests that the catalyst does not only promotes degradation but also the mineralization of 4-NP.

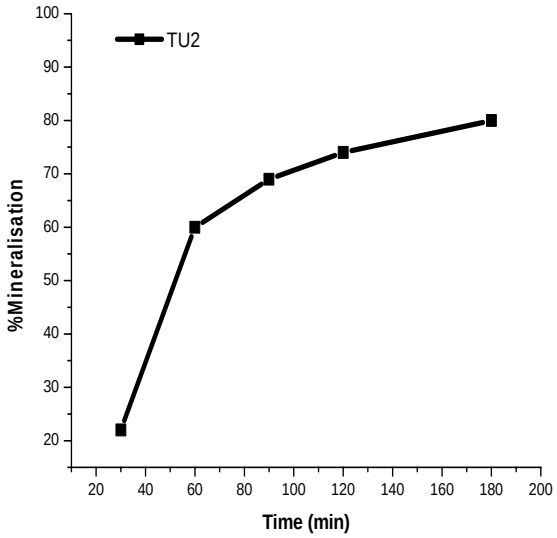

Fig.6.3 % Mineralisation of 4-NP against time
Amount of catalyst 1g/L; 4-NP concentration 20ml of 10^{-4}M

6.2.2 Effect of catalyst concentration

The effect of catalyst concentration on the degradation 4-nitrophenol was investigated by employing different concentrations of TU2 catalyst varying from 0.5 to 3 g/L. 20ml of 10^{-4}M of solution was used in all cases and it was irradiated for one hour using visible light.

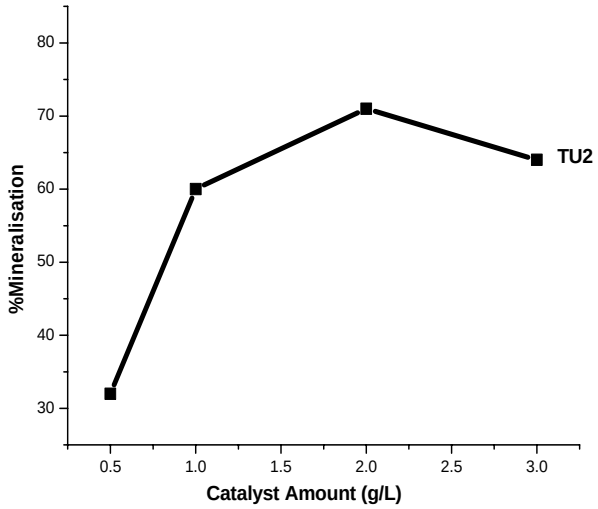

Fig.6.4 % Mineralization of 4-NP against amount of catalyst
Irradiation time 1 hour; 4-NP concentration 20ml of 10^{-4}M

The percentage mineralization increases with increase of catalyst concentration and then decreases.

6.2.3 Effect of dopants

To evaluate the photocatalytic activity of doped TiO_2 and to find out the optimum content of dopant, a set of experiments for 4-nitrophenol degradation with an initial concentration of 20ml of 10^{-4}M under visible irradiation was carried out in aqueous suspension using TiO_2, Ag-TiO_2 ,$MoTiO_2$, N-S TiO_2,N-TiO_2 catalysts with different concentration of dopants and percentage degradation was studied by taking absorbance at 315nm . The experimental results are shown in fig.6.5. The experimental results demonstrated that after 60 minutes reaction 4-nitrophenol in all the solution was degraded. Among them, N-S codoped titania (TU2) achieved the highest efficiency of the 4-nitrophenol degradation. Higher dopant content in TiO_2 seems to be detrimental to the photodegradation.

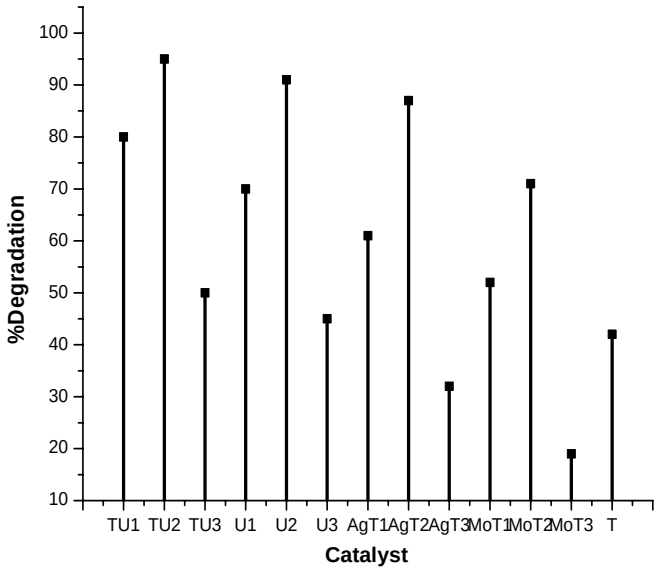

Fig.6.5 % Degradation of 4-NP using different catalysts Irradiation time 1hour; Amount of catalyst 1g/L; 4-NP concentration 20ml of 10^{-4}M

Comparative photocatalytic mineralisation of 4-nitrophenol in presence of TiO_2 with different dopants was also investigated under visible light. N-STiO_2 nanoparticles show better results (60% degradation) as compared to pure TiO_2 nano particles (22% degradation) in 1 hour as shown in Fig. 6.6. This is due to the positive effect of dopants on the photoactivity of TiO_2 for degradation of 4-Nitrophenol. It may be explained by its ability to trap electrons, thus, reducing the recombination of light-generated electron-hole pairs at TiO_2 surface. The high surface area, crystallinity of anatase phase and low bandgap also affect their activity.

In photocatalytic degradation, 4-nitro phenol is finally converted into inorganic products like CO_2, H_2O [20].

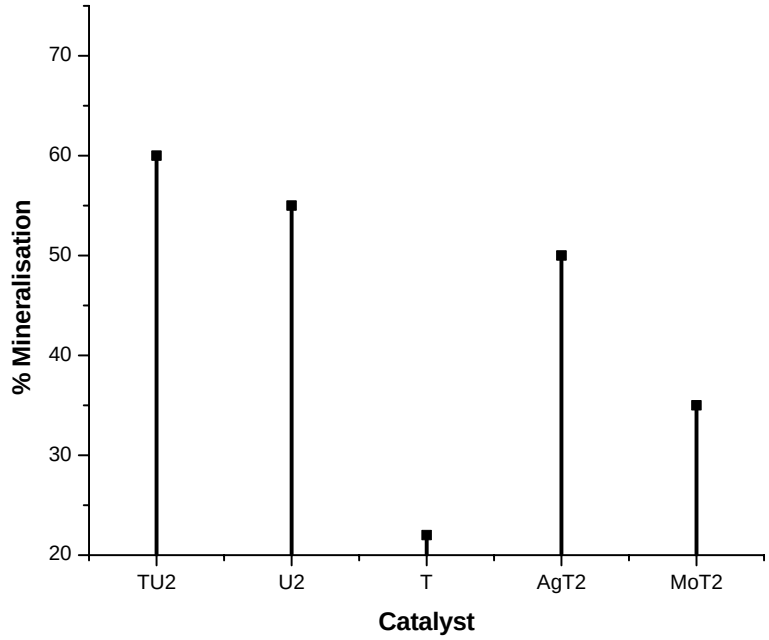

Fig.6.6 % Mineralisation of 4-NP using different catalysts Irradiation time 1hour; Amount of catalyst 1g/L; 4-NPconcentration 20ml of 10^{-4}M

6.2.4 Effect of light source

Experiments were conducted under dark condition. 20ml of 10^{-4}M 4-NP solution and 1g/L of TU2 catalyst was used for the studies. Experiments were also conducted in absence of catalysts. Table 6.1 shows the mineralization of 4-NP in the absence of light and in the absence of catalyst.

Table 6.1 %Mineralisation of 4-NP in the absence of light/catalyst

Studies	% mineralisation(time 1h)
Without Catalyst	4
Without Light	2

Negligible degradation was observed in the absence of catalyst under irradiation using 150W Xe lamp. Without catalyst TOC does not decrease at all suggesting that direct photolysis cannot mineralise nitrophenol[8].

References

[1] M. S. Dieckmann, K. A. Gray, Water Res., 30(1996)1169.

[2] N. Takahashi, T. Nakai, Y. Satoh, Y. Katoh, Water Res., 28(1994)1563.

[3] D. Ollas, E. Pelizzetti, N. Serpone, Environ Sci Technol., 25(1991)1522.

[4] M. R. Hoffmann, S. Martin, Choi, D. W. Bahnemann, Chem Rev., 95(1995) 69.

[5] J. Pearl, X. Domenech, D. F. Ollis, J. Chem Technol Biotechnol., 170 (1997) 117.

[6] A. Khodja, T. Sehili, J. F. Pilichowski, P. B. Boule, J Photochem Photobiol A:Chem., 141(2001)231.

[7] D. Chen, A. K. Ray, Water Res., 32(1998)3223.

[8] Kashif Naeem, Feng Ouyang, Journal of Chemistry, 6(S1)(2009) S422.

[9] V. Augugliaro, M. J. Lopez-Munos, L. Palmisano, J. Soria, Applied Catalysis A, 10 (1993) 7.

[10] V. Augugliaro, L. Palmisano, M. Schiavello, Applied Catalysis, 69 (1991) 323.

[11] E. Kusvuran, O. Erbatur, Journal of Hazardous Materials, 106 (2004) 115.

[12] F. J. Benıtez, J. Beltran-Heredia, J. L. Acero, M. L. Pinilla, Industrial and Engineering Chemistry Research, 36 (1997) 638.

[13] I. Casero, D. Silicia, S. Rubio, D. Perez Bendito, Water Research, 31 (1997) 1985.

[14] O. Legrini, E. Oliveros, A. M. Braun, Chemical Reviews, 93 (1993) 671.

[15] K. Tanaka, W. Luesaiwong, T. Hisanaga, Journal of Molecular Catalysis A, 122 (1997)67.

[16] R. W. Matthews, Journal of Catalysis, 111(1988)264.

[17] J. M. Herrmann, Catalysis Today, 53(1999)115.

[18] Hinda Lachheb, Ammar Houas, Jean-Marie Herrmann, International Journal of Photoenergy, 2008(2008)1.

[19] D. Behar, C. Gonzalez, P. Neta, Journal of Physical Chemistry A, 105 (2001)7607.

[20] Hassan Ilyas, Ishtiaq A. Qazi,Wasim Asgar, M. Ali Awan, Zahir-ud-din Khan, Journal of Nanomaterials,2011(2011)1.

.....ൠ.....

Chapter

7

Photocatalytic Degradation of Acetophenone

Contents

Heterogeneous photocatalysis on TiO_2 has been shown to provide an effective method to degrade organic pollutants. Addition of dopants into TiO_2 significantly increased its photocatalytic activity. Acetophenone shows high percentage of photocatalytic degradation using doped TiO_2.

7.1 Introduction

Acetophenone is an organic compound with the formula $C_6H_5COCH_3$. It is the simplest aromatic ketone [1].

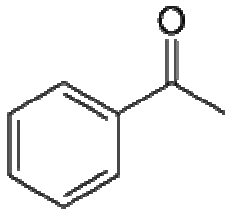

Fig. 7.1 Structure of Acetophenone

Acetophenone is found in emissions from vehicular exhaust, waste incineration, residential fuel oil, and coal combustion. It is also found in the vaporization of certain perfumes. Oxidation by other oxidants and photolysis do not appear to be important for the removal of acetophenone in the atmosphere. Exposure to acetophenone vapor may cause skin irritation and transient corneal injury. Oral exposure can cause central nervous system depression, hematologic effects, and weakened pulse in humans. Inhalation exposure may produce respiratory depression and shortness of breath. Aspiration may result in chemical pneumonitis [2,3].

7.2 Activity Studies

TiO_2 is a promising photocatalyst in a great a variety of areas such as photodegradation of pollutants in water, air etc [4]. In this work metal and non metal doped titania were used for the photocatalytic degradation of acetophenone in water. The irradiation experiments were carried out with a light source of 150 W Xe lamp in visible region. The concentration of acetophenone solution was 10^{-4} M and 20ml of solution was used for experiment. The concentration of TiO_2 was set as 1g/L. Samples were

withdrawn at different time intervals during the photodegradation and centrifuged immediately and percentage mineralisation was studied using TOC analysis. Total organic carbon (TOC) of the solution was measured using a Elemental Vario TOC analyser. The effects of operational parameters, such as time, catalyst concentration, light source, dopants were examined.

7.2.1 Effect of time

Photocatalytic degradation of acetophenone in TiO_2 was performed by taking 20ml of 10^{-4}M aqueous solution and 1g/L of catalyst. Prior to irradiation, the solution was magnetically stirred in the dark for 30 minutes to ensure the establishment of an adsorption/desorption equilibrium. Irradiations were carried out under visible light using 150W Xe lamp. The percentage degradation was studied within a time range of 15 to 60 minutes. After a regular interval of time, the samples were collected and immediately centrifuged. The photocatalytic activity was evaluated by measuring the loss of acetophenone in solution.

The quantitative determination of acetophenone was performed by measuring its absorbance at 246nm with a UV-Visible spectrophotometer [5]. The percentage degradation was computed using following equation: percentage degradation = $[C_o- C_t/C_o]$ x 100 where, C_o and C_t are the concentrations at time zero and time t, respectively. Fig.7.2 shows the percentage degradation versus irradiation time of aqueous solution of acetophenone.

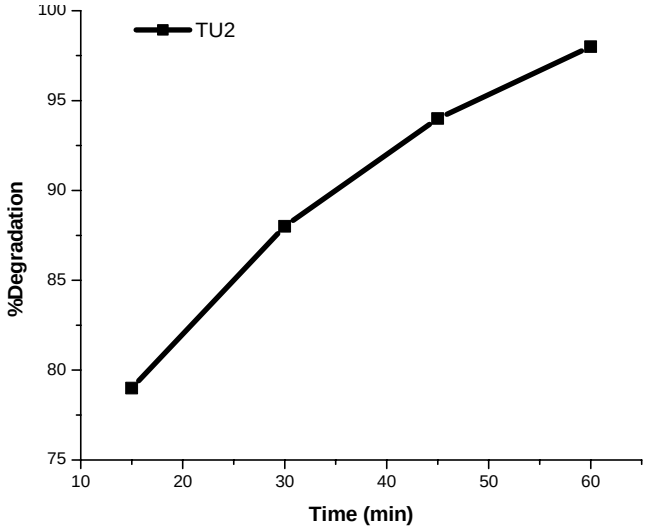

Fig. 7.2 % Degradation of Acetophenone against time
Amount of catalyst 1g/L; Acetophenone concentration 20ml 10^{-4}M

The determination of the total decomposition of organic compound can be evaluated by measuring the total organic carbon (TOC) in the irradiated solution. In the present study, the percentage mineralisation of acetophenone was studied within a time range of 30 minutes to 3 hours and the corresponding results are reported in fig. 7. 3

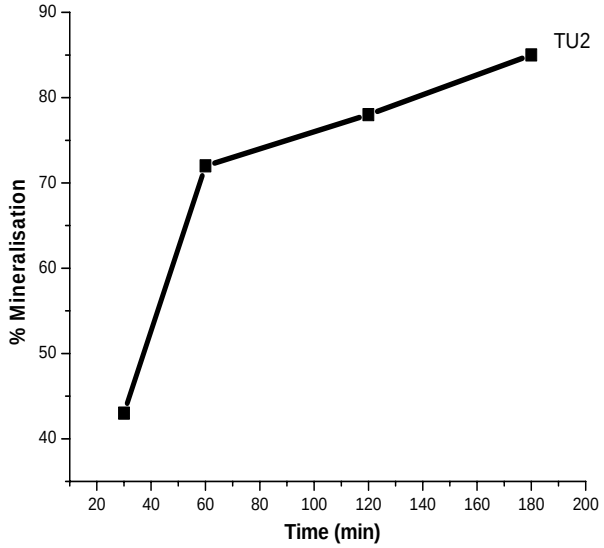

Fig.7.3 % Mineralisation of Acetophenone against time
Amount of catalyst 1g/L; Acetophenone concentration 20ml 10^{-4}M

85% mineralisation was obtained after 3 hours. These values show that the TiO_2 catalysts synthesized in this study are very efficient for the mineralization of acetophenone. It shows that even though there is a large decrease in UV/Vis absorbance, the TOC values are decreased slowly, since total degradation involves many consecutive reactions before reaching CO_2.

7.2.2 Effect of catalyst concentration

The effect of catalyst concentration on the degradation of acetophenone was investigated by employing different concentrations of TU2 catalyst varying from 0.5 to 3 g/L. 20ml of 10^{-4}M of acetophenone solution was used in all cases and the solution was irradiated for 1 hour using visible light. It is interesting to note that the percentage mineralisation increases with the increase in catalyst concentration and then decreases.

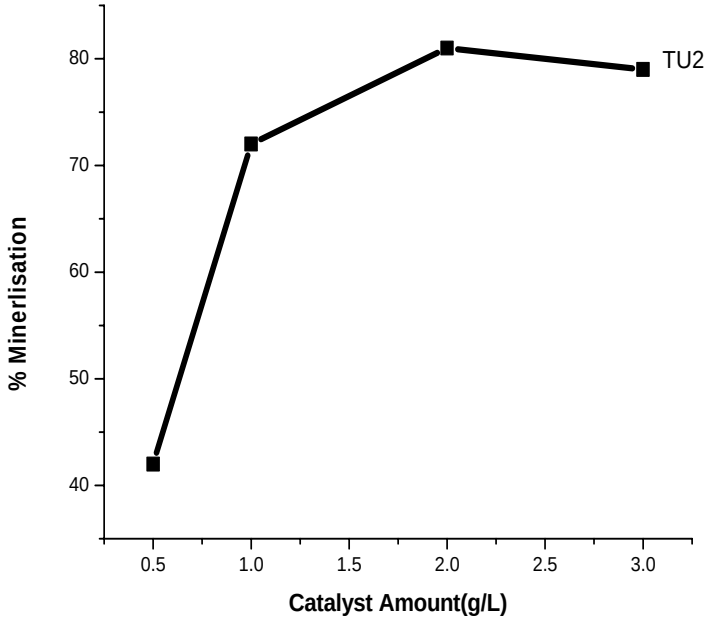

Fig.7.4 % Mineralisation of Acetophenone against amount of catalyst Irradiation time 1 hour; Acetophenone concentration 20ml 10^{-4}M

As the catalyst loading is increased, there is an increase of surface area of the catalyst available for adsorption and degradation. The increase in opacity and light scattering by particle are the reasons for the decrease in degradation at higher catalyst loading.

7.2.3 Effect of dopants

The photocatalytic degradation of acetophenone was studied using all doped samples with different concentration of dopants. The line diagram represents the percentage degradation of acetophenone using all ratios of metal and non metal doped catalyst within a time of 30 minutes under visible light irradiation. The doped samples show higher activity compared to undoped titania. The extent of degradation decreases by increasing the dopant content beyond the optimum value. The percentage degradation decreases because excess-dopant introduces electron–hole recombination centres although the catalysts with higher amount of dopant can absorb more visible-light [6-12]

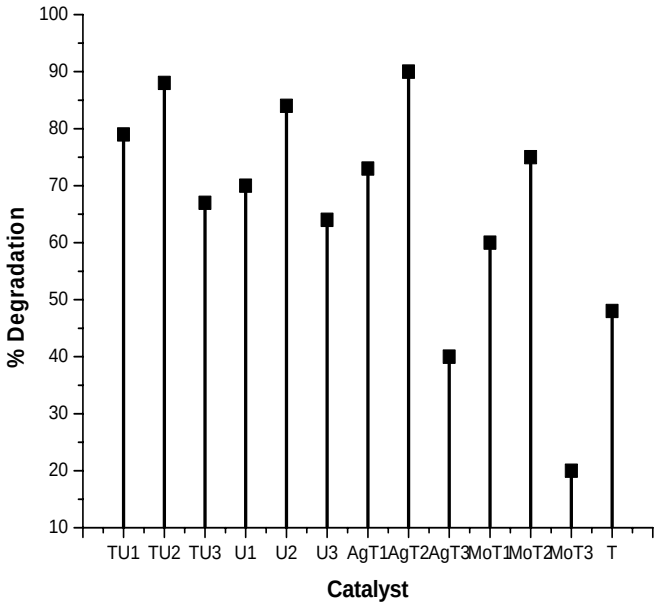

Fig.7.5 % Degradation of Acetophenone using different catalysts Irradiation time 30 minutes; Amount of catalyst 1g/L; Acetophenone concentration 20ml of 10^{-4}M

Percentage mineralisation of acetophenone was studied using undoped titania (T) and all samples with optimal concentration of dopants (TU2, U2, AgT2, MoT2). The line diagram represents the percentage mineralisation using metal and non metal doped catalyst within a time of 1 hour. The experiment was carried out using 20ml of 10^{-4}M acetophenone solution and 1g/L of catalyst under visible light irradiation.

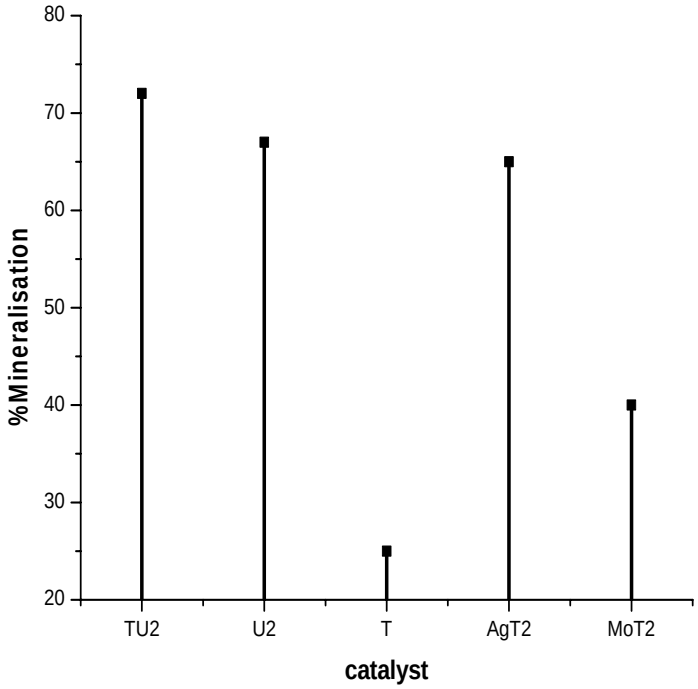

Fig.7.6 % Mineralisation of Acetophenone using different catalysts Irradiation time 1hour; Amount of catalyst 1g/L; Acetophenone concentration 20ml of 10^{-4}M

The percentage mineralisation depends on the employed sample .The TOC results after 1 hour of irradiation has shown that acetophenone is photodegraded when the doped TiO_2 is used, whereas it is scarcely mineralized in the presence of pure titania. High mineralisation percentage was obtained by employing TU2 and U2 actalysts while a percentage of only 20% was observed with pure titania.

The photocatalytic process is highly dependent on the hydroxyl group present on the surface, which attacks the contaminant present in water. The higher surface area is helpful in accommodating higher hydroxyl groups, which leads to higher photocatalytic degradation[13]. The optimum band-gap also plays a major role in the photocatalytic activity of doped titania [14,15]. Similarly, doping improves the trapping of electron and inhibits e^--h^+ recombination [16-19].

7.2.4 Effect of light source

Aqueous solution of acetophenone was irradiated by 150 W Xe lamp in the presence or absence of TiO_2. The role of photocatalytic degradation and the effect of direct photolysis on the degradation of acetophenone were studied.

Table 7.1 %Mineralisation of Acetophenone in the absence of light/catalyst

Studies	% mineralisation (time 1h)
Without Catalyst	4
Without Light	6

The blank study carried out in the presence of light without any catalyst shows that during light irradiation, direct photolysis could not mineralize acetophenone. Degradation of acetophenone was only 4% within 60 minutes in the direct photolysis indicating that the degradation in the presence of TiO_2/light is particularly due to the photocatalytic reaction of the TiO_2 particles, followed by the formation of an electron–hole pair on the surface of catalyst.

References

[1] www.wikipedia.org

[2] www.chemicalland21.com/industrialchem

[3] www.epa.gov/ttn/atw/hlthef/acetophe.html

[4] Yanfang Shen, Tianying Xiong, Hao Du,Huazi Jin, Jianku Shang, Ke Yang, J Sol-Gel Sci Technol., 50(2009)98.

[5] Praveen K. Surolia, Rajesh J. Tayade, Raksh V. Jasra, Ind. Eng. Chem. Res.,46 (2007) 6196.

[6] M. I. Litter, Appl. Catal.B, 23(1999) 89.

[7] V. Brezova, A. Blazkova, L. Karpinsky, J. Groskova, B. Havlınova, V. Jorık, M. Ceppan, J. Photochem. Photobiol .A, 109 (1997) 177.

[8] R. J. Tayade, R. G. Kulkarni, R. V. Jasra, Ind. Eng. Chem. Res., 45 (2006) 5231.

[9] W. Choi, A. Termin, M. R. Hoffmann, J. Phys. Chem., 98 (1994) 13669.

[10] X. Li, P. Yue, C. Kutal, New J. Chem., 27 (2003) 1264.

[11] V. Vamathevan, H. Tse, R. Amal, G. Low, S. McEvoy, Catal. Today, 68 (2001) 201.

[12] Chien-Cheng Pan, Jeffrey C.S. Wu, Materials Chemistry and Physics, 100 (2006) 102.

[13] Rajesh J. Tayadea, Praveen K. Suroliaa, Ramchandra G. Kulkarnib, Raksh V. Jasra, Science and Technology of Advanced Materials,8 (2007) 455 .

[14] Ye Cong, Jinlong Zang, Feng Chen, Masakazu Anpo, J. Phys.Chem. C, 111 (2007) 6976.

[15] Aditi R. Gandhe, Julio B. Fernandes, Bulletin of the Catalysis Society of India, 4 (2005) 131.

[16] Jinkai Zhou, Yuxin Zhang, X. S. Zhao, Ajay K. Ray, Ind. Eng. Chem. Res., 45 (2006) 3503.

[17] Jun Zhang, Chunxu Pan, Pengfei Fang, Jianhong Wei, Rui Xiong, Applied Materials and Interfaces, 2 (2010)1173.

[18] Vaclav S tengl, Snejana Bakardjieva, J. Phys. Chem. C, 114(2010) 19308.

[19] Yi Xie, XiujianZhao, Journal of Molecular Catalysis A: Chemical, 285 (2008) 142.

.....ഌ.....

Chapter

8

Summary and Conclusions

Contents

8.1 Summary

Semiconductor photocatalysis has received much attention during last three decades as a promising solution for both energy generation and environmental problems. Semiconductor photocatalysis is initiated by electron-hole pairs after bandgap excitation. When a photocatalyst is illuminated by light with energy equal to or greater than band-gap energy, the valence band electrons can be excited to the conduction band, leaving a positive hole in the valence band: the electrons (and holes) migrate to the surface of the semiconductor and participate in various oxidation and reduction reactions with adsorbed species such as water, oxygen, and other organic or inorganic species. The positive hole can oxidize pollutants directly, but mostly they react with water to produce the hydroxyl radical (•OH), which is a very powerful oxidant. •OH rapidly attacks pollutants and mineralize them into CO_2 and H_2O. TiO_2, the most popular photocatalyst because of its relatively high activity, chemical stability, availability with low production costs, and non-toxicity has been widely studied and proven to have a potential to completely oxidize a variety of organic compounds, including persistent organic pollutants. TiO_2 has a wide band-gap energy of 3.0 ~ 3.2 eV which prevents the utilization of visible-light that accounts for most of solar energy. In the present study we prepared metal and non-metal doped titania which shows absorption in visible light region. The prepared catalysts were characterized by various techniques such as X-ray Diffraction Analysis(XRD), BET surface Area, X-ray Photoelectron Spectroscopy(XPS), Scanning Electron Microscopy(SEM), Energy Dispersive X-ray Analysis(EDX), UV-Vis.Diffuse Reflectance Spectroscopy(UV-Vis.DRS),CHNS Elemental analysis, Fourier Transform Infrared Spectroscopy(FTIR), Transmission Electron Microscopy(TEM) and Thermogravimetric Analysis(TG). The

activity of the prepared samples was studied by the degradation of different organic pollutants. The extent of photocatalytic degradation was tested using UV –Visible spectrophotometer and mineralization was examined by measuring the Total Organic Carbon (TOC) in the solution.

8.2 Conclusions

Chapter 1 contains an introduction of photocatalysis. It includes the mechanism, history, application and advantages of photocatalysis. It also includes the role of semiconductors as photocatalysts, the band edge position of different semiconductors and the advantage of TiO_2 as a photocatalyst. The band gap of titania, the different crystalline phases of titania and the different preparation methods are included. The band gap of titania is 3.24eV which falls in UV region. Doping is an effective method to modify titania and to improve its activity in visible light. Among advanced oxidation processes the photocatalytic degradation has proved to be an effective tool for degrading organic pollutants. The aim of this research is to develop a photocatalyst with high photoactivity, which is capable of degrading and mineralizing different organic compounds under visible light.

Chapter 2 explains catalyst preparation and different characterization techniques. The materials used, the preparation method and catalyst notations are included. TiO_2 doped with metals and non metals are prepared through sol-gel technique. It also gives a brief account of different characterization techniques such as X-ray Diffraction Analysis(XRD), BET surface Area, X-ray Photoelectron Spectroscopy(XPS), Scanning Electron Microscopy(SEM) Energy Dispersive X-ray Analysis (EDX), UV-Vis Diffuse Reflectance Spectroscopy(UV Vis.DRS),CHNS Elemental analysis, Fourier Transform Infrared Spectroscopy (FTIR), Transmission Electron Microscopy(TEM) and

Thermogravimetric Analysis(TG).The method used to study the photocatalytic degradation was also incorporated in this chapter.

Chapter 3 discusses the physiochemical characteristics of the catalysts. The XRD results showed that the catalysts showed good crystallinity with fully anatase phase. Crystallite size was determined by using Scherrer's equation. The BET surface area of all the catalyst was measured. The present sol gel method adopted is a good route for the preparation of photocatalyst with high surface area. The UV-Vis DRS results showed that the presence of small amount of dopant in the catalyst gives rise to a red shift of its absorbance wavelength and decreases the band gap of titania. EDX is used to confirm the existence of dopants in the doped catalysts. The presence of N and S in the doped catalysts was studied by CHNS analysis. The surface morphology was obtained from SEM and TEM images. The HRTEM images showed that particles are highly ordered. The SAED image of N doped titania showed well distinct spots due to high crystallinity. The presence of N in N doped titania was again confirmed by XPS analysis. From the TG analysis the calcination temperature was fixed to be 400^{o}C.

Chapter 4 discusses the photocatalytic degradation of different dyes in aqueous solution in visible light region. Dyes (Acid Orange 7, Acid Red1, Methylene Blue, Crystal Violet and Acid Blue 25) were selected for the photocatalytic degradation. The effect of operational parameters, such as time, dye concentration, catalyst concentration, light source, doping of TiO_2 on the degradation of aqueous dye solutions were examined. The reusability of catalyst was also checked. The percentage degradation was studied spectrophotometrically. The mineralization was studied by using TOC analysis. The doped catalyst shows higher degradation in visible light compared to undoped titania. The N-S codoped catalyst showed highest visible

light activity. The high visible light activity of doped catalysts is due to its low band gap, good crystallinity and high surface area. The catalysts showed good activity at optimal dopant concentration. Effective destruction of these dyes is possible in the presence of light and catalysts suggesting that the degradation occurs through photocatalytic mechanism.

Chapter 5 focuses on the photocatalytic degradation of some pesticides in aqueous solution under visible light. The prepared catalysts were used in the photocatalytic degradation of some pesticides: 2,4-D , 2,4,5-T, Monolinuron, Dazomet and Phosphamidon. This chapter explains the effect of operational parameters i.e., time, catalyst concentration, dopants, light source on the degradation of pesticides. The results indicated that doping enhances the photoactivity of titania in visible light. The presence of optimum amount of dopants may prevent the charge carrier recombination; in addition the absorbance in visible region also influences the activity of catalysts. Negligible mineralisation was observed under light irradiation in absence of catalysts, which proves that the mineralization of these pesticides proceeds exclusively due to photocatalytic processes. In the case of all these pesticides more than 60% mineralisation was observed after one hour using TU2 as catalyst.

Chapter 6 explains the photocatalytic degradation of 4-nitophenol. The effects of operational parameters, such as time, catalyst concentration, light source, dopants were examined. The results suggested that the catalyst does not only promotes degradation but also the mineralization of 4-nitrophenol. Negligible mineralization was observed in absence of catalyst under light irradiation indicating that direct photolysis cannot mineralize nitrophenol. Doped catalysts showed higher mineralization compared to undoped titania. This is due to the positive effect of dopants on the photoactivity of TiO_2 at

degradation of *4*- nitrophenol that may be explained by its ability to trap electrons, thus, reducing the recombination of light-generated electron-hole pairs at TiO_2 surface. The high surface area , crystallinity, anatase phase, low bandgap also effects their activity.

Chapter 7 explains the photocatalytic degradation of acetophenone .The effect of different operational parameters on photocatalytic degradation was discussed. Negligible mineralisation was observed in the absence of catalyst or light. The N-S codoped catalyst showed highest visible light activity.

Chapter 8 presents summary and conclusion of the present work.

8.3 Future Outlook

For effectively utilizing the solar energy, developing a photocatalyst with high visible activity is still a big challenge in this research field. In the present study some metal and non-metal doped catalyst were prepared which showed high activity in visible light region Quite recently, however, anion doping and multielemental doping have been receiving much attention as a method for controlling the optical properties of TiO_2 . The present sol gel method adopted is a good route for the preparation of photocatalyst with high activity. There are other different methods of preparation which can also be tried for developing efficient catalysts. Here the photocatalytic degradation of some dyes and pesticides are studied .The work can be extended for the degradation of many other organic pollutants and for the purification of water and air. In this work we mainly focus on the percentage mineralization. Studies can be extended for identifying the reaction intermediates and reaction pathway.

.....ꕥ.....

PAPERS PRESENTED IN INTERNATIONAL/ NATIONAL CONFERENCES

[1] Preparation, characterization and photocatalytic activity of N doped TiO_2 - Dhanya T.P. and S. Sugunan*. (Indian Analytical Science Congress-2008)

[2] S-N codoped TiO_2 photocatalyst with visible light activity prepared by sol-gel method - DhanyaT.P.and S. Sugunan*. (National Conference on Advances in Physical and Theoretical Chemistry held at Department of Chemistry Calicut -March 2009)

[3] N doped anatase titania with enhanced photocatalytic activity in visible light - DhanyaT.P. and S. Sugunan*. (Matcon2010- International conference on Materials for the millennium held at Department of Applied Chemistry, CUSAT, Cochin- January 2010)

[4] Visible light responsive S-N codoped TiO_2 photocatalyst for the degradation of 2,4 D –DhanyaT.P. and S.Sugunan* (CTric 2011 held at Department of Applied Chemistry, CUSAT, Cochin - March 2011)

[5] Enhanced photocatalytic activity of silver doped titania synthesized through sol gel method – DhanyaTP. and Dr. S.Sugunan* (CTric 2012 held at Department of Applied Chemistry, CUSAT, Cochin - January 2012)

[6] Enhanced photocatalytic activity of nitrogen doped titania synthesized through sol gel method-DhanyaT.P. and S.Sugunan* (National conference on Advances in organic and physical chemistry held at Department of Chemistry Calicut -March 2012)

.....ഉാ.....